International
Progress Report

IPR-03-38

Äspö Hard Rock Laboratory

Status report of the Colloid investigation conducted at the Äspö HRL during the years 2000-2003

Marcus Laaksoharju (comp.)

GeoPoint AB

March 2003

Svensk Kärnbränslehantering AB
Swedish Nuclear Fuel
and Waste Management Co
Box 5864
SE-102 40 Stockholm Sweden
Tel +46 8 459 84 00
Fax +46 8 661 57 19

Äspö Hard Rock
Laboratory

Report no.	No.
IPR-03-38	F91K
Author	Date
Marcus Laaksoharju (comp.)	2003-03-15
Checked by	Date
Ignasi Puigdomenech	2003-06-23
Approved	Date
Christer Svemar	2003-09-26

Äspö Hard Rock Laboratory

Status report of the Colloid investigation conducted at the Äspö HRL during the years 2000-2003

Marcus Laaksoharju (comp.)

GeoPoint AB

March 2003

Keywords: Colloid, colloid generation, colloid concentration, saline groundwater, bentonite, microbes, groundwater sampling

Foreword

SKB decided year 2000 to initiate an international colloid project at Äspö-Hard Rock Laboratory in Sweden to study the stability, generation and mobility of colloids. The participating organisations in the project were: INE/Forshungszentrum Karlsruhe, Germany; POSIVA, Finland and SKB, Sweden. Project contributors and SKB managers are acknowledged for excellent work and support of the project during the years 2000-2003.

Main project contributors (in alphabetic order):

Gunnar Buckau; Claude Degueldre; Trygve Eriksen; Ioana Gurban; Wolfgang Hauser;Ola Karnland; Bernhard Kienzler; Mia Mäntynen; Karsten Pedersen; Minna Rantanen; Margit Snellman; Ulla Vuorinen; Susanna Wold;

SKB and INE managers:

Fred Karlsson; Bernhard Kienzler; Ignasi Puigdomenech; Peter Wikberg

Abstract

SKB decided year 2000 to initiate an international colloid project at Äspö-Hard Rock Laboratory in Sweden. The objectives of the colloid project are to: (i) Study the role of bentonite clay as a source for colloid generation, (ii) Verify the colloid concentration at Äspö-HRL and, (iii) Investigate the potential for colloid formation/transport in natural groundwater concentrations. The experimental concepts for the Colloid project are: laboratory experiments with bentonite clay, background field measurements of natural colloids, borehole specific bentonite colloid generation experiment and a fracture specific transport experiment. The activities concerning the laboratory experiments and background field measurements are described in this work since the other activities are ongoing or planned. The following conclusions were made:

- The dissolution of bentonite and hence the colloid formation is dependent of background electrolyte and its concentration.
- Natural colloidal particles consist of organics, inorganic colloids (clay, calcite, ironhydroxide) and of microbes.
- Microbes form few but large particles, organic particles are small but can be many. Microbe content is increasing with the content of organic carbon
- The colloid concentration is decreasing with depth and salinity
- The colloid content at Äspö is less than 300 ppb
- The colloid content at repository level is less than 50 ppb
- The groundwater variability obtained in the sampled boreholes reflect well the natural groundwater variability along the whole HRL tunnel

Sammanfattning

År 2000 initierade SKB ett internationellt kolloidprojekt i berglaboratoriet på Äspö. Syftet med projektet är: (i) Studera bentonitlerans roll som kolloidkälla, (ii) Verifiera den naturliga kolloidhalten i grundvattnen på Äspö och, (iii) Studera kolloidformations och transport potentialen i naturliga grundvatten. De experimentella koncepten för kolloidprojektet är: laboratorie försök med bentonit lera, bakgrundsmätningar av den naturliga kolloidhalten i grundvatten, borrhåls specifika kolloidgenereringsförsök och sprickspecifika kolloidtransportförsök. I detta arbete beskrivs laboratorieförsöken med bentonit lera och bakgrundsmätningar av den naturliga kolloidhalten, eftersom de övriga aktiviteterna är pågående eller planeras. Av det utförda arbetet kan man dra följande slutsatser:

- Upplösning av bentonit och således kolloidhalten styrs av bakgrunds elektolyten och dess koncentration.
- Naturliga kolloider i grundvatten består av organiska och oorganiska (lera, kalcit, järnhydroxider) partiklar samt av mikrober.
- Mikroberna bildar ofta få men stora partiklar medan organiskt material bildar ofta små men många partiklar. Mikrobhalten ökar med ökad halt av organiskt material.
- Kolloidhalten på Äspö minskar med ökat djup och salthalt.
- Kolloidhalten på Äspö är mindre än 300 ppb
- Kolloidhalten på förvarsdjup på Äspö är mindre än 50 ppb
- Variationerna i salthalten i de mätta borrhålen täcker in den naturliga salthaltsvariationen som påträffas längs med hela Äspö tunneln.

Contents

1 Background and objectives

Colloids are small particles in the size range 10^{-3} to 10^{-6} mm. The colloidal particles are of interest for the safety of a repository for spent nuclear fuel because of their potential to transport radionuclides from a defect waste canister to the biosphere.

SKB has for more than 10 years conducted field measurements of colloids. The outcome of those studies performed nationally and internationally concluded that the colloids in the Swedish granitic bedrock consist mainly of clay, silica and iron hydroxide particles and that the mean concentration is around 20-45 ppb which is considered to be a low value /Laaksoharju et al., 1995/. The low colloid concentration is controlled by the attachment to the rock, which reduces both the stability of the colloids and their mobility in aquifers.

It has been argued that e.g. plutonium is immobile owing to its low solubility in groundwater and strong sorption onto rocks. Field experiments at the Nevada Test Site, where hundreds of underground nuclear tests were conducted, indicate however that plutonium is associated with the colloidal fraction of the groundwater. The $^{240}Pu/^{239}Pu$ isotope ratio of the samples established that an underground nuclear test 1.3 km north of the sample site is the origin of the plutonium /Kersting et al., 1999/.

The findings of potential transport of solutes by colloids and access to more sensitive instruments for colloid measurements motivated a Colloid Project at Äspö HRL (Hard Rock Laboratory). The project was initiated by SKB in 2000 and is planed to continue until the end of the year 2006.

The participating organisations in the project are:

- INE/Forshungszentrum Karlsruhe, Germany
- POSIVA, Finland
- SKB, Sweden

The objectives of the Colloid project are to study:

- The stability and mobility of colloids.
- Measure colloid concentration in the groundwater at Äspö.
- Bentonite clay as a source for colloid generation.
- The potential of colloids to enhance radionuclide transport.

The results from the project will be used mainly in the future development of safety assessment modelling of radionuclide migration. The project was conducted during.

The aim of this report is to present the results obtained during the time period 2000-2003. The persons contributing with scientific project results are referred to in the text below and the contributions not printed elsewhere are presented as Appendix 1-11 in this report.

2 Experimental concept

The experimental concepts for the Colloid project are: laboratory experiments, background measurements, borehole specific experiment and fracture specific experiment. The aim of the laboratory experiments is to study the behaviour of the bentonite clay at prevailing groundwater conditions at Äspö HRL. Background measurements of colloids aim at establishing the natural colloid content at the Äspö groundwaters. The borehole and fracture specific experiment aim at describing the colloid generation and transport potential of the bentonite clay but since these experiments are ongoing or in a planning phase they are not described further here. The laboratory and background measurements are described in the next sections.

2.1 Laboratory experiments

2.1.1 Initial laboratory tests

The mobility of radionuclides associated within a bentonite barrier of a repository for spent nuclear fuel may change if the bentonite complex to colloids. Clay and humic/fulvic colloids can enter the bentonite with the saturating groundwater but clay colloids can also be generated by the bentonite itself. The colloid formation of bentonite in contact with different solutions and the stability of the colloids have been studied.

The role of the bentonite clay as a source for colloid generation at varying groundwater salinity (NaCl/CaCl) was studied in laboratory experiments (Wold and Eriksen, 2001). Bentonite clay particles were dispersed in water solutions with different salinity and the degree of sedimentation was studied, see Figure 1. The results from the laboratory test indicate that the bentonite colloid formation is strongly correlated with the ionic strength of the solution. Very low concentration of colloids formed in suspensions with ionic strengths 0.1 and 1 M. This is valid for experiments both with dry (as in Figure 1) and wet prepared bentonite. At 0 and 0.01 M colloids were formed in the experiments with wet prepared bentonite. In the case with dry prepared bentonite where the solutions are shaken initially, the sedimentation is slow and no measurement was possible. At high ionic strength the colloid formation is minor. At ionic strength 0.01 M where colloid formation is favourable the colloid formation seems to increase when using a temperature of 60 °C for the solution compared with a solution of 20 °C, (Wold and Eriksen, 2001).

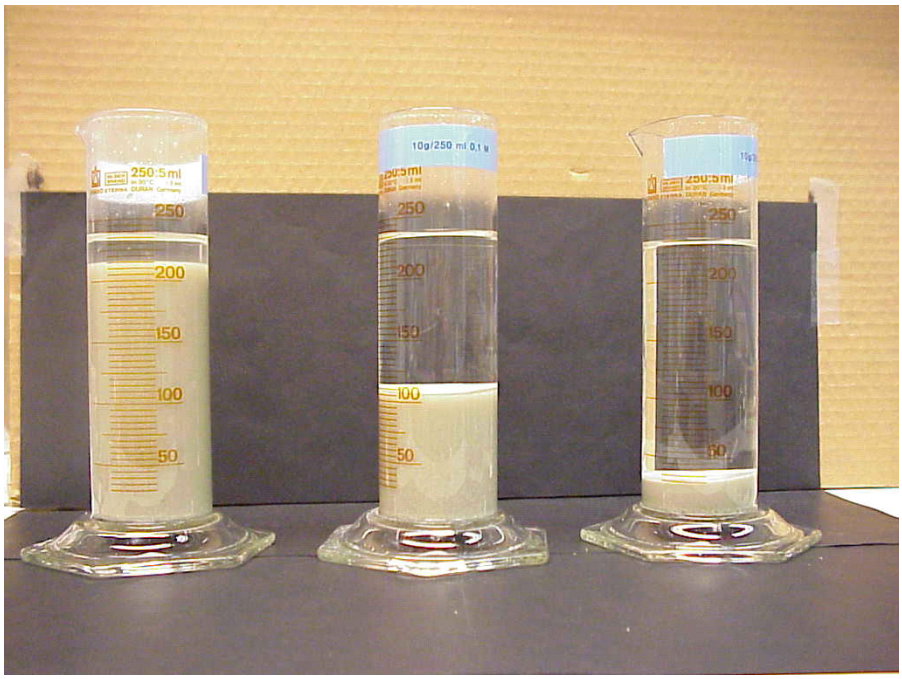

Figure 1: *The salinity of the water can influence the colloid generation. The experiment show different degrees of sedimentations of bentonite clay dependent of the ionic strengths (NaCl) in the water. A high or low ionic strength can result in instability and colloid formation. The experimental conditions: Dry bentonite, 10 g/250 ml in contact with 0.01, 0.1 and 1 M solution at 20 °C after 1.5 weeks (Wold and Eriksen, 2001 and 2002).*

2.1.2 Detailed laboratory tests (Appendices 1 and 2)

The laboratory experiment on bentonite was extended to investigate in more detail the influences of background electrolytes $NaClO_4$ and $CaCl_2$ at 0, 0.001, 0.01, 0.1 and 1 M, type and amount of bentonite (MX-80, Na- and Ca-bentonite), temperature (20 and 60 °C), and pH (Karnland, 2002; Wold and Eriksen, 2002a). Colloid concentration as well as colloidal size distributions was measured in the solutions after 7 to 21 days with PCS–dynamic light scattering. ICP-MS and ICP-AES analysis were performed where especially Si, Al, Fe, Mg and Ca in the solutions were monitored. Al in the solutions is assumed to be a marker for clay colloids generated by the bentonite.

The results indicate that colloid formation is a function of the dissolution of bentonite. The dissolution of bentonite is very slow in pH 8 to 8.5 in 20 °C but increases with temperature and when changing pH to <8 or >8.5. The dissolution of bentonite is dependent of background electrolyte and its concentration. In low ionic strength of Na^+ the osmotic pressure is high which results in a loose gel structure in the bentonite. Colloids can form and migrate out in solution.

Increasing Ca^{2+} decreases the distance between the montmorillonite sheets in bentonite and dissolution of Na-bentonite is therefor faster than MX-80 and Ca-bentonite dissolution. Colloidal stability in the solutions is mainly controlled by ionic strength. Aggregation and flocculation increases with ionic strength and colloids form larger units and sedimentate out from solution with time see Figure 2 (Karnland, 2002; Wold and Eriksen, 2002a).

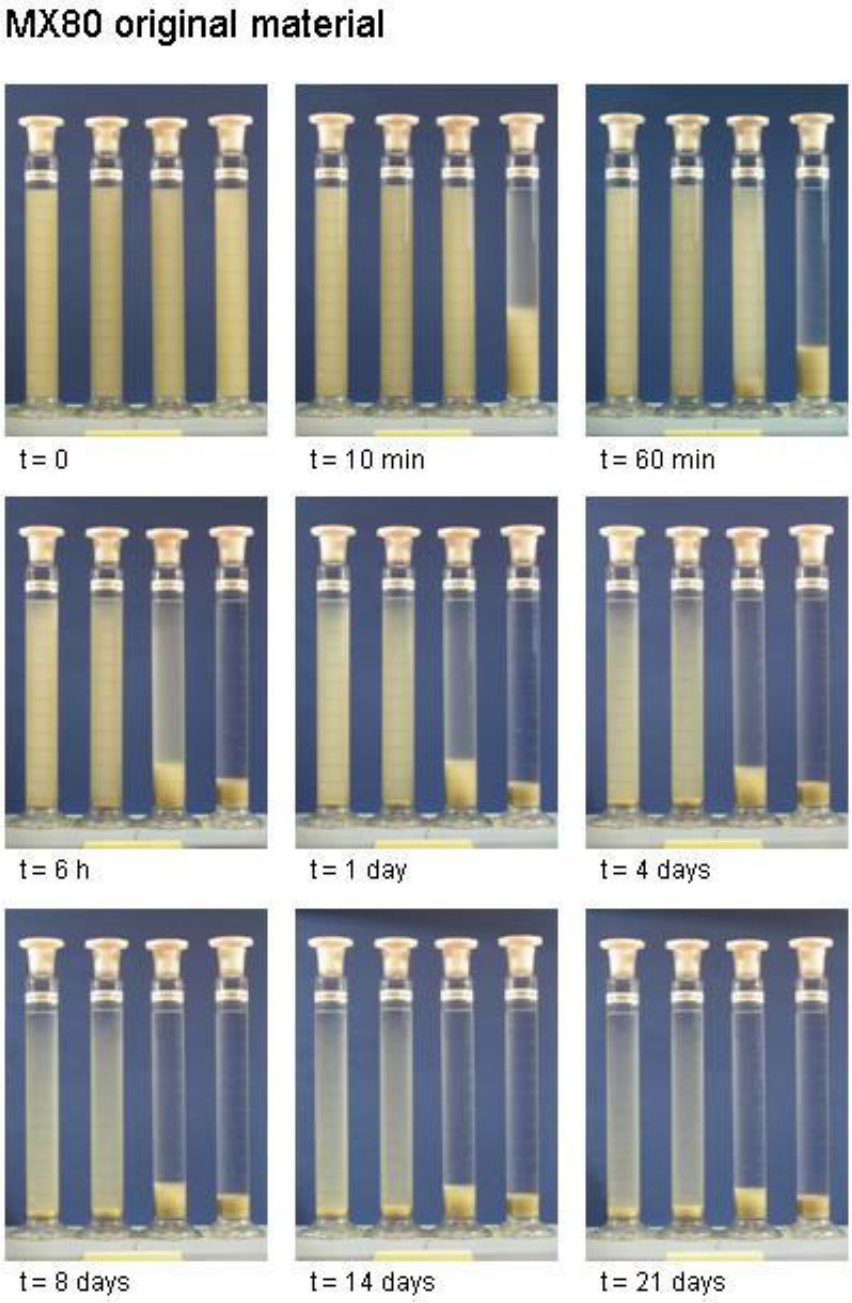

Figure 2: *Photographs of the MX-80 material in 250 ml water solutions after different sedimentation periods in time. From left to right in each picture, NaCl was added in order to give a concentration of: 0 M, 0.001 M, 0.01 M and 0.1 M (Karnland, 2002).*

2.2 Background Colloid measurements along Äspö HRL

The aim of this activity was to measure the natural background colloid concentrations from 8 different boreholes along the Äspö HRL-tunnel (Figure 3) by applying different techniques. The boreholes represent different water types with a TDS (Total Dissolved Solids) of 286-21760 mg/l, since it is well known that the colloid stability can change with the ion content of the groundwater. Some of the techniques were applied on all boreholes but others only on some specific boreholes. Also additional samplings outside the selected boreholes were employed. The techniques used and some of the major findings are presented below more detailed descriptions are found in the referred appendices.

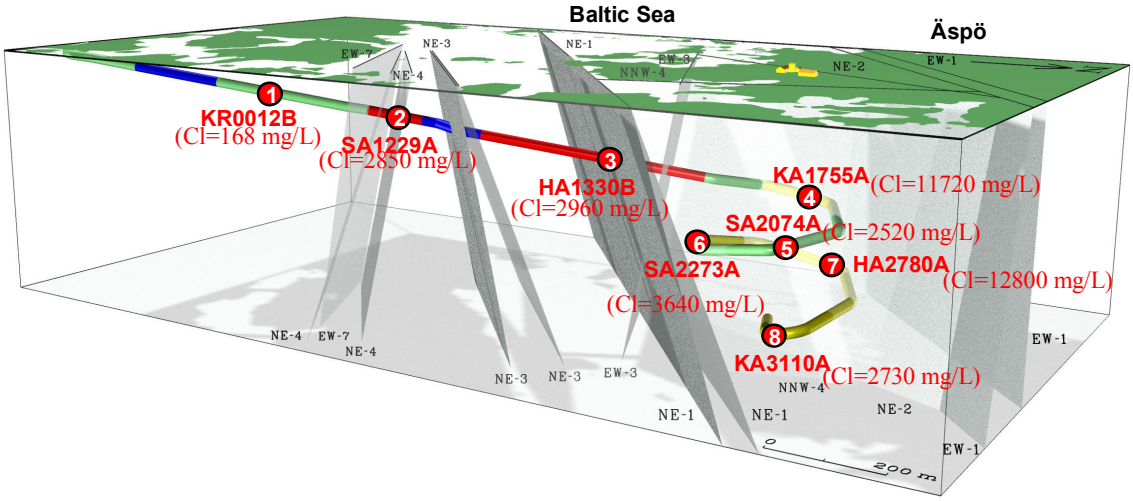

Figure 3: *The 8 boreholes sampled for colloids along the Äspö HRL tunnel. The Cl content of the groundwater is given within brackets. The reason for the large differences in the salinity along the tunnel is that the boreholes intersect different fracture zones with different orientations containing groundwater with different origins and ages.*

2.2.1 LIBD measurements (Appendix 3)

The colloid content was measured on-line from the boreholes by using a new high pressure detection cell connected to a modified laser based equipment LIBD (Laser-induced Breakdown-Detection) which has been developed by INE in Germany (Figure 4). The advantage is that the resolution of this equipment is higher compared with standard light scattering equipments. It is therefore possible to detect the colloid content at much lower concentrations than previously possible (Hauser et al, 2002). The results from the measurements show increased colloid stability and concentration in low salinity groundwaters (Figure 5) and in waters with high humic like organics. From EQ3/6 thermodynamic calculations the suparsaturation with regard to mainly carbonates was used as an indicator that these phases may form many of the colloids. The method was also used to indicate how sensitive the measurements are for contamination of atmospheric gasses (Hauser et al, 2002).

Figure 4: *The equipment for Laser-induced Breakdown-Detection (LIBD) of colloids is installed in a van in order to allow mobility and on-line measurements at boreholes (Hauser et al., 2002).*

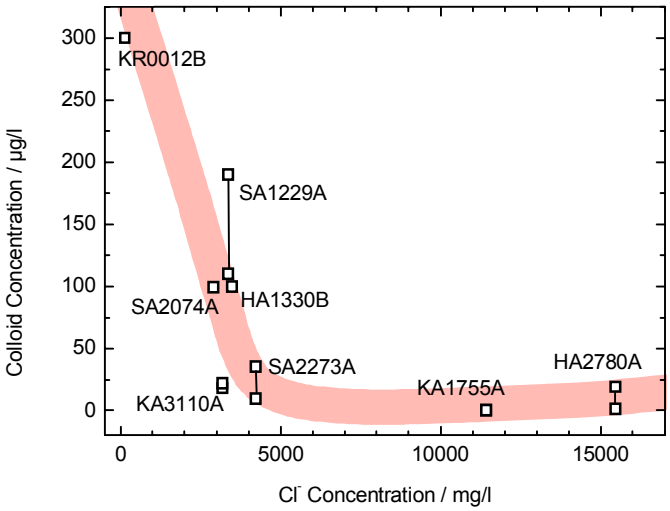

Figure 5: *The natural colloid concentration is decreasing with groundwater salinity but also with depth (Hauser et al, 2002).*

2.2.2 Humic measurements (Appendix 4)

A feasibility study was conducted for the isolation of sufficient amounts of fulvic acid from Äspö groundwaters. Dissolved organic carbon (DOC) and UV/Vis spectroscopy of original water samples as well as fulvic acid concentrates is used for quantification of the fulvic acid. The study shows that sufficient fulvic acid is available in all waters. It is also shown that sorption of fulvic acid on precipitates generated during shipping and handling of groundwater samples is not a problem.

For chemical, spectroscopic and isotopic (especially ^{14}C) characterization around 200 mg fulvic acid is required (around 100 mg C). In groundwaters where the fulvic acid concentration is around 1 mgC/L or higher, 100 L of groundwater can be sampled and sent to the laboratory for direct treatment. In two of the twelve investigated water samples the fulvic acid concentrations are so low that on-site pre-concentration by reverse osmosis appears to be the method of choice (Buckau and Wolf, 2002).

2.2.3 Ultrafiltration (appendix 5)

Two boreholes were sampled (sampling point 6 and 7, see Figure 3) and the sampled groundwater was ultrafiltrated in an inert atmosphere. An example of the results from the SEM micrograps and EDS spectra analysis are presented in Figure 6. The SEM/EDS results indicate that the dominating particle phases may be calcite, silica, ironhydroxide and clay particles. The obtained results did not allow calculation of the actual concentration of the elements associated with the different phases nor the amount of particles (Vuorinen 2002).

a)

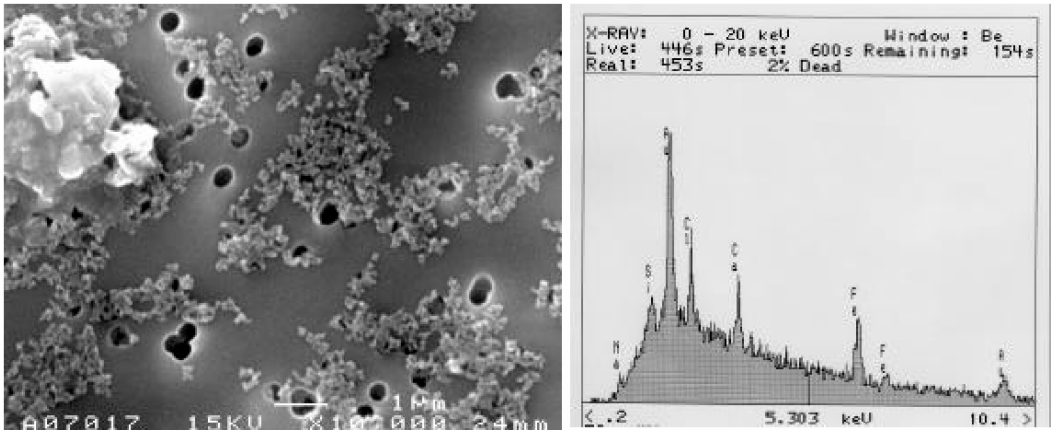

b)

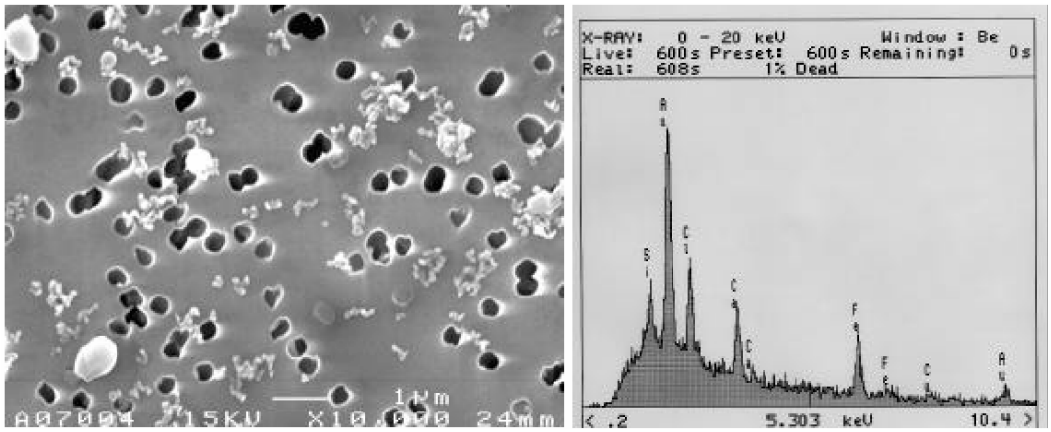

Figure 6: *SEM micrographs (to the left) of the 0.4 μm membrane (magnification = x10 000) and the EDS spectrum (to the right). a) The sample from the borehole SA2273A contains some large particles but also some small aggregates the EDS spectra indicate the presence of Fe, Ca, Si (Au is a method artefact; Cl is a due to saline groundwater precipitation). b) The sample from the borehole HA2780A shows a more homogeneous size distribution but similar elemental peaks (Vuorinen 2002).*

2.2.4 Comparison of groundwater analytical results (Appendix 6)

Groundwater sampling and analytics can be challenging when dealing with deep groundwaters. The POSIVA group wanted for quality assurance reasons to sample the boreholes used for colloid sampling located in the deeper part of the tunnel (sampling locations HA2780A, SA2273A and KA1755A, see Figure 3). The results show good agreement with the SKB analytical results (Appendix 7) despite some different sampling occasions and considering the ±5% uncertainty in the measurements (Rantanen and Mäntynen, 2002).

2.2.5 Groundwater analytical results (Appendix 7)

The complete groundwater analytical results of the boreholes sampled for the colloid project was performed by SKB, following the routines for class 4 (complete chemical characterisation) and class 5 (complete chemical characterisation including special isotope analysis). The results are presented in appendix 7 (Mattsén 2002) the salinity (Cl) distribution along the tunnel is depicted in Figure 3.

2.2.6 Colloid filtration and PCS measurements (Appendix 8)

Two different techniques for colloid concentration measurements was applied: on-line filtration and PCS-Dynamic light scattering measurement applied on pressurised groundwater samples. A filter system, with 3000, 450, 220 nm and 50 nm, were connected in series to the borehole. The filters were flushed with argon to prevent artefact colloid formation from groundwater in contact with atmospheric gases. Groundwater volumes of 50-1000 ml were flushed through the filter system. The filters were analysed by using ICP-MS and ICP-AES. The inorganic colloids in Äspö-waters are presumably composed of iron hydroxides, silica and clay mineral. The analysed Fe, Si and Al were therefore assumed to represent the inorganic colloid phases in the Äspö groundwaters. The colloid concentrations in the Äspö ground waters are in the range of 1-149 ppb. Colloids in the size range >50<220 nm are dominating in all the Äspö-water samples except for the water sampled in borehole SA 2273 A. The colloid concentrations are low and it is therefore questionable to define the exact size distributions. All the samples contained lower colloid concentrations than the PCS detection limit of 0.6 mg/l (Wold and Eriksen, 2002). This method is therefore not suitable for natural groundwaters.

2.2.7 Microorganisms in the groundwater (Appendix 9)

Microorganisms generally range in size between 2×10^{-4} to 10^{-2} mm, thereby overlapping colloid particles in size. Their organic character, with many different functional groups directed outwards from the cell surface, e.g. phosphates, amines, hydroxyl- and carboxyl-groups, makes them potent as radionuclide sorbents. The sampled boreholes along the Äspö-HRL represented different water types since it is well known that the colloid stability but also the microorganisms can change with the ion content of the groundwater. A test rack with 50 ml sterile plastic tubes with screw lids filled with 3 ml 30 % formaldehyde were used for sampling. The water was filtered and the filters were examined by using microscopy under fluorescene light in order to count the microbes. The numbers ranged more than two orders of magnitude, with the highest numbers in the shallowest and the deepest borehole investigated, KR0012B and KA3110A. A comparison of the obtained data with earlier data on total numbers of microorganisms in Fennoscandian Shield groundwater is shown in Figure 7. The obtained data lies within the range of all available data. There was an obvious difference in size and appearance between the boreholes, from 0.2 μm up to several μm. The borehole HA1330B showed the largest cells, most other boreholes had small, or very small cells, see Figure 8 (Pedersen, 2002). The microbial content is increasing with the organic content in the groundwater (see Figure 9). Generally shallow water contains more organic material than deep groundwater.

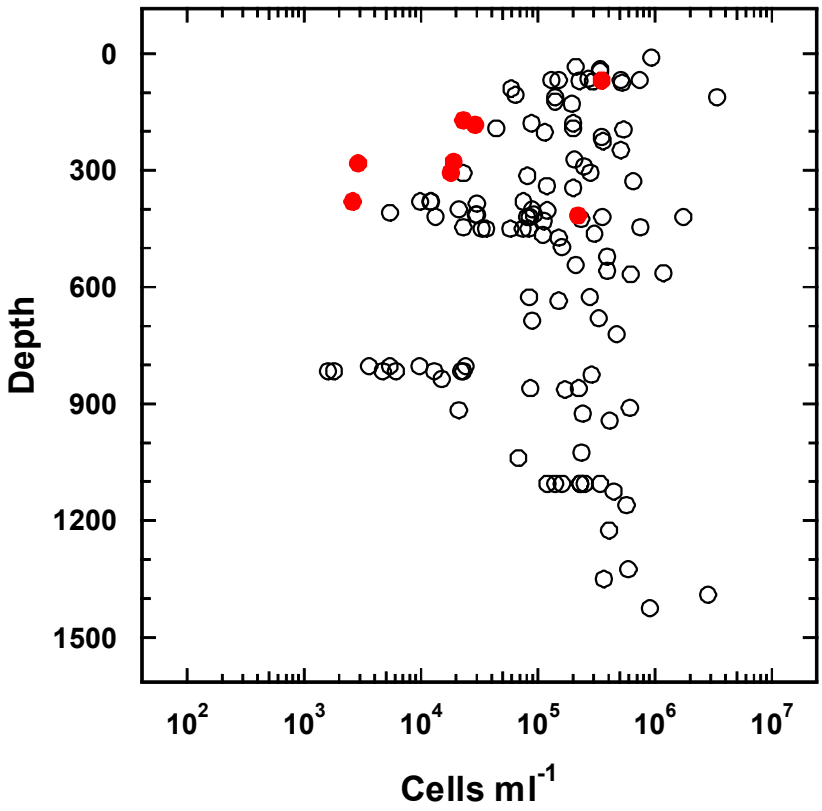

Figure 7. *The means of the number of microorganisms along the depth of the Äspö-HRL. The results are compared with data from Stripa research mine, Laxemar boreholes KLX and investigation sites in Finland (Olkiluoto, Hästholmen, Kivetty, Romuvaara) and the natural uranium analogue in Palmottu, Finland.(Pedersen, 2002).*

a)

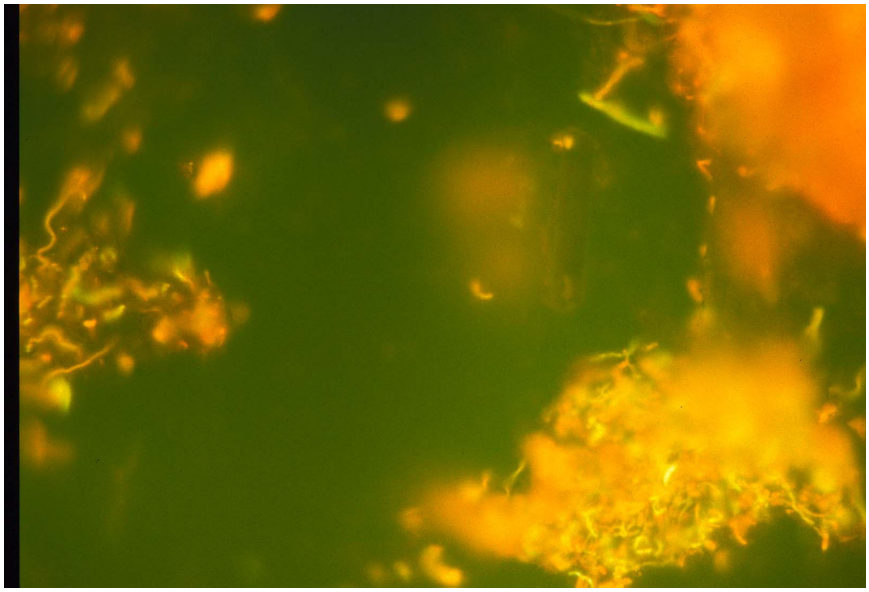

b)

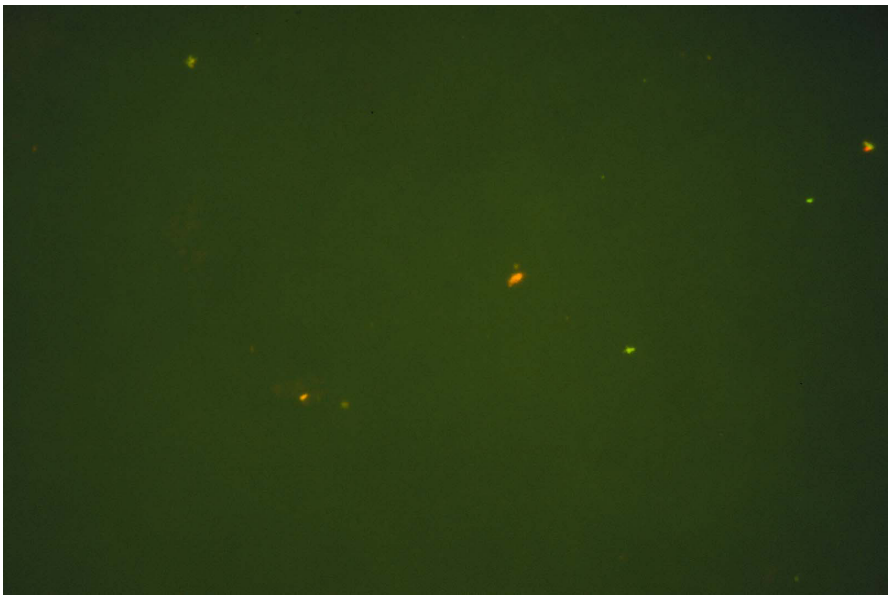

Figure 8. *a) A borehole with large cells (HA1330B) and b) a borehole with small cells (HA2780). The pictures represent the 2B filters with a frame size 130 x 85 µm (Pedersen 2002).*

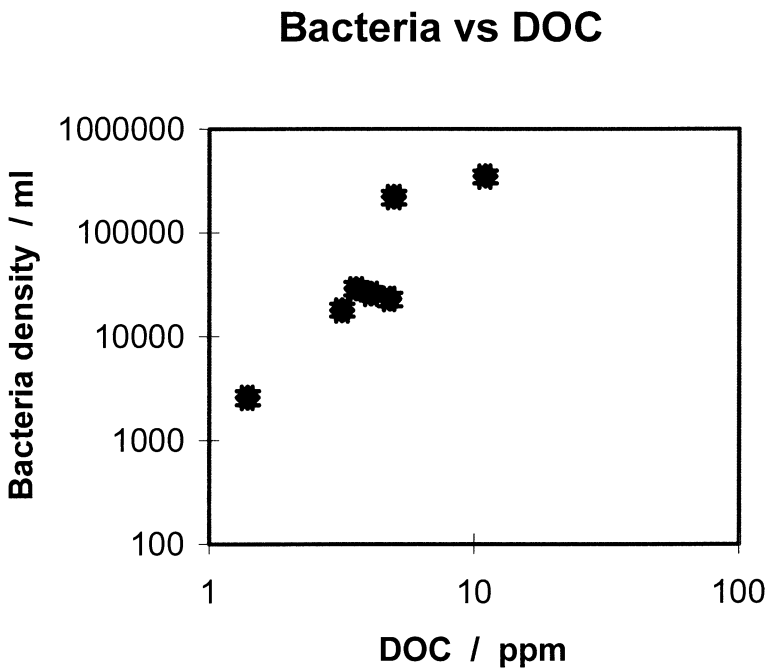

Figure 9: *The microbial content is increasing with the organic content in the groundwater (Dugueldre 2002).*

2.2.8 Measurements of the electrical conductivity along the Äspö HRL tunnel (Appendix 10)

The aim of the sampling was to measure the electrical conductivity of all the major water venues at the Äspö tunnel and to compare it with borehole data to assure that the borehole data reflects the natural groundwater and also colloid variability at the site. A total of 195 groundwater samples were collected along the tunnel in total. The results are shown in Figure 10.

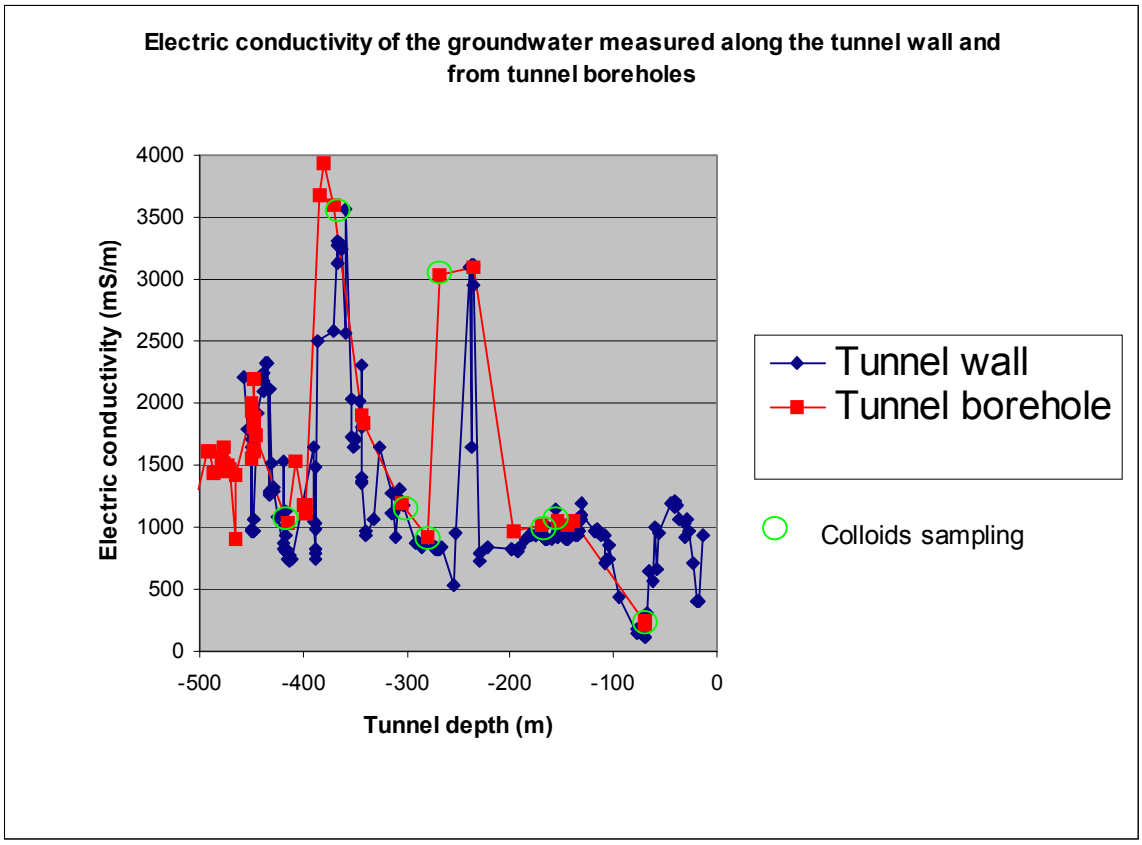

Figure 10: *Electrical conductivity measured along the tunnel walls (blue) and electrical conductivity data measured in the tunnel boreholes (red) versus the tunnel depth. The green circles indicated the 8 boreholes used for colloid sampling (Gurban, 2002).*

The results indicate that both data sets give the same basic information concerning groundwater composition (salinity) but greater detail variability is seen in the data collected along the tunnel. This indicates that data collected along the tunnel reflects local variability better than data from boreholes, but when sampling the tunnel wall close to the boreholes the groundwater salinity is the same in the borehole as in the water dripping from the wall. These results support the colloid project, by showing that the groundwater composition obtained from the boreholes reflect well the major groundwater variability obtained in the whole tunnel (Gurban, 2002).

2.2.9 Review comments (Appendix 11)

The project contributions (Appendices 1-10) have been reviewed by an external reviewer (Degueldre, 2002). Many of the important findings were summarised during this review process e.g. that the natural colloidal particles at Äspö consist of organics, inorganic colloids (clay, calcite, ironhydroxide) and of microbes. Microbes form few but large particles, organic particles are small but can have a high concentration especially in shallow waters (Figure 7). The colloid concentration is decreasing with depth and salinity.

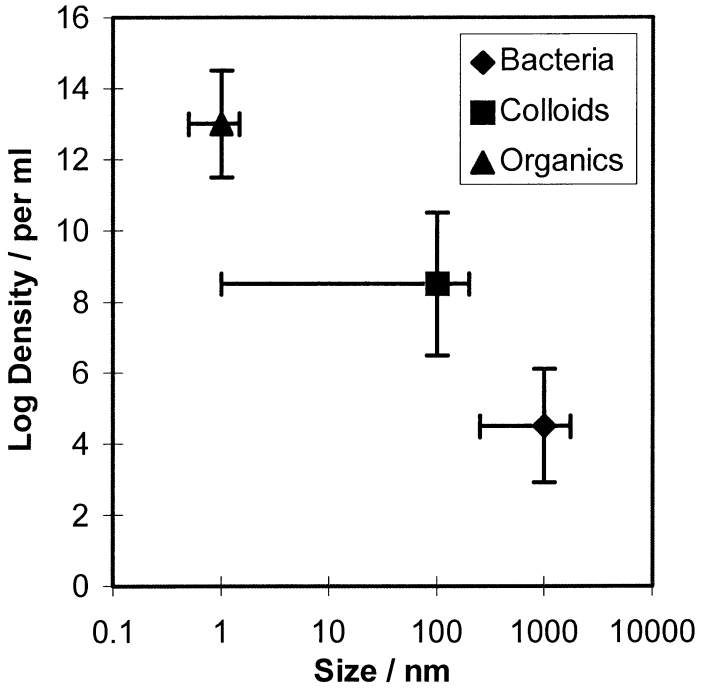

Figure 7: *Schematic presentation of concentration and size distribution of the dominating colloidal particles at Äspö HRL (Degueldre, 2002).*

3 Conclusions

The major result from the laboratory experiments is that dissolution of bentonite is dependent of background electrolyte and its concentration. In low ionic strength of Na^+ the osmotic pressure is high which results in a loose gel structure in the bentonite. Colloids can form and migrate out in solution. The dissolution of bentonite is very slow in pH 8 to 8.5 in 20 °C but increases with temperature and when changing pH to <8 or >8.5. (Karnland, 2002; Wold and Eriksen, 2002a).

The major finding from the background colloid measurements at Äspö HRL is that despite different techniques and sometimes large uncertainties in the measurements that the colloid content at repository level is at ppb level (Degueldre 2002; Hauser et al., 2002; Wold and Eriksen 2002; Vuorinen 2002; Gurban 2002; Wold and Eriksen 2002; Mattsén 2002; Rantanen and Mäntynen 2002; Pedersen 2002). These results support the earlier measurements and modeling of colloids which indicated low colloid concentrations at deep groundwaters at Äspö (Laaksoharju et al., 1995).

The following conclusions can be made:

The dissolution of bentonite and hence the colloid formation is dependent of background electrolyte and its concentration.

Natural colloidal particles consist of organics, inorganic colloids (clay, calcite, ironhydroxide) and of microbes.

- Microbes form few but large particles, organic particles are small but can be many
- Microbe content is increasing with the content of organic carbon
- The colloid concentration is decreasing with depth and salinity
- The colloid content at Äspö is less than 300 ppb
- The colloid content at repository level is less than 50 ppb
- The groundwater variability obtained in the sampled boreholes reflect well the natural groundwater variability along the whole HRL tunnel

4 References

Buckau G, Wolf M, 2002. Origin, stability and mobility of humic colloids in Äspö groundwater: Feasibility study. *See, Appendix 4.*

Gurban I, 2002. Electric conductivity measurements along the Äspö tunnel. *See, Appendix 10.*

Hauser W, Götz R, Geckeis H, Kienzler B, 2002. In-situ Colloid Detection in Granite Groundwater along the Äspö Hard Rock Laboratory Access Tunnel. *See, Appendix 3.*

Karnland O, 2002. Colloid stability in Wyoming bentonite clay. *See, Appendix 1.*

Kertsting A, Efurd D, Finnegan D, Rokop D, Smith D, Thopmson J, 1999. Migration of plotonium in the ground water at the Nevada Test Site. Nature, Vol 397, January 1999, pp 56-59.

Laaksoharju M, Degueldre C, Skårman C, 1995. Studies of colloids and their importance for repository performance assessment. SKB Technical Report TR 95-24, Stockholm, Sweden.

Mattsén C, 2002. Compilation of groundwater chemistry data October 2001. *See, Appendix 7.*

Pedersen K, 2002. Total number of microorganisms in groundwater sampled during background colloid measurements along the Äspö HRL-tunnel. *See, Appendix 9.*

Rantanen M, Mäntynen M, 2002. Groundwater sampling in Äspö tunnel. *See, Appendix 6.*

Vuorinen U, 2002. Characteristics of natural colloids in two groundwater samples from the Äspö HRL-tunnel. *See, Appendix 5.*

Wold S, Eriksen T, 2001. Formation of inorganic colloids in solutions of different ionic strength in contact with bentonite. SKB ITD-01-02.

Wold, S Eriksen T, 2002a. Formation of inorganic colloids in solutions in contact with bentonite. *See, Appendix 2.*

Wold S, Eriksen T, 2002b. Background inorganic colloid measurements in different Äspö-waters. *See, Appendix 8.*

Degueldre C, 2002. Review comments to the Äspö Colloid Wordkshop 5:th of March 2002. *See, Appendix 11.*

Appendix 1

Colloid Stability in Bentonite
–
A Laboratory Study

Ola Karnland

Clay Technology AB

Background

Highly compacted bentonite clay is planned to be used as a buffer material in the KBS3 type repository for spent nuclear fuel. The main component in bentonite is montmorillonite, which consists of mineral flakes with a thickness of approximately 1 nanometer. Consequently, there is a potential risk that these flakes will act as colloids if the highly compacted buffer material is exposed to water and free to expand. Such dispersion may jeopardize the buffer function by loss of material to fractures and possible continuous transport by groundwater. Further, radioactive material may be adsorbed on the clay particles and thereby transported to the biosphere. It is not likely that the bentonite will disperse into the ground-water, but it can not be excluded that some process such as rock displacement or gas penetration will lead to partial dispersion of the montmorillonite. The main question is then, under which conditions do such a dispersion lead to a stable colloidal system.

Objectives

The main objectives in this laboratory test series are to:

- quantify bentonite colloid stability at different salt concentration,
- quantify the difference between mono- and divalent cat-ions with respect to colloid stability,
- examine the role of original salt content in the bentonite,
- test if chemical analyses is a possible tool to detect clay colloids in ground water.

The test solution concentrations were chosen in order to identify limits and were not aimed to be representative for repository ground water. However, the highest examined concentrations are in the same range as the concentrations in Äspö ground-water.

Test program

The main test series included 15 tests in which a water solution of 250 ml and 1g of bentonite material were placed in a mixing cylinder (Table 1). The original clay was used in 4 tests, and Na- and Ca-converted clay was used in 4 tests, respectively. Two tests were made with the final supernatant in the Na-conversion stage, described below, which included some colloids observed by naked eye (CoA13, CoA14). Three additional tests including Na converted clay exposed to $CaCl_2$ solutions were made (CoA16-CoA18). Two reference analyses with water only were made, one with starting de-ionized water (CoA15) and one with the same starting water but treated as the clay samples and placed in the test cylinders for the maximum testing time (CoA19).

The clay was actively dispersed in the solutions by daily shaking for a few minutes during a period of 1 week. The cylinders were thereafter left to rest in order to permit natural sedimentation by gravitation only.

Table 1 Test Program.

Project Colloids
Series CoA

	solution				solution analyses					Mineral	
test no	V	C	salt	bentonite	ICP/AES	IC	colloids	κ	pH	XRD	ICP/AES
	ml	mM						S/cm			
CoA01	250		none	MX-80	1	1	1	138	8.2	1	1
CoA02	250	1	NaCl	MX-80	1	1	1	264	7.4		
CoA03	250	10	NaCl	MX-80	1	1	1	1400	6.8		
CoA04	250	100	NaCl	MX-80	1	1	1	11400	6.6		
CoA05	250		none	MX-80 Na	1	1	1	64	8.4	1	1
CoA06	250	1	NaCl	MX-80 Na	1	1	1	215	7.3		
CoA07	250	10	NaCl	MX-80 Na	1	1	1	1300	7		
CoA08	250	100	NaCl	MX-80 Na	1	1	1	11800	6.7		
CoA09	250		none	MX-80 Ca	1	1	1	33	8.5	1	1
CoA10	250	1	$CaCl_2$	MX-80 Ca	1	1	1	258	6.3		
CoA11	250	10	$CaCl_2$	MX-80 Ca	1	1	1	2400	6.1		
CoA12	250	100	$CaCl_2$	MX-80 Ca	1	1	1	20000	5.8		
CoA13	250		prevalent	MX-80 Na f	1	1	1	181	7.8		
CoA14	250		prevalent	MX-80 Na f	1	1	1	207	7.8		
CoA15	250		none	none	1	1	1	1.2	8.4		
CoA16	250	1	$CaCl_2$	MX-80 Na	1	1	1	286	7.1		
CoA17	250	10	$CaCl_2$	MX-80 Na	1	1	1	2300	6.2		
CoA18	250	100	$CaCl_2$	MX-80 Na	1	1	1	19000	5.9		
CoA19	250	0	none	none	1	1	1	1.7	8.4		

Test material

Wyoming bentonite sold under the commercial name MX-80 was the source material for the three types of test materials which were used. It was delivered in a 25 kg sack by Askania AB and produced by Volclay LTD, Mersyside, UK.

According to an old characterisation (Müller-Vonmoos, 1983) the material is dominated by natural sodium montmorillonite clay (~ 75% by weight). The rest consists of quartz (~15%), feldspars (~7%), carbonates (~1.4%) sulphides (~0.3%), organic carbon (~0.4%). Dispersed in distilled water the clay fraction (d < 2 μm), make up around 80%. The mean mineralogical composition of the montmorillonite part is given by:

$(Al_{3.10}\,Fe^{3+}_{0.4}\,Fe^{2+}_{0.02}\,Mg_{0.48})$ $(Si_{7.92}\,Al_{0.08})$ $O_{20}\,(OH)_4$ $Na_{0.48}\,Ca_{0.04}\,Mg_{0.02}$

octahedral cations tetrahedral cations structural O/OH exchangeable cations

The cation exchange capacity is around 0.8 eq/kg bulk material and around 1.0 eq/kg clay in the minus 2μm fraction. The natural exchangeable cat-ions are sodium (~85%), calcium (~10%), magnesium (~4%) and small amounts of potassium (~0.3%). The

specific surface area is around 550 m^2/gram material and the grain density is around 2.75 g/cm^3.

In this study the bentonite material was used in its original state, and in cleaned and Na- and Ca-converted states, respectively. The latter two materials were produced in the following way. Ten grams of the original MX-80 material was dispersed in 1 liter of de-ionized water and the fraction coarser than $2*10^{-6}$m was settled as calculated by Stoke´s law and removed by decantation. NaCl or $CaCl_2$ was added to give a concentration of 3 M in the decanted dispersion, respectively. The dispersion was left to settle and the supernatant was removed and new de-ionized water was added. This procedure was repeated, and as the salt concentration was lowered the settlement was enhanced by centrifugation. The electrical conductivity of the supernatants were measured after each washing in order to ensure that only insignificant amounts of salt finally was left in the material. The material was thereafter dried at 105°C and the material was analyzed by ICP/AES (Table 2) and by XRD (Figure 1).

Table 2 Results from ICP/AES analyses of the bentonite materials. Figures in the first section indicate % and in the second section ppm.

Element	MX-80	MX-Na	MX-Ca
Al2O3	20.6	21.1	20.2
CaO	1.39	0.118	2.67
Fe2O3	3.93	3.88	3.79
K2O	0.572	0.216	0.306
S	0.301	0.0921	0.149
MgO	2.5	2.43	2.24
MnO2	0.0131	0.0041	0.0067
Na2O	2.32	2.76	0.217
P2O5	0.0589	0.0739	0.0468
SiO2	62.1	63.1	60.1
TiO2	0.172	0.164	0.157
LOI	6.1	6	6.5
Summa	100.1	99.9	96.4
Ba	326	72.2	144
Be	1.44	1.54	1.55
Co	<6	6.54	<5
Cr	274	<10	<10
Cu	<6	<5	11.3
La	57.9	65.2	61.3
Mo	<6	<5	<5
Nb	34.7	32.9	32.2
Ni	<10	<10	<10
S	3010	921	1490
Sc	5.8	6.54	6
Sn	<20	<20	<20

Sr	271	27.7	35.8
V	4.75	<2	<2
W	<60	<50	<50
Y	42.6	49.3	40.8
Zn	101	54.4	63.7
Zr	212	200	199

The chemical formula of the converted montmorillonite material was roughly calculated based on the ICP/AES analyses of the Na and Ca converted material, respectively. The Si, Al, Mg and Fe results were used to give a best fit to the ideal montmorillonite formula $Si_8\ Al_{(4-y)}\ Mg_y\ O_{20}\ (OH)_4 + Na_{(x+y)}$. Since silica obviously still is present in the form of quartz, according to the XRD analyses, the silica content was reduced in order to meet the expected cation exchange capacity of 1.0 eq/kg. In both cases the reduction was 6% units in ICP/AES analyses.

The calculated formula for the Ca material was $Si_{7.72}\ Al_{0.28}\ Al_{3.12}\ Mg_{0.48}\ Fe_{0.41}\ O_{20}\ (OH)_4\ Ca_{0.38}$ and the formula for the Na material was $Si_{7.74}\ Al_{0.26}\ Al_{3.11}\ Mg_{0.49}\ Fe_{0.40}\ O_{20}\ (OH)_4\ Na_{0.75}$.

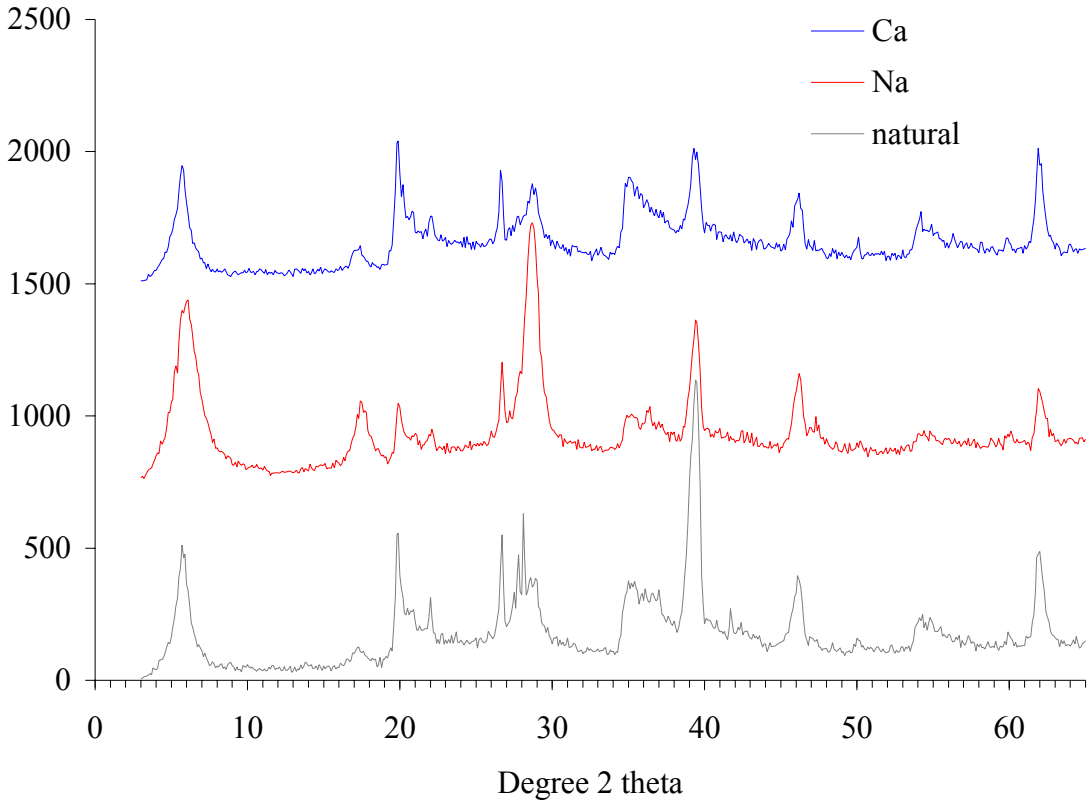

Figure 1 XRD analyses of the bentonite material used in the test series. Upper curve shows result from Ca converted material, middle curve from Na converted material and lower curve from the original MX-80 material. The main

difference is the loss of accessory minerals (mainly feldspars) in the treated material.

Analyses

The cylinders were photographed after defined time intervals during the sedimentation and the results are shown in Figures 13-16.

After 21 days of sedimentation the upper 30 ml of solution was removed and analyzed with respect to (Table 3-7):

- Electrical conductivity (Figure 2),
- pH (Figure 3),
- major cat-ions and some trace elements by ICP/AES (Figure 5-12),
- SO_4^{2-}, by IC,
- Colloid content (Figure 4).

In addition, pure test water was analyzed before and after 21 days of exposure to a test cylinder. Further, 2 water solutions from the production of Na-converted bentonite material were analyzed. These samples represent the finest part of the Na converted material since it was not removed from the dispersion despite the intensive centrifugation (4000 rpm for 30 minutes).

Table 3 Analyze results from the MX-80 test solutions.

Sample			**CoA01**	**CoA02**	**CoA03**	**CoA04**
planned	**clay**	**cation**	Na/Ca	Na/Ca	Na/Ca	Na/Ca
		mass,g	1	1	1	1
	solution	**cation**		Na	Na	Na
		anion		Cl	Cl	Cl
		C, M	low	0.001	0.010	0.100
		volume, ml	250	250	250	250
measured	ICP/EAS, mg/L	**Al**	92.7	47.0	2.245	0.028
		B	0.423	0.536	0.175	0.067
		Ba	0.054	0.053	0.025	0.178
		Ca	4.97	4.65	2.18	15.85
		Cd	0.002	0.002	0.000	0.000
		Co	0.000	0.000	0.001	0.001
		Cr	0.002	0.002	0.000	0.000
		Cu	0.000	0.001	0.001	0.001
		Fe	19.20	21.60	0.487	0.011
		K	1.340	1.470	1.957	3.426
		Li	0.027	0.030	0.014	0.016
		Mg	11.000	12.100	0.692	3.560
		Mn	0.030	0.028	0.001	0.009
		Mo	0.009	0.010	0.012	0.006
		Na	31.00	50.50	230.37	1715.00
		Ni	0.000	0.000	0.001	0.000
		P	0.125	0.127	0.169	0.017
		Pb	0.005	0.010	0.002	0.001
		S	7.680	4.530	5.31	5.99
		Si	243.0	128.0	9.772	1.921
		Sr	0.160	0.160	0.0711	0.5410
		Ti	0.52	0.56	0.014	0.000
		V	0.009	0.009	0.001	0.000
		Zn	0.467	0.039	0.002	0.006
	IC, mg/L	**Cl^-**	1.1	27.7	386.3	3609.6
		SO_4^{2-}	6.1	4.2		
		NO_3^-	0.1	<0.01		
		PO_4^{3-}	<0.02	<0.02		
	titration, (mM)	**[HCO_3^-]**	0.8	0.8	0.5	0.5
	TOC, mg/L	**C-inorg.**	7.8	7.6	7.0	6.0
		C-org	4.6	2.1	1.4	2.6
Sample	**mass/250 ml**	**mg tot**	231	167	352	2943
Sample	**mass/250 ml**	**mg MM Si**	202	107	8	2

Table 4 Analyze results from the MX-Na test solutions.

Sample			**CoA05**	**CoA06**	**CoA07**	**CoA08**
planned	**clay**	**cation**	Na	Na	Na	Na
		mass,g	1	1	1	1
	solution	**cation**		Na	Na	Na
		anion		Cl	Cl	Cl
		C, M	low	0.001	0.010	0.100
		volume, ml	250	250	250	250
measured	ICP/EAS	**Al**	292.0	233.0	188.0	0.041
		B	1.230	1.140	1.040	0.077
		Ba	0.018	0.017	0.018	0.016
		Ca	0.85	0.90	0.61	0.86
		Cd	0.006	0.005	0.004	0.000
		Co	0.001	0.000	0.000	0.001
		Cr	0.004	0.003	0.002	0.000
		Cu	0.011	0.009	0.008	0.001
		Fe	57.50	55.40	45.50	0.000
		K	0.535	0.664	0.576	1.500
		Li	0.066	0.064	0.063	0.006
		Mg	30.500	29.300	24.000	1.996
		Mn	0.059	0.055	0.047	0.001
		Mo	0.000	0.000	0.000	0.000
		Na	48.60	70.60	302.00	2120.00
		Ni	0.000	0.000	0.000	0.000
		P	0.115	0.083	0.093	0.069
		Pb	0.001	0.000	0.004	0.007
		S	0.960	1.330	0.628	0.91
		Si	760.0	610.0	500.0	4.348
		Sr	0.024	0.022	0.020	0.0210
		Ti	1.58	1.49	1.36	0.001
		V	0.019	0.018	0.015	0.000
		Zn	0.151	0.474	0.061	0.000
	IC	**Cl^-**	0.4	33.4	333.5	3710.9
		SO_4^{2-}	1.2	1.1	0.4	
		NO_3^-	0.0	<0.01	<0.01	
		PO_4^{3-}	0.1	<0.02	<0.02	
	titration, (mM)	**[HCO_3^-]**	0.3	0.3	0.2	0.2
	TOC	**C-inorg.**	4.1	3.8	2.4	2.0
	TOC	**C-org**	2.5	3.4	2.2	0.7
Sample	**mass/250 ml**	**mg tot**	657	571	768	3209
Sample	**mass/250 ml**	**mg MM Si**	633	508	416	4

Table 5 Analyze results from the MX-Ca test solutions.

Sample			**CoA09**	**CoA10**	**CoA11**	**CoA12**
planned	**clay**	**cation**	Ca	Ca	Ca	Ca
		mass,g	1	1	1	1
	solution	**cation**		Ca	Ca	Ca
		anion		Cl	Cl	Cl
		C, M	low	0.001	0.010	0.100
		volume, ml				
measured	ICP/EAS	**Al**	20.2	0.210	0.047	0.073
		B	0.481	0.223	0.172	0.197
		Ba	0.019	0.034	0.095	0.125
		Ca	8.17	35.17	361.35	5200.00
		Cd	0.001	0.000	0.000	0.000
		Co	0.001	0.000	0.001	0.003
		Cr	0.001	0.000	0.000	0.002
		Cu	0.001	0.001	0.001	0.000
		Fe	4.88	0.048	0.001	0.001
		K	0.464	0.439	0.468	0.708
		Li	0.008	0.004	0.007	0.011
		Mg	2.730	0.271	0.924	1.219
		Mn	0.009	0.000	0.000	0.001
		Mo	0.001	0.000	0.000	0.000
		Na	0.82	0.80	0.74	1.43
		Ni	0.000	0.000	0.000	0.009
		P	0.014	0.008	0.000	0.000
		Pb	0.008	0.000	0.000	0.000
		S	0.560	0.90	6.10	48.17
		Si	11.2	10.100	9.986	9.777
		Sr	0.007	0.0160	0.1016	0.7778
		Ti	0.15	0.001	0.000	0.000
		V	0.002	0.000	0.000	0.000
		Zn	0.018	0.007	0.015	0.022
	IC	**Cl^-**	0.2	75.0	687.6	6820.6
		SO_4^{2-}	0.4			
		NO_3^-	0.0			
		PO_4^{3-}	<0.02			
	titration, (mM)	**[HCO_3^-]**	0.4	0.2	0.1	0.1
	TOC	**C-inorg.**	3.1	2.0	2.0	1.0
	TOC	**C-org**	1.3	0.9	0.7	1.4
Sample	**mass/250 ml**	**mg tot**	28	68	587	6639
Sample	**mass/250 ml**	**mg MM Si**	9	8	8	8

Table 6 Analyze results from the MX-Na/Ca test solutions.

Sample			**CoA05**	**CoA16**	**CoA17**	**CoA18**
planned	**clay**	**cation**	Na	Na	Na	Na
		mass,g	1	1	1	1
	solution	**cation**		Ca	Ca	Ca
		anion		Cl	Cl	Cl
		C, M	low	0.001	0.01	0.1
		volume, ml				
measured	ICP/EAS	**Al**	292.0	198.0	0.1	0.0
		B	1.230	1.151	0.091	0.000
		Ba	0.018	0.041	0.025	0.038
		Ca	0.85	20.13	429.00	3525.00
		Cd	0.006	0.002	0.000	0.000
		Co	0.001	0.000	0.000	0.000
		Cr	0.004	0.000	0.000	0.000
		Cu	0.011	0.012	0.000	0.000
		Fe	57.50	48.15	0.00	0.00
		K	0.535	1.97	0.46	0.83
		Li	0.066	0.060	0.014	0.016
		Mg	30.500	27.51	2.61	2.91
		Mn	0.059	0.029	0.000	0.000
		Mo	0.000	0.000	0.000	0.000
		Na	48.60	56.03	84.54	90.50
		Ni	0.000	0.071	0.000	0.004
		P	0.115	0.241	0.043	0.032
		Pb	0.001	0.049	0.000	0.000
		S	0.960	1.04	5.84	78.50
		Si	760.0	425.9	5.9	6.0
		Sr	0.024	0.027	0.087	0.623
		Ti	1.58	1.337	0.000	0.000
		V	0.019	0.002	0.000	0.000
		Zn	0.151	0.060	0.001	0.008
	IC	**Cl^-**	0.4	68.42	610.09	4568.00
		SO_4^{2-}	1.2	0.85	0.84	0.74
		NO_3^-	0.0	0.00	0.07	0.05
		PO_4^{3-}	0.1	0.15	0.00	0.00
	titration, (mM)	**[HCO_3^-]**	0.3	0.30	0.30	0.00
	TOC	**C-inorg.**	4.1	2.7	1.7	1.7
	TOC	**C-org**	2.5	1.8	1.2	1.0
Sample	**mass/250 ml**	**mg tot**	657	468	626	4546
Sample	**mass/250 ml**	**mg MM Si**	633	355	5	5

Table 7 Analyze results from the final solutions from the preparation of the MX-Na material, and from test water before and after exposure to a test cylinder.

Sample			**CoA13**	**CoA14**	**CoA15**	**CoA19**
planned	**clay**	**cation**	Na	Na		
		mass, g				
	solution		undefined	undefined	test water start	test water final
		C, M	low	low	low	low
		volume, ml				
measured	ICP/EAS	**Al**	117.0	216.0	0.0	0.0
		B	0.560	0.943	0.017	0.010
		Ba	0.005	0.008	0.001	0.001
		Ca	0.23	0.41	0.00	0.11
		Cd	0.002	0.004	0.000	0.000
		Co	0.001	0.001	0.000	0.000
		Cr	0.001	0.003	0.000	0.000
		Cu	0.002	0.003	0.000	0.000
		Fe	23.80	42.20	0.04	0.00
		K	0.350	0.305	0.022	0.00
		Li	0.025	0.046	0.000	0.008
		Mg	13.000	23.200	0.075	0.01
		Mn	0.029	0.050	0.000	0.000
		Mo	0.002	0.000	0.000	0.000
		Na	48.80	61.00	0.01	0.06
		Ni	0.000	0.000	0.000	0.000
		P	0.106	0.131	0.000	0.000
		Pb	0.001	0.004	0.000	0.000
		S	0.756	0.648	0.008	0.00
		Si	289.0	500.0	0.6	1.1
		Sr	0.007	0.014	0.000	0.000
		Ti	0.57	1.04	0.00	0.000
		V	0.009	0.015	0.000	0.000
		Zn	0.034	0.060	0.000	0.000
	IC	**Cl^-**	29.6	28.3	<0.02	2.00
		SO_4^{2-}	0.8	0.9	<0.02	0.00
		NO_3^-	<0.01	<0.01	<0.01	0.06
		PO_4^{3-}	<0.02	<0.02	<0.02	0.00
	titration, (mM)	**[HCO_3^-]**	0.6	0.7	0.0	0.00
	TOC	**C-inorg.**	6.2	6.9	0.4	0.0
	TOC	**C-org**	1.8	3.8	1.6	2.5
Sample	**mass/250 ml**	**mg tot**	288	481	0	
Sample	**mass/250 ml**	**mg MM Si**	241	416	0	1

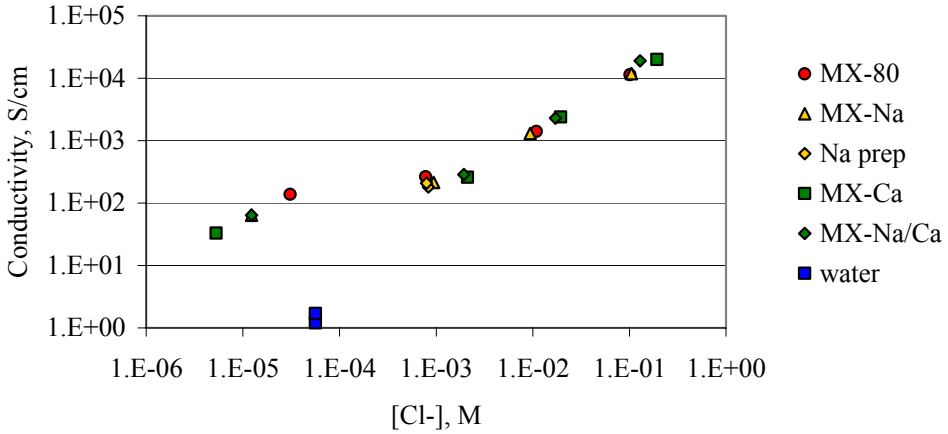

Figure 2 Electric conductivity of the analyses solutions/dispersions versus measured chloride concentration.

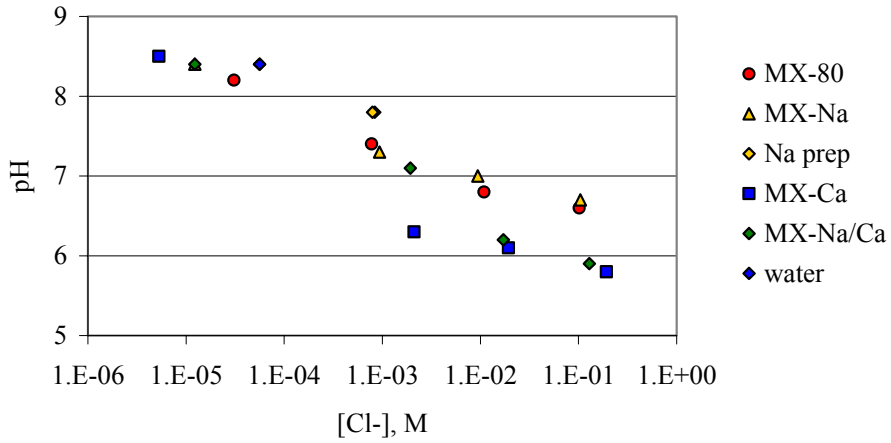

Figure 3 pH of the analyzed solutions/dispersions versus measured chloride concentration.

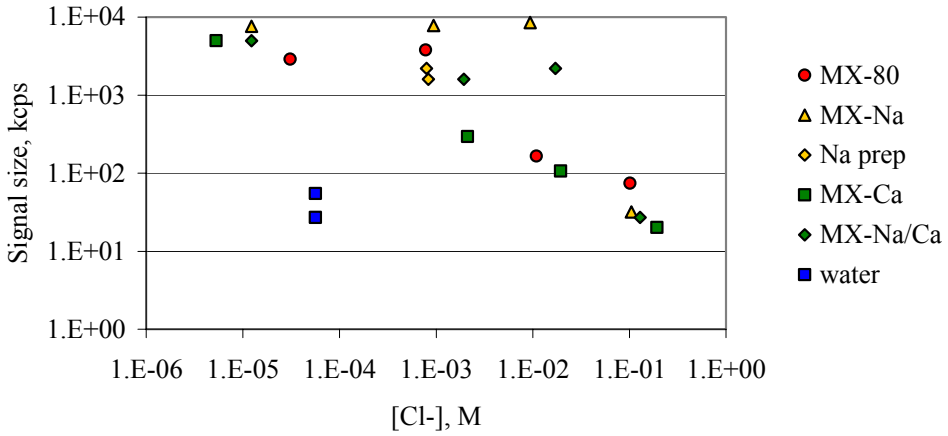

Figure 4 Signal size of the analyzed solution/dispersion versus chloride concentration.

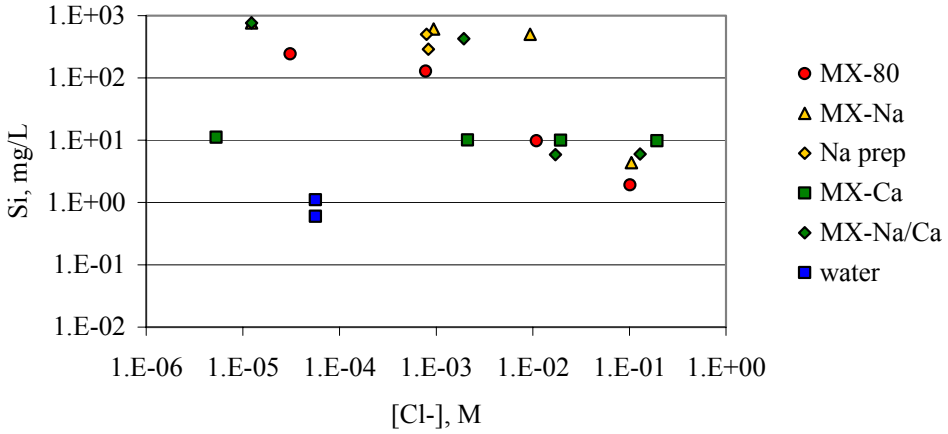

Figure 5 Si content in the analyzed solution/dispersion versus chloride concentration.

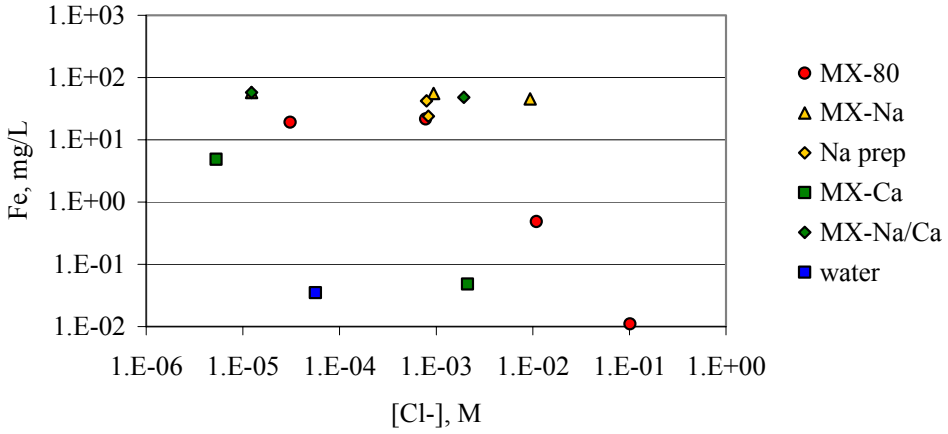

Figure 6 Fe content in the analyzed solution/dispersion versus chloride concentration.

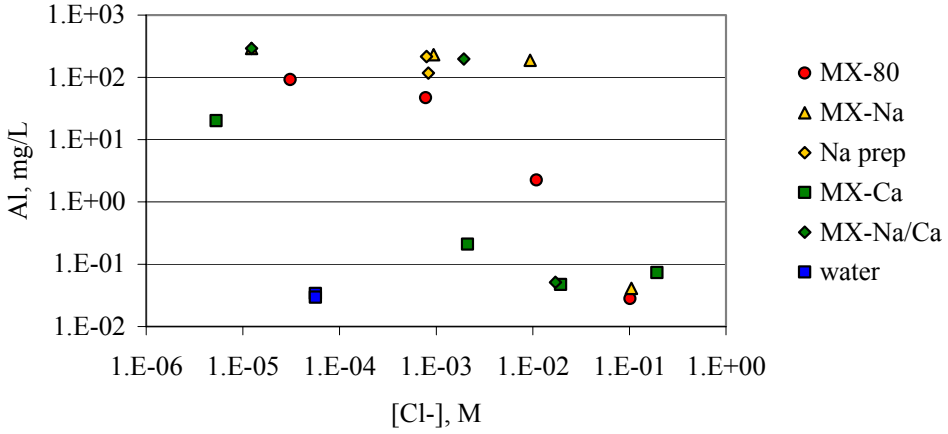

Figure 7 Al content in the analyzed solution/dispersion versus chloride concentration.

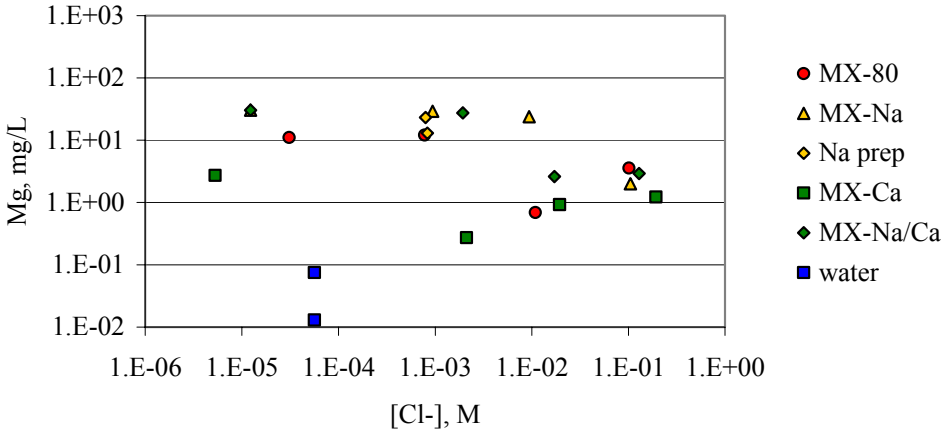

Figure 8 Mg content in the analyzed solution/dispersion versus chloride concentration.

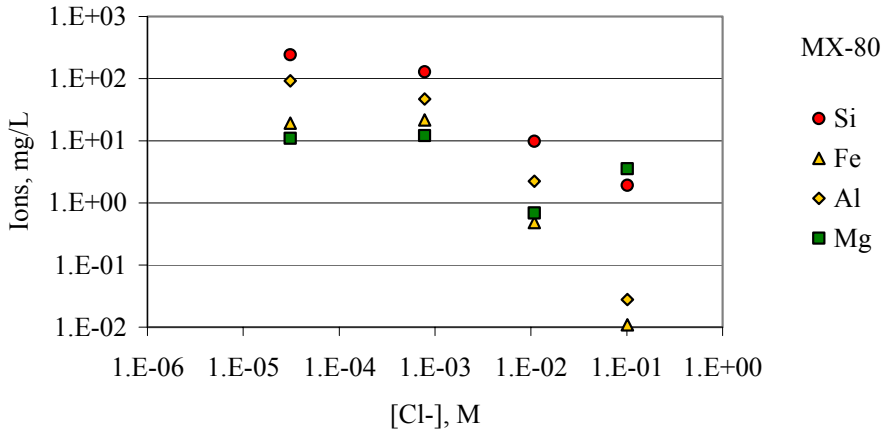

Figure 9 Si, Fe, Al and Mg content in the MX-80 sample/NaCl solutions versus chloride concentration.

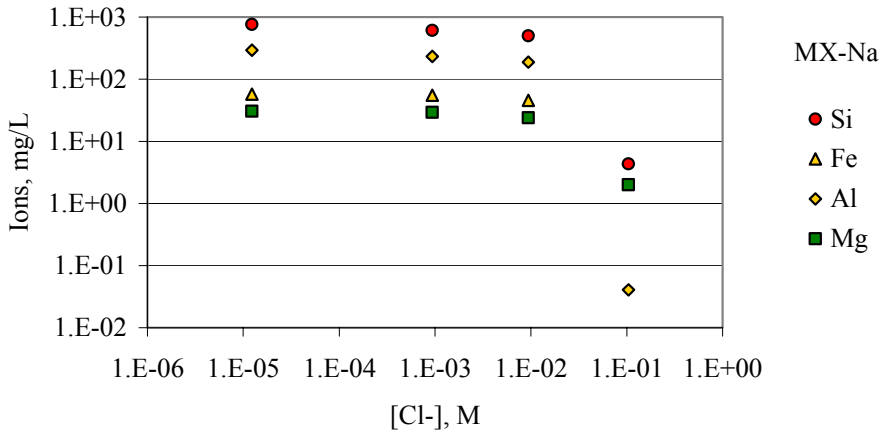

Figure 10 Si, Fe, Al and Mg content in the MX-Na sample/NaCl solutions versus chloride concentration.

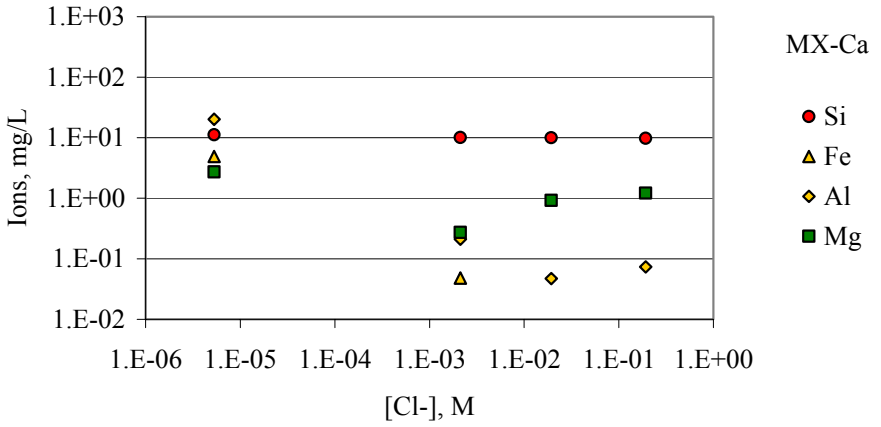

Figure 11 Si, Fe, Al and Mg content in the MX-Ca sample/$CaCl_2$ solutions versus chloride concentration.

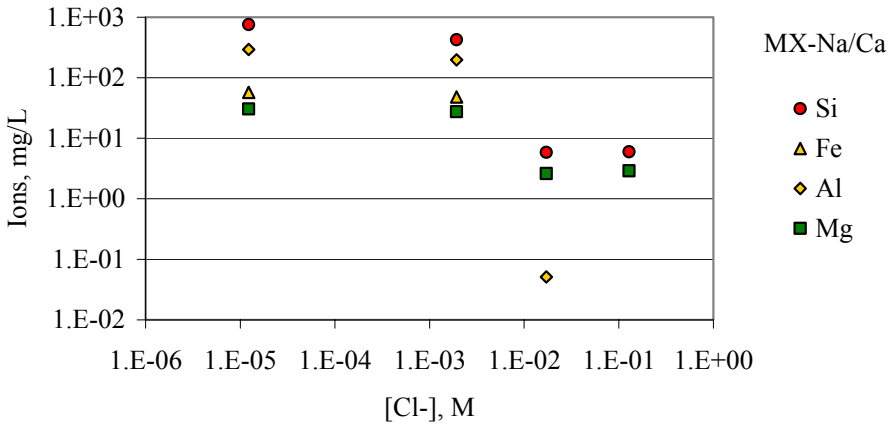

Figure 12 Ion concentrations in the MX-Na sample/$CaCl_2$ solutions versus chloride concentration.

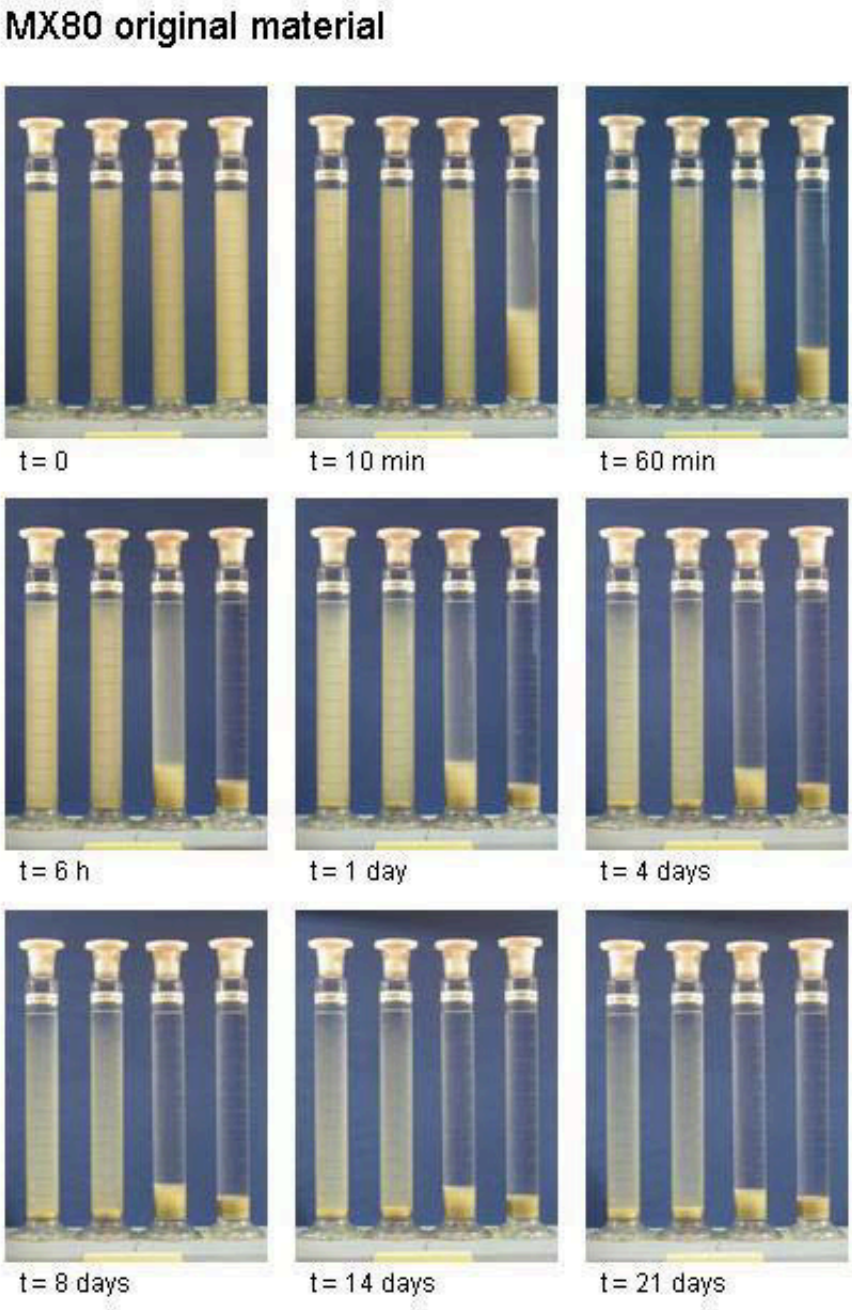

Figure 13 Photographs of the MX-80 material in 250 ml water solutions after different sedimentation periods. From left to right in each picture, NaCl was added in order to give a concentration of: 0.000 M, 0.001 M, 0.01 M and 0.1 M.

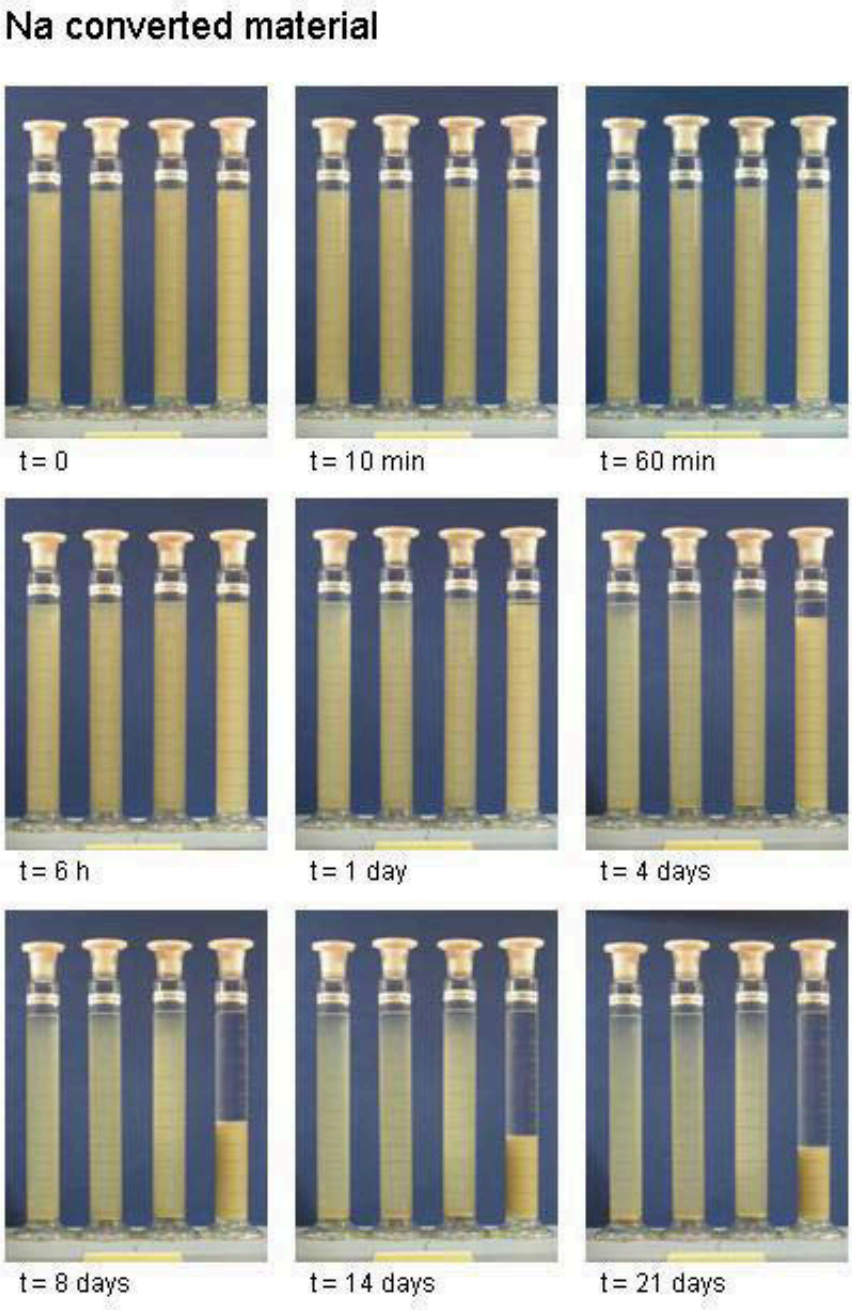

Figure 14 Photographs of the MX-Na material in 250 ml water solutions after different sedimentation periods. From left to right in each picture, NaCl was added in order to give a concentration of: 0.000 M, 0.001 M, 0.01 M and 0.1 M.

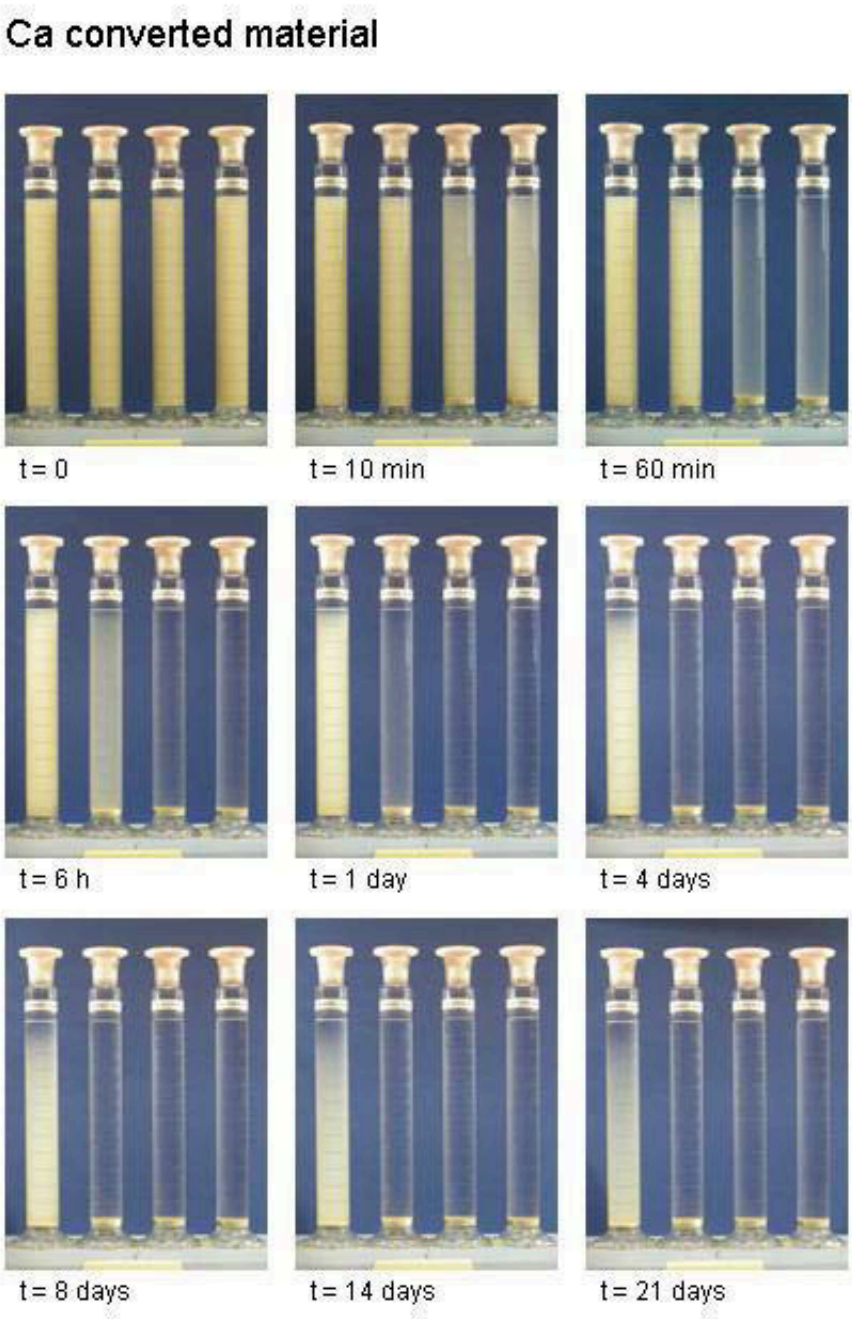

Figure 15 Photographs of the MX-Ca material in 250 ml water solutions after different sedimentation periods. From left to right in each picture, NaCl was added in order to give a concentration of: 0.000 M, 0.001 M, 0.01 M and 0.1 M.

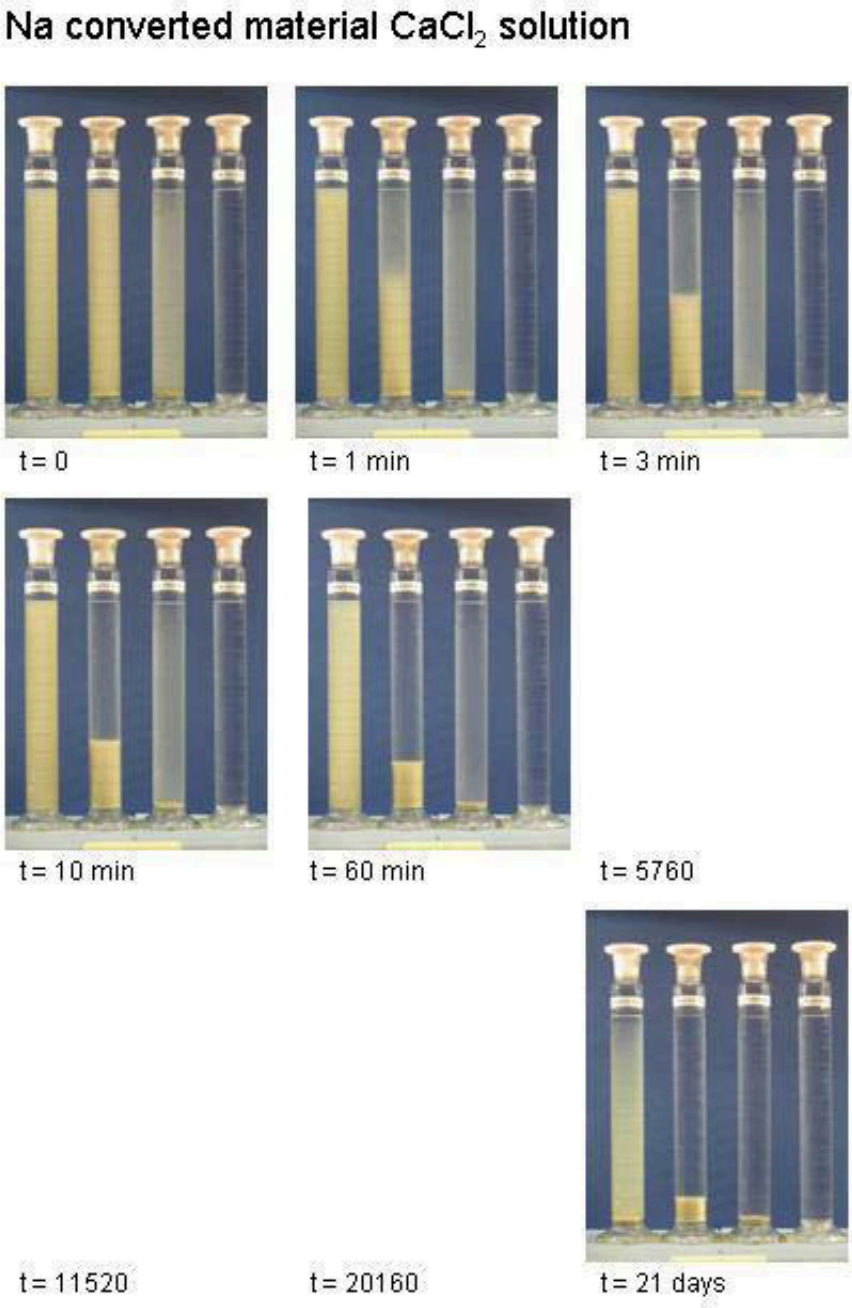

Figure 16 Photographs of the MX-Na material in 250 ml water solutions after different sedimentation periods. From left to right in each picture, $CaCl_2$ was added in order to give a concentration of: 0.001 M, 0.01 M, 0.1 M. The rightmost cylinder only contains water and no bentonite material.

Discussion

According to double layer theory it is possible to roughly estimate the separation between the montmorillonite flakes at different salt concentrations and type of ions by use of:

$$\kappa = \sqrt{\frac{2Z^2F^2C_0}{\varepsilon_0\varepsilon_r RT}} \qquad \text{(eq. 1)}$$

where κ generally is called the Debye-Hückel parameter and

Z	= charge of the cations
F	= Faradays constant
C_0	= electrolyte concentration
ε_0	= permittivity of vacuum
ε_r	= relative permittivity of the solvent
R	= gas constant
T	= temperature

The thickness of the diffuse layer is 1/κ and for the actual montmorillonite in sodium state the calculated basal spacings are shown in Figure 17.

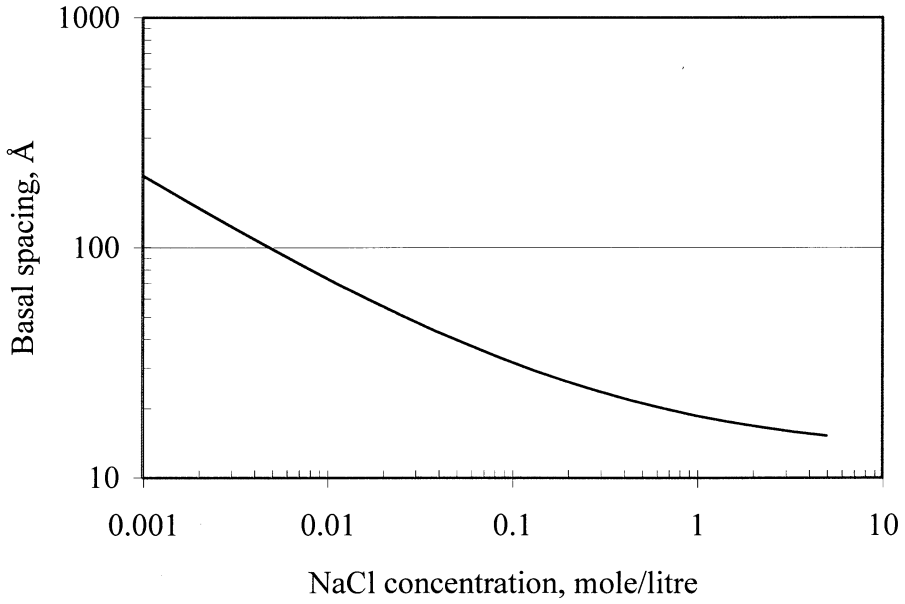

Figure 17 Basal spacing in bentonite calculated from the Debey-Hückel parameter according to eq.1.

Figure 18 shows experimental results from Norrish (1954), which is in fair agreement with the results calculated by use of the Debye-Hückel parameter.

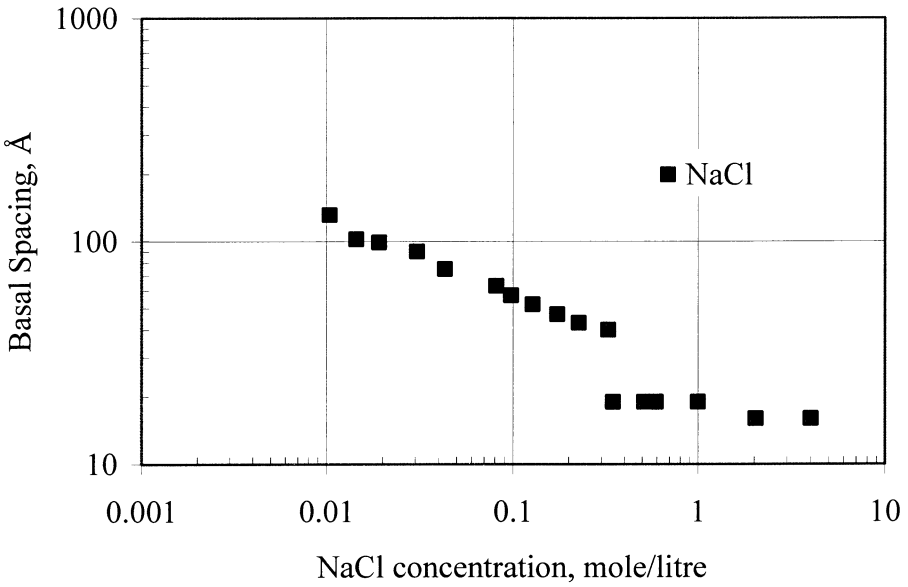

Figure 18 Norrish experimental data.

E.g. The distance between the montmorillonite flakes is calculated to be around 200 Å in the lowest examined NaCl concentration (0.001 M). The sample containing 1 g of clay is then expected to have a volume of approximately 7 cm^3. In Figure 14 it is obvious that the volume of the expanded clay has a larger volume also in the test with the highest salt concentration (0.1 M). However, in all samples there is a clear tendency of clay volume decrease with time, and the calculated values likely represent a final equilibrium stage.

The dramatic effect of Ca-ions compared with Na-ions is in agreement with the Schultze-Hardy rule for lyophobic sols which are stabilized only by double-layer interaction. The critical coagulation concentration is largely dependent on the valence of the clay counter-ions but practically independent of the specific character of the various ions and of the charge and type of the co-ions. Typical critical coagulation concentrations for monovalent ions are 100 mM, for divalent ions 1 mM, and for trivalent 0.1 mM.

Ion chromatography (IC) analysis of test solution is not possible to perform without pre-filtration, due to practical reasons, and the results are thereby only representative for dissolved substances. However, the ICP-AES technique admits analyses of untreated solutions including colloids. The present analyses show typical montmorillonite ratios between Si, Al, Fe and Mg in the tests where colloids are present according to laser measurement (Figure 9 – 12). The analyses give typical montmorillonite "fingerprints" which may be used for qualitative information of the colloids, and to some extent also for quantification (Figure 9 and 10), at least at relatively high content of colloids.

Conclusions

The results from the settlement tests may be summarized in the following way:

- The colloid stability is strongly affected by the salt concentration in the test solutions; the critical concentration for a relatively fast coagulation in the sodium case is between 10 and 100 mM.
- Divalent ions have a much more pronounced effect on the stability compared to monovalent ions; the critical concentration for a relatively fast coagulation in the calcium case is around 1 mM.
- Concentration lower than critical coagulation concentrations do not stop sedimentation but makes it much slower.
- The bentonite material seems in principle to follow the Shultze-Hardy rule.

The results do in principle confirm previous laboratory tests (Le Bell, 1978).

Further, the ICP/AES analyses of test solutions show that the results are typical for the clay mineral and can be used for identification and to some extent also for quantification of colloids in the water.

References

Müller-Vonmoos M., Kahr G., 1983. Mineralogiche Untersuchungen von Wyoming Bentonit MX-80 und Montigel. NTB 83-12, Baden.

Le Bell J.C., 1978. Colloid chemical apects of the “confined bentonite concept”. KBS Teknisk Rapport 97, Stockholm 1978.

Norrish K., 1954. The swelling of montmorillonite. Trans. Faraday Soc. 18, 120-134.

Appendix 2

Formation of inorganic colloids in solutions in contact with bentonite – Effects of type of bentonite, temperature, pH and ionic strength in solution

Susanna Wold and Trygve Eriksen
Royal Institute of Technology
Department of Chemistry / Division of Nuclear Chemistry

1 Background

Complexation of radionuclides by colloids may change the mobility of radionuclides in natural systems. Colloids are small particles between 1 and 1000 nm and are due to the Brownian motion kept in solution. Groundwater contains clay- and humic/fulvic colloids, which are negatively charged at neutral pH, and have high affinity for positively charged metal ions. Colloids can be brought into the bentonite barrier in a repository for spent nuclear fuel by the groundwater. Another possibility is formation of stable colloids by the bentonite which may migrate away from the bentonite into the water environment.
The colloid formation in solutions in contact with bentonite and the influence of background electrolyte concentration, type and amount of bentonite and temperature on colloid formation has been studied.

2 Experimental

Two types of bentonite were used in the experiments.

1. MX-80. Clay content of 85 % and montmorillonite 80-90 wt % of this fraction. Remaining silt fraction contains quartz, feldspar and some micas, sulfides and oxides.
2. Na-bentonite. Prepared from MX-80 with removal of the accessory minerals (Wieland et al. 1994).

Sodium perchlorate solutions 0.01, 0.1 and 1 M were used in the experiments. All solutions were prepared from analytical grade chemicals an millipore deionized, triple distilled water.

Experimental setup

Graduated glass cylinders of 250 ml with a diameter of 5 cm with glass lids were used throughout the experiments. Different amounts of bentonite were poured into the solutions of varying ionic strength using two techniques.

1. Dry bentonite was poured into the solutions so that particles could sedimentate separately. The suspensions were left standing for one day where after the suspensions were shaken. This bentonite is referred to as dry bentonite.
2. Dry bentonite was poured into graduated cylinders and was wetted by solution and left for moistening for 5 minutes whereafter the solutions were poured into the cylinders. This bentonite is referred to as wet bentonite.

The cylinders were placed in a thermostat box for one week set to 20 °C and 60°C. The precision of temperature is ± 0.2 °C. pH and conductivity were measured once a day in the solutions.
An u-formed syringe was used for sampling to avoid disturbance of the bentonite.

PCS – Dynamic light scattering

The signal in the PCS is roughly proportional to the concentration of colloids. To enable measurements of particle concentration as well as particle size distributions, the PCS equipment was calibrated with solutions containing latex colloids with defined size distributions.
The colloidal size distribution and colloidal concentration was measured at the wavelength 488 nm with a dynamic light scattering instrument 90 Plus Particle Size Analyzer equipped with a 2 W Lexus Laser Model 95 Ion Laser. The data were evaluated with Brookhaven size particle software.

ICP-MS and ICP-AES analysis

To follow the chemistry in the water in contact with the bentonite, 20 ml water samples were acidified with 0.5 ml 65 % suprapure HNO_3 in acid washed vessels and sent to SGAB commercial laboratory for ICP-MS, ICP-AES analysis. The ICP analysis provides the concentration of a wide range of metals. Montmorillonite is assumed to be the potential provider of colloids even if the assessory minerals also can contribute. Al, Si are markers for the dissolution of montmorillonite into the bulk-water. There is, however a relation between Al concentration and colloid concentration, which is not valid for Si, since SiO_2 is more soluble (Degueldre et al.1996).

3 Results and discussion

Purified Na bentonite and bentonite acts very different to the commercial, the results will therefor treated separately.

Very low concentrations, ≤ 0.5 mg/l colloids are found in solutions of 0.1 and 1 M $NaClO_4$ independently how the bentonite is initially introduced to the solutions or amount of bentonite added. The mean size of the colloids is in the range of 50 to 500 nm. At 60 °C the colloid concentration is slightly higher than at 20 °C, but the tendency is otherwise the same.

The aluminum- and the colloid concentration follow each other, why it seems reasonable to use Al as a marker for colloids. The Al is generally higher but in the same size magnitude as the colloid concentration. Filtration of the samples to separate the colloids from the solved metals are recommendable, but the volumes in these experiments are too low to enable collection of detectable concentrations of colloids. Ocular it can be seen that the bentonite is expanded in low but not in high background electrolyte concentration. The osmotic pressure is high when Na^+ concentration is low in the water. When the gel structure is loose colloids can form and migrate away from the bentonite.

At both temperatures, 20°C and 60°C the colloid concentrations are lowest in pH 7.8 to 8.4 with increasing concentration in both lower and higher pH. Huertas et al (2001) has shown that the dissolution of montorillonite in granitic solutions depends strongly on pH with a minimum around pH 8-8.5. The dissolved ions from bentonite should be separated from the colloids, but our results indicate that the colloid concentration is related to the dissolution of bentonite. At low ionic strength of Na^+ the osmotic pressure is high and the gel structure in the clay is very loose and colloids can form and migrate out in the water bulk. It is very different whether the metal ion in the electrolyte is Na^+ or Ca^{2+}, this is however not studied here.

Colloid stability depends on ionic strength of solution. High ionic strength favors aggregation and flocculation (Luckham and Rossi 1999), therefor colloids will with time sedimentate out from the solution.

At high ionic strength very low colloid concentration is found as the low osmotic pressure in the montmorillonite minimizes the probability of formation of colloids. If colloids form aggregation/flocculation will form larger units of the colloids which will sedimentate.

The Na bentonite expanded very much in the experiments with background electrolyte concentrations of 0.01 and 0.1 M. Almost no clear water zone was found. The water contained high Al concentrations compared to the parallel experiments with bentonite. The colloid

concentrations were also higher than in the bentonite cases. In the Na bentonite experiments the osmotic pressure is high. Also there are no ions with higher charge like Ca^{2+} and Mg^{2+} which can compress the montmorillonite sheets. The texture is very loose, and ions and colloids can migrate out in the water.

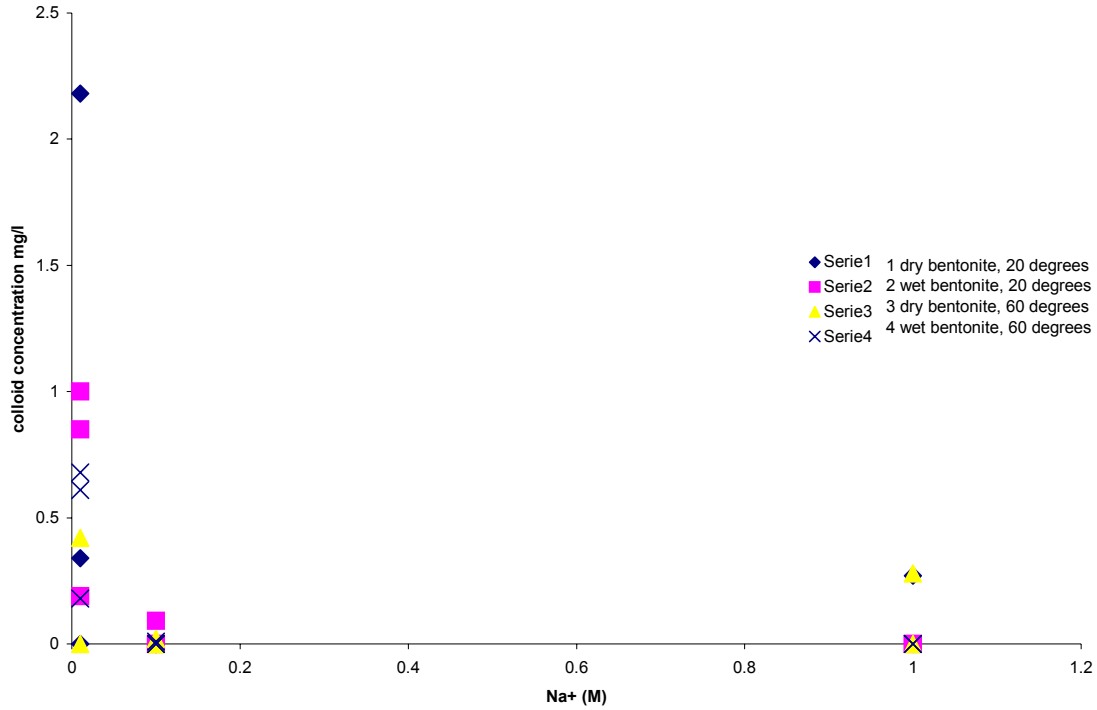

Figure 1. Colloid concentration as a function of Na^+ concentration in supporting electrolyte. The data set includes both experiments with MX-80 and Na-bentonite. The highest value origins from a Na-bentonite experiment.

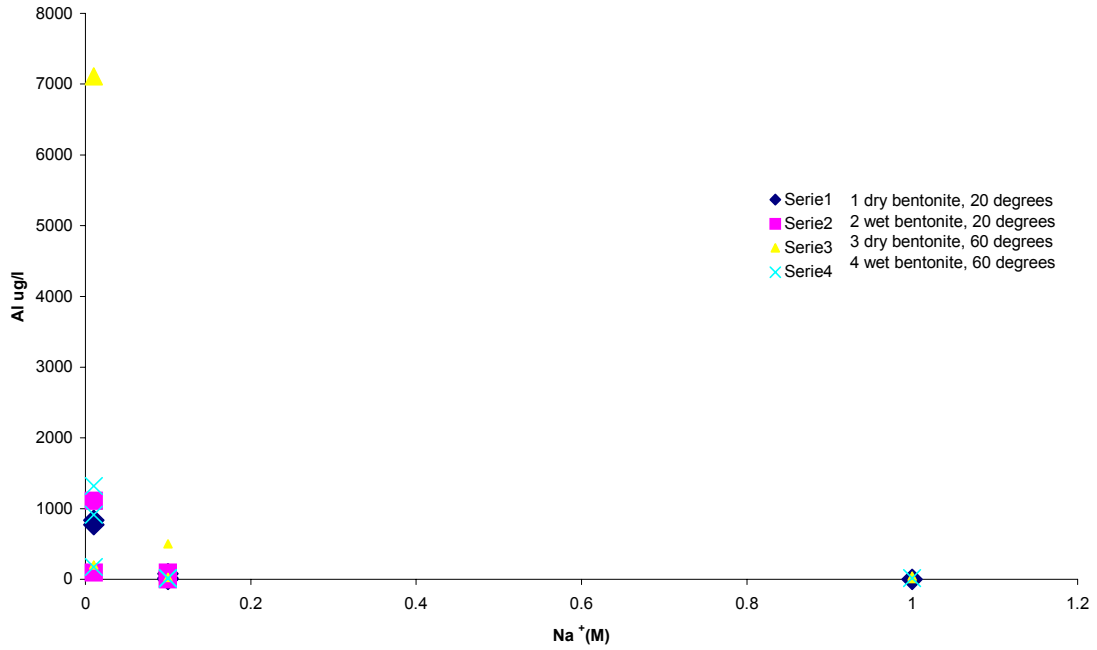

Figure 2. Aluminium concentration as a function of Na^+ concentration in supporting electrolyte. The data set includes both experiments with MX-80 and Na-bentonite. The highest value origins from a Na-bentonite experiment.

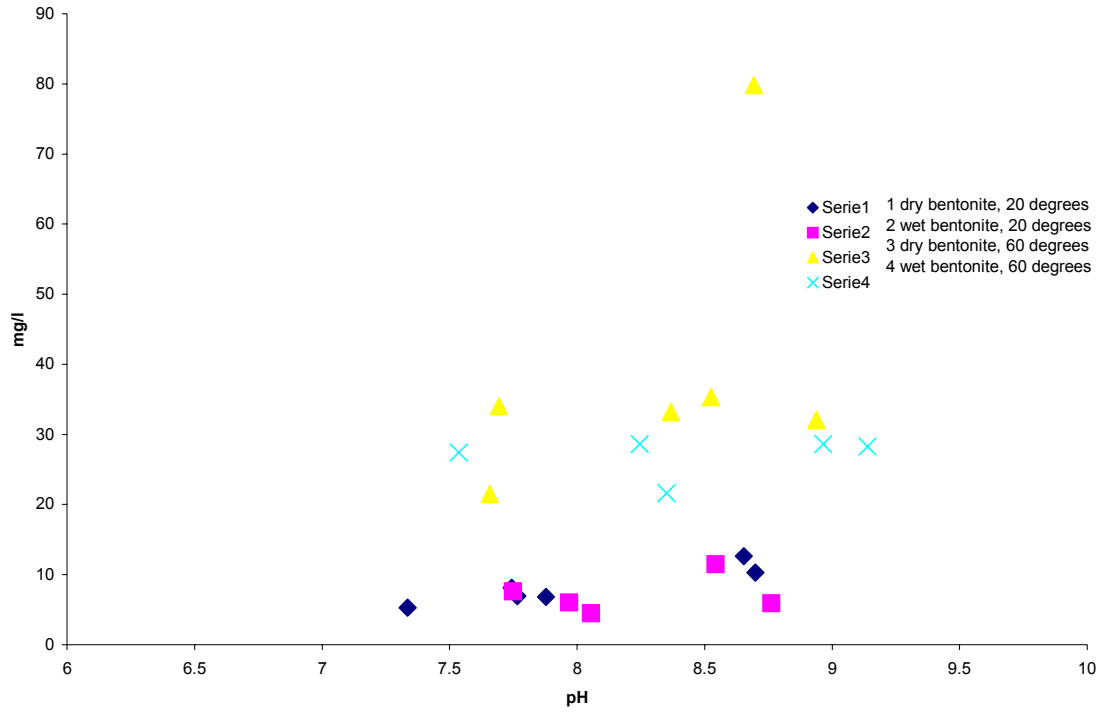

Figure 3. Silica and Aluminum concentration as a function of pH. The data set includes both experiments with MX-80 and Na-bentonite. The highest value origins from a Na-bentonite experiment.

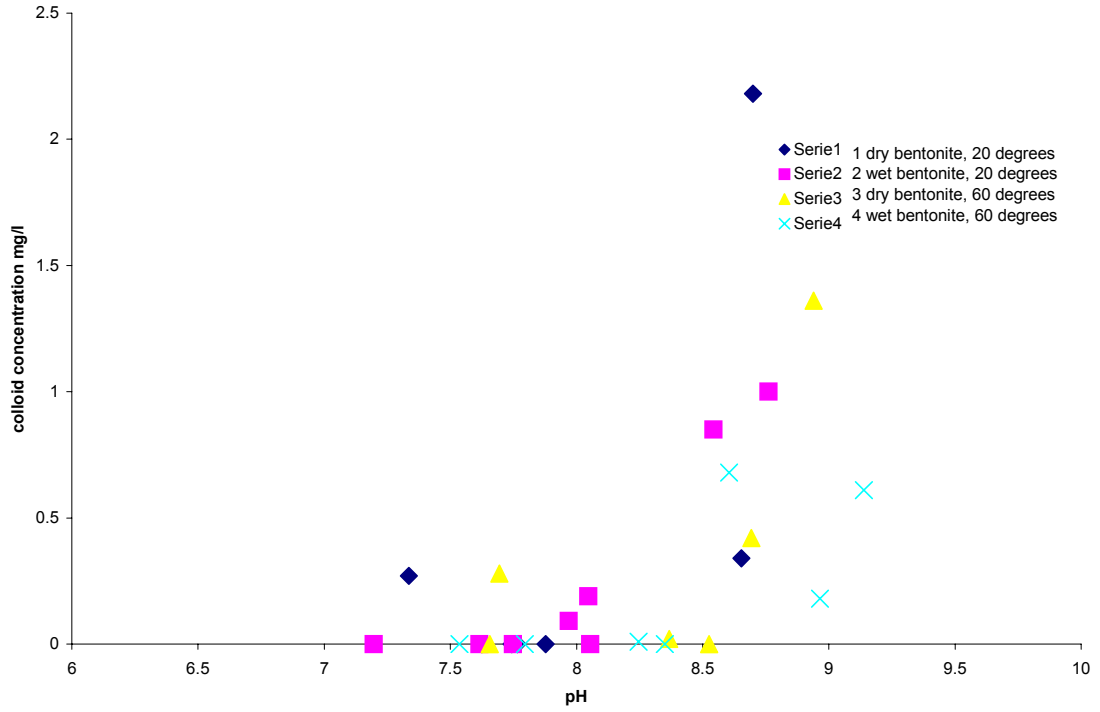

Figure .4 Colloid concentration as a function of pH. The data set includes both experiments with MX-80 and Na-bentonite. The highest value origins from a Na-bentonite experiment.

Table 1. Overview of analytical data

sample	volume ml	clay	type	grams	ion strength (M)	C	pH	delta cond	konc mg/l* laser	Ca mg/l <0,5	Fe mg/l <0,02	K mg/l <2	Mg mg/l <0,5	Mg+Ca mg/l	Na mg/l 259	Si mg/l 0.564	Al µg/l 14.9	Si + Al mg/l	Al mg/l 0.0149	Mn µg/l <2
1	250	MX-80	d	5.0125	0.01	20	8.699	0.061216905	2.18	2.96	0.251	6.06	0.574	3.534	293	9.51	771	10.281	0.771	1.2
10	250	MX-80	d	10	0.01	20	8.654	0.072148495	0.34	3.68	0.273	4.62	0.732	4.412	343	11.8	833	12.633	0.833	1.3
4	250	MX-80	d	5.1296	0.1	20	7.878	0.218631802	0	37.1	<0,004	12.9	5.15	42.25	2170	6.82	1.54	6.82154	0.00154	58.6
11	250	MX-80	d	10	0.1	20	7.765	0.109315901	0	42.9	0.0153	13.5	5.44	48.34	2100	6.93	14.2	6.9442	0.0142	101
12	250	MX-80	d	10	1	20	7.335	0.218631802	0.27	153	0.0478	30.7	21.5	174.5	22400	5.27	<4	5.27	0	107
16	100	Na	d	2	0.01	20		no sedimentation	-	-	-	-	-	-	-	-	-	-	-	-
5	250	MX-80	d	5.0632	1	20	7.625	0.11	0.00	-	-	-	-	-	-	-	-	-	-	-
17	100	Na	d	2	0.1	20	7.743	0.109315901	0	2.12	0.0278	2.63	3.3	5.42	1950	8.04	77.7	8.1177	0.0777	6.94
2	250	MX-80	w	5.0689	0.01	20	8.761	0.050285315	1	2.34	0.0347	6.63	0.352	2.692	282	5.81	95	5.905	0.095	0.535
3	250	MX-80	w	5.0273	0.1	20	8.054	0.174905442	0	27.1	<0,004	9.55	3.88	30.98	2200	4.49	7.25	4.49725	0.00725	45.6
6	250	MX-80	w	5.0274	1	20	7.615	0	0.00	-	-	-	-	-	-	-	-	-	-	-
7	250	MX-80	w	10.0427	0.01	20	8.046	0.11	0.19	-	-	-	-	-	-	-	-	-	-	-
9	250	MX-80	w	10.0134	1	20	7.196	0.22	0.00	-	-	-	-	-	-	-	-	-	-	-
8	250	MX-80	w	10.0565	0.1	20	7.969	0.174905442	0.092	30.2	<0,004	14.1	4.6	34.8	2150	6.04	2	6.042	0.002	84.3
13	100	Na	w	2	0.01	20	8.543	0.03279477	0.85	0.161	0.333	0.608	0.445	0.606	243	10.4	1110	11.51	1.11	3.31
14	100	Na	w	2	0.1	20	7.748	0.109315901	0	1.96	0.0304	3.05	3.09	5.05	2010	7.53	97.5	7.6275	0.0975	8.54
28	250	MX-80	d	5.0152	0.01	60	8.939	1.880164577	1.36	3.03	0.0798	5.15	0.483	3.513	364	31.9	205	32.105	0.205	1.2
34	250	MX-80	d	10.0467	0.01	60	8.693	0.659781931	0.42	40.5	5.45	11.5	12.6	53.1	690	72.7	7110	79.81	7.11	80.5
29	250	MX-80	d	5.1344	0.1	60	8.367	0.136760797	0.02	44.7	0.013	12.2	4.37	49.07	2560	33.2	29	33.229	0.029	83.4
35	250	MX-80	d	10.1375	0.1	60	8.525	0.010825512	0	47	0.233	17.9	4.79	51.79	2160	34.8	501	35.301	0.501	156
30	250	MX-80	d	5.0191	1	60	7.694	0.475596449	0.28	115	<0,02	25.6	11.1	126.1	25100	34	43.6	34.0436	0.0436	87.5
23	100	Na	d	1.632	0.1	60		no sedimentation	-	-	-	-	-	-	-	-	-	-	-	-
22	100	Na	d	2.0494	0.01	60		no sedimentation	-	-	-	-	-	-	-	-	-	-	-	-
36	250	MX-80	d	10.0176	1	60	7.657	1.97	0	191	<0,02	35.4	26.8	217.8	23500	21.5	8.72	21.50872	0.00872	154
20	100	Na	w	2	0.1	60		no sedimentation	-	-	-	-	-	-	-	-	-	-	-	-
25	250	MX-80	w	5.0077	0.01	60	8.965	1.13	0.18	3.34	0.226	5.07	0.574	3.914	347	27.7	915	28.615	0.915	0.871
31	250	MX-80	w	5.0551	0.01	60	9.139	0.898525696	0.61	4.21	0.0764	5.32	0.63	4.84	468	28.1	172	28.272	0.172	1.33
26	250	MX-80	w	5.0066	0.1	60	8.35	0.787074488	0	23.3	0.0069	8.83	3.38	26.68	1980	21.6	17.9	21.6179	0.0179	62.8
32	250	MX-80	w	5.0263	0.1	60	8.245	0.116660377	0.01	42	0.0047	11.9	4.86	46.86	2520	28.6	10.5	28.6105	0.0105	73
33	250	MX-80	w	5.0744	1	60	7.536	0.085484215	0	105	<0,02	27.1	10.9	115.9	27600	27.4	14.5	27.4145	0.0145	81.5
19	100	Na	w	2.034	0.01	60	8.604	0.104943265	0.68	0.454	0.417	0.744	0.644	1.098	301	13.8	1320	15.12	1.32	3.9
27	259	MX-80	w	5.0136	1	60	7.795	2.40445	0											

* Detectionlimit of colloid concentration is 0.6 mg/l why all values below the detectionlimit should be seen as < 0.6 mg/l.

References

Degueldre C, Pfeiffer H.-R, Alexander B, Wernli B and Bruetsch R. (1996) Colloid properties in granitic groundwater in granitic groundwater systems. I: Sampling and characterisation. Applied Geochemistry, 11 (677-695).

Luckham P and Rossi S. (1999) The colloidal and rheological properties of bentonite suspensions. Advances in Colloid and Interface Science, 82 (43-92).

Wieland E, Wanner H, Albinsson Y, Wersin P and Karnland O. (1994) A surface chemical of the bentonite/water interface and its implication for modelling the near field chemistry in a repository for spent fuel. SKB Technical Report 94-26.

Appendix 3

In-situ Colloid Detection in Granite Groundwater along the Äspö Hard Rock Laboratory Access Tunnel

Wolfgang Hauser, Robert Götz, Horst Geckeis,
Bernhard Kienzler
Institut für Nukleare Entsorgung (INE)
Forschungszentrum Karlsruhe GmbH
Postfach 3640
D-76021 Karlsruhe
Germany

1. Motivation

In safety assessment for a repository of radioactive waste, aquatic colloids existing in natural water play a role as carrier for the migration of radionuclides, mainly actinide ions from the waste to the biosphere [1, 2, 3, 4, 5]. Apart from actinide oxide/hydroxide colloids, colloids released from backfill bentonite and background colloids present in natural groundwater are of particular importance. In this study the amount of background colloids in natural groundwater in the Swedish Hard Rock Laboratory (HRL) granite formation is determined. The aim is to investigate the colloid occurance in different groundwater types without any interferences by sampling.

The average size of colloids in natural water ranges from less than 50 nm up to a few hundred nm with particle concentrations from ppt (ng/l) to a few hundred ppb (µg/l) [1, 2]. With conventional light scattering techniques, aquatic colloids of dilute concentrations are often not detectable [6, 7, 8, 9]. The Laser-Induced Breakdown Detection (LIBD) has been developed for the ultra-trace detection of colloids. The advantage of this method is a several orders of magnitude higher sensitivity particularly for colloids with a size < 100 nm [10, 11, 12, 13].

A mobile LIBD setup built for in-situ measurements [14], equipped with a new high-pressure detection cell is used for the background colloid detection in natural groundwater along the access tunnel of the granite Hard Rock Laboratory Äspö, situated at Oskarshamn / Sweden. The investigations are performed within the scope of an international collaboration between the German ‘ Institut für Nukleare Entsorgung (INE)’ of the ‘ Forschungszentrum Karlsruhe’ and the Swedish ‘ Svensk Kärnbränslehantering AB (SKB)’ in the frame of the SKB project COLLOID [15].

2. Experimental

LIBD instrumentation

The principle of LIBD is based on the generation of a dielectric breakdown in the focus region of a pulsed laser beam [9, 10, 11, 12, 13, 16, 17]. As the threshold energy (irradiance) to incite breakdown for solids is lower than for liquids or gas, the breakdown can be generated selectively on particles dispersed in solution at suitable pulse energy [11]. A schematic diagram of the mobile LIBD set-up used in the present work is shown Fig. 1. A pulsed laser beam with a frequency of 15 Hz at 532 nm wavelength from a small Nd:YAG-laser (Co ntinuum Minilite I) is focused (15 mm focal length) into the center of a flow-through detection cell, after passing through a variable attenuator and a beam splitter. The plasma generated at a

breakdown event is monitored by a microscope equipped with a CCD monochrome camera triggered by the incident laser pulse and recorded by a PC controlled image processing system. A breakdown shock wave propagated in the sample solution is detected simultaneously by an acoustic sensor (piezoelectric transducer) [18] that is connected to the surface of the cell. Both, the energy and the acoustic signal are recorded by an analog-digital converter interface in a PC. The mobile instrumentation of LIBD is combined with a Millipore ultra-pure water processing unit for on-line cleaning the flow-through detection cell of LIBD. The whole system, which is set up to a compact mobile unit is transported by a van for the field experiment.

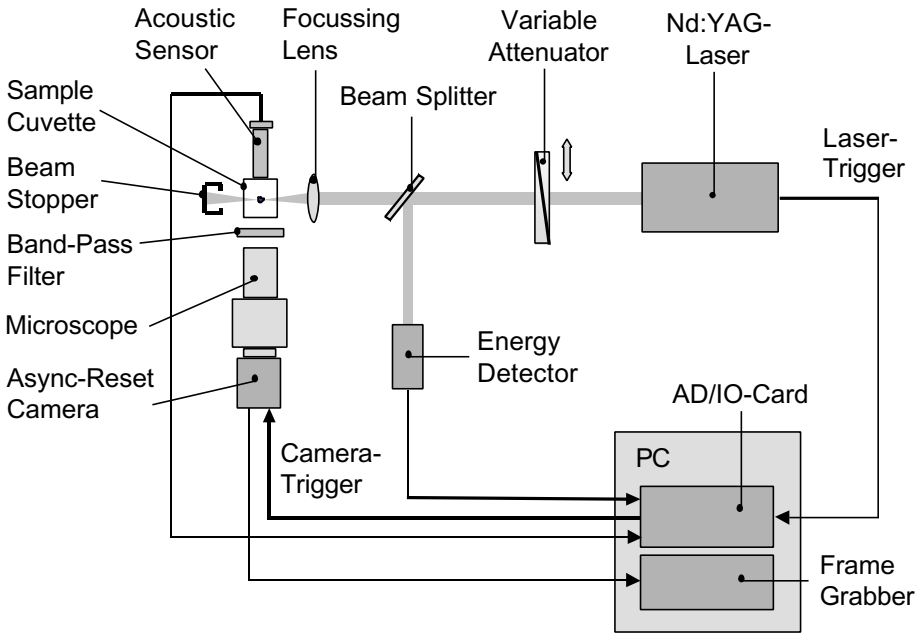

Fig. 1: Schematic diagram of the mobile laser-induced breakdown detection system

High-pressure flow-through detection cell

The LIBD has been operated up to now under low pressure conditions with commercially available quartz detection cells (fluorescence cells) for batch or flow-through sampling. These cells have a sample volume of 3 ml at 10 mm absorption length. A new flow-through detection cell had to be developed constraining a water pressure of 32 bar for the investigations in the Äspö tunnel, down to a depth of about –420 m. Fig. 2 presents the new high-pressure detection cell developed by INE. Without changing the optical path of the laser light, the detection cell fits into the same mount used for the silica cell. The new cell, fabricated from PEEK (polyether etherketone) is lined outside with a stainless steel housing

(black parts in Fig. 2). Four optical windows, one at each side are applied for the passing laser light (absorption length 12 mm), the microscope and for inspection. They consist of sapphire with 2 mm thickness. The groundwater flow enters the inner cell volume of 0.8 ml from the base via a PEEK tubing. The outlet is on the top of the cell. The high-pressure detection cell is successfully tested for a water pressure up to 60 bar.

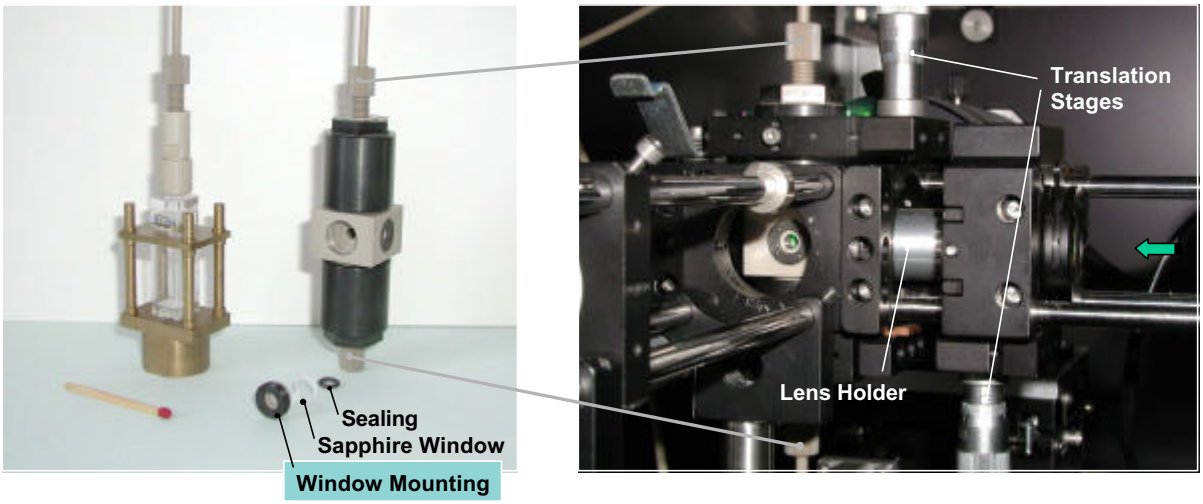

Fig. 2: LIBD high-pressure flow-through detection cell
(left: flow-through silica detection cell)

LIBD calibration with the high-pressure flow-through detection cell

The quantitative measurement of colloids in the field experiment requires the stable alignment of all optical components of the LIBD system. The exact adjustment of the beam alignment is performed by optical inspection with a laser beam profiler. According to the method described in [14], the laser pulse energy is adjusted to a constant value, at which the highest signal-to-background ratio is attained for the colloid detection. Such operational energy is selected by comparing the breakdown probability of ' ultra-pure water' with that of colloid dispersion as a function of the laser pulse energy. The breakdown probability is appraised by the ratio of the observed breakdown events to the total number of laser trigger pulses [11]. The LIBD sensitivity, as determined with the pure water dispersion of polystyrene reference particles for the smallest size available (19 nm diameter), is attained down to a few ppt at the threshold energy of 1.4 mJ.

The calibration of the system with a silica detection cell (Hellma cuvette) for the derivation of a colloid mass concentration, or number density, and an average colloid size by measuring the breakdown probability and the spatial extension of the breakdown event distribution in the laser pulse focus area has been described in detail [13, 14]. For the in-situ measurements the

quartz detection cell is replaced by the high-pressure cell. Because of its different optical and geometrical properties, the LIBD system has to be re-calibrated completely.

Concentration calibration (constant energy detection)

The result of the concentration calibration with polystyrene reference particles of different size, from 19 nm up to 993 nm is plotted in Fig. 3.

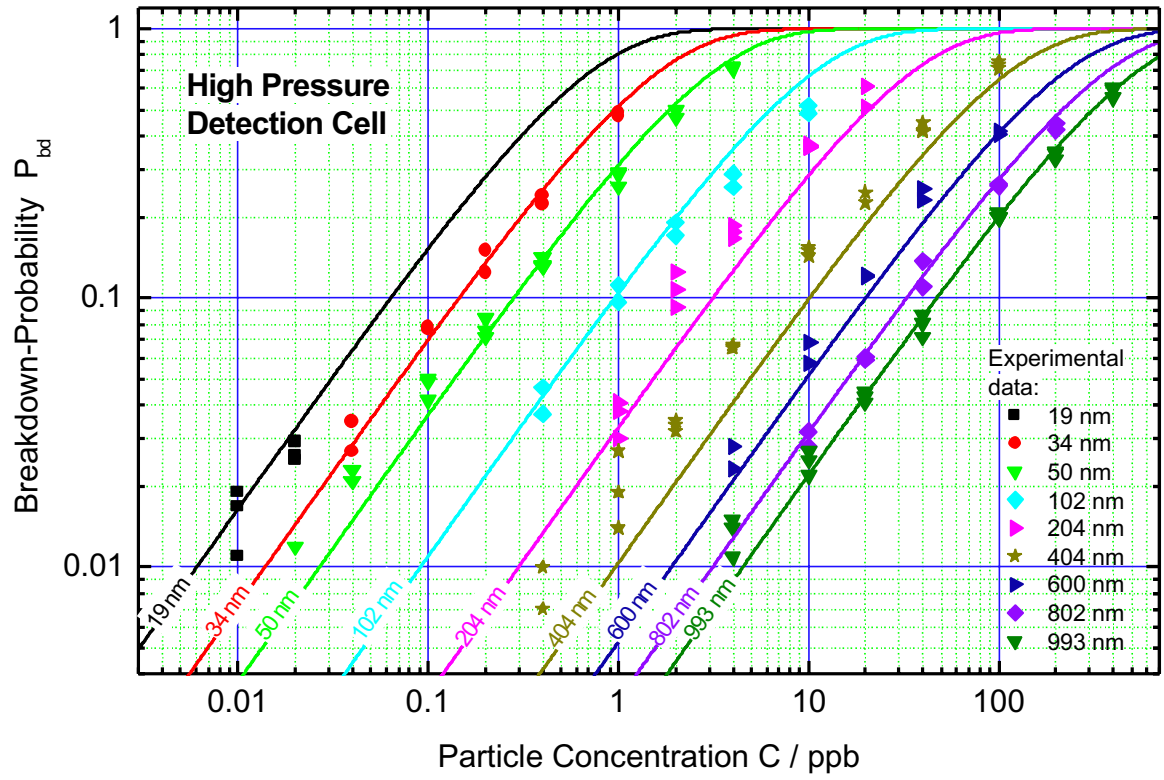

Fig. 3: LIBD concentration calibration with constant laser pulse energy (1.4 mJ) for the high pressure detection cell

Following the calibration, an effective focus volume V_{eff} (m^3) as a function of the particle diameter d(nm) is derived as

$$V_{eff} = 167.7 \times 10^{-18}\, d^{1.29} \qquad (1)$$

With this effective focus volume the mass concentration C_p (ppb) of colloids in a given sample solution can be evaluated from the breakdown probability according [14] with the known parameters for the present experiment:

$$C_p = 10^9 (\rho_P / \rho_D)(1 - (1 - P_{bd})^{Vp\,/\,Veff}) \qquad (2)$$

Where ρ_P the density of the particles (polystyrene particles $\rho_P = 1.05$ g/cm^3, for natural inorganic colloids $\rho_P = 2.7$ g/cm^3 is taken), ρ_D the density of the dispersion medium (0.998

g/cm^3) and V_p the particle volume calculated by $(4/3)\pi(d/2))^3$ with a hard sphere particle diameter d in nm.

Size calibration (constant energy detection)

The spatial extension of the breakdown event distribution in the laser pulse focus area is found to be a direct function of the particle size [12, 13]. Such a distribution is determined in the direction of the laser beam axis (x-coordinate) by monitoring the number of breakdown events in the 2-D spatial area along the x-axis. The number of events N(x) can be well fitted to a Gaussian function by

$$N(x) = (A(x) / (w(x))(\pi / 2)^{1/2} \exp(-2\,(x / w(x))^2 . \qquad (3)$$

A(x) corresponds to the area below the Gaussian curve. The full width at half maximum (FWHM) w(x) is related directly to the effective focus volume V_{eff} as given by Eq. (1), thus increasing with a particle size increase. It has been demonstrated that w(x) is correlated linearly with the particle size (d). For the setup with the high-pressure detection cell, the average size of the predominant colloid population can be estimated according to the empirical relation:

$$d = (w(x) - (179.4 \pm 3)) / (0.647 \pm 0.011) , \qquad (4)$$

with w(x) in µm and d in nm.

For the practical application of this detection and evaluation method the limiting boundaries for the colloid detection must be taken into account. From Fig. 3 it can be concluded that this method gives precise results for breakdown probabilities below about 0.8. For breakdown probabilities close to 1 the upper detection limit is reached, as there is no definite relation between breakdown probability and particle concentration. According Fig. 3 it is, for example, not possible to determine colloid concentrations above 4 ppb for 50 nm particles. Therefore, an alternative method must be applied, particularly for high concentrated colloid dispersions.

"S-curve" interpretation

As the effective focus volume V_{eff} of the breakdown event distribution in the laser focus region is related linearly with the particle size [12], each effective volume has its own laser threshold energy. This means that the laser threshold energy can also be correlated to the

particle size. Therefore, an average size of colloids can be determined also by a calibration of the laser threshold energy alone.

This threshold energy can be derived by detecting the breakdown-probability as a function of the laser pulse energy (s-curve detection). In Fig. 4 the breakdown probability is plotted as a function of the laser pulse energy for 993 nm and 19 nm polystyrene reference particle dispersions with different particle concentrations and ultra-pure water. For 993 nm particle dispersions the breakdown probability significantly deviates from 0 (P_{bd} = 0.005) at the same threshold energy of 0.15 mJ for all particle concentrations. Above this size specific threshold energy the breakdown probability increases with the pulse energy. This threshold energy increases with decreasing particle diameter. For 19 nm dispersions the threshold energy is 1.15 mJ (P_{bd} = 0.005).

Furthermore Fig. 4 demonstrates that the slope of the s-curves increases with the particle concentration without any variation in the threshold energy. For 19 nm and 993 nm particles significant changes in the shape of the s-curves are detected at low as well as at high concentrations. Therefore this method, designated as s-curve interpretation method can alternatively be applied for the estimation of an average particle diameter and concentration. Compared to the prescribed constant energy method (see Fig. 3), the s-curve interpretation method (Fig. 4) enlarges the detection range especially to higher particle concentrations. This is demonstrated in Fig. 4, where the s-curves for 993 nm particle concentrations > 1 ppm are clearly separated.

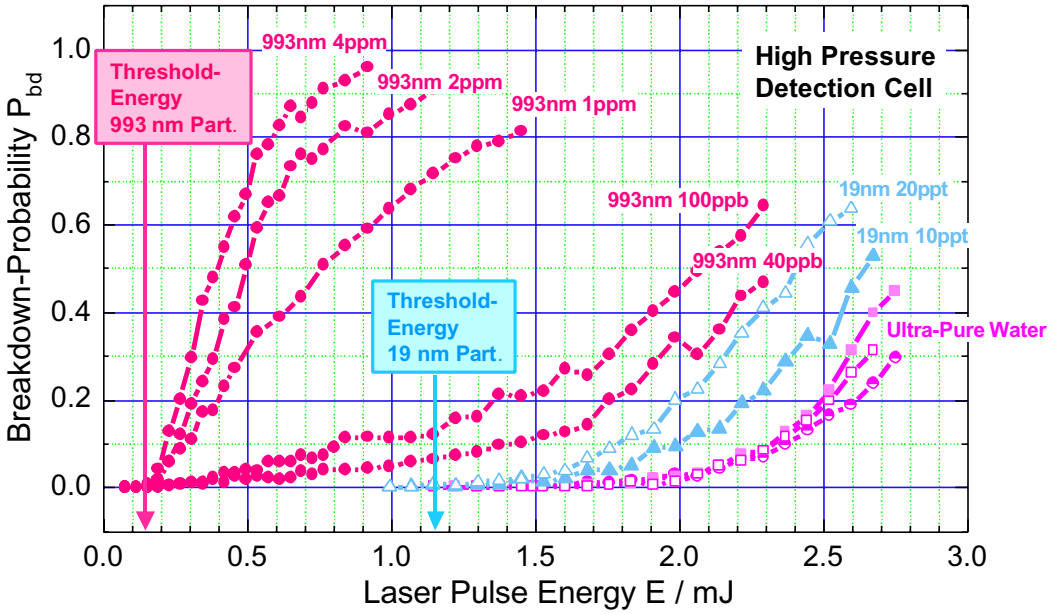

Fig. 4: Breakdown-probability as a function of laser pulse energy for different polystyrene reference particle dispersions and ultra-pure water (S-curve interpretation)

However, in low colloid concentrated dispersion (optically transparent) the constant energy method provides the same precision of the result with much less detection time.

Configuration of the detection system in the Äspö HRL tunnel

Along the 3.6 km long access tunnel of the Äspö Hard Rock Laboratory at depth from –70 m down to – 416 m eight sampling locations with lined boreholes are selected by SKB [15]. Each borehole, designated in Fig. 5 contains one representative type of groundwater which can be characterized as a mixture of water of different origin, e.g. meteoric, baltic sea, brine, glacial [19].

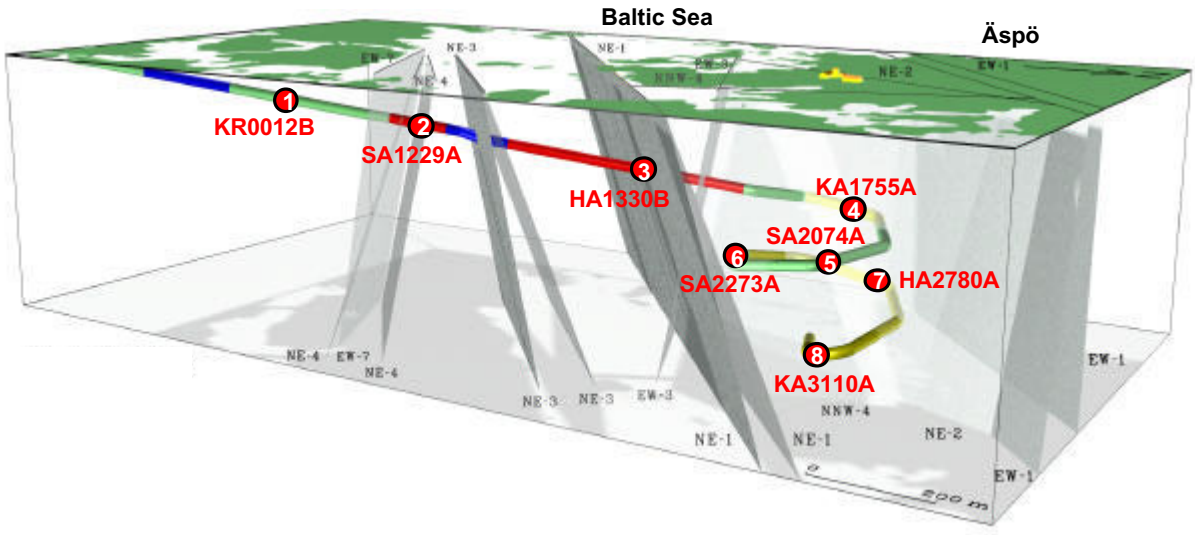

Fig. 5: LIBD sampling locations [15]

The complete LIBD detection system including the ultra-pure water processing unit is transported to Äspö, where all experiments are performed in the closed, heated transportation van. The instrumented van is installed close to the sampling boreholes, mostly on a ramp to guarantee a horizontal orientation of the setup (see Fig. 6). For continuous operation, the water processing unit is supplied with fresh drinking water from an external reservoir, separately provided at each location.

Fig. 6: LIBD instrumentation in the Äspö Hard Rock Laboratory access tunnel

The boreholes are equipped with packers and internal tubings for collecting the groundwater in a preset sampling section of the granite rock fracture, several meters from the tunnel wall. The preset sections are between 9 m up to 72 m long, as summarized in the sampling data of Table 1. From the sampling section the groundwater is conducted by an internal max. 6 m long stainless steel or plastic tubing to the borehole valve, installed at the tunnel wall.

Table 1: Summary of borehole sampling configuration and bypass valve data

Borehole ID		Borehole Data			Bypass Valve Data		
		Elevation m	Sampling Section m	Internal Tubing Length m	External Tubing Length m	Max. Flow Rate ml/min.	Max. Pressure bar
1	KR0012B	- 69	1.2 – 10.6	1.2 (s)	0	325	5.9
2	SA1229A	- 168	6.0 – 20.5	6.0 (s)	40 (p)	1 150	12.9
3	HA1330B	- 182	5.6 – 32.5	5.6 (s)	55 (p)	290	≥ 8.0
4	KA1755A	- 235	88.0 – 160.0	5.0 (p)	100 (p)	1 140	13.3
					0	2 400	14.4
5	SA2074A	- 282	6.0 – 38.7	6.0 (s)	0	210	21.3
6	SA2273A	- 306	5.8 – 20.0	5.8 (s)	75 (p)	1 050	16.2
7	HA2780A	- 370	3.7 – 43.3	3.7 (s)	70 (p)	2 000	14.3
8	KA3110A	- 416	20.1 – 28.6	5.5 (p)	0.5 (p)	2 400	32.8

(p) Plastic tubing
(s) Stainless steel tubing

In order not to block the tunnel with the van, the LIBD setup had to be placed mostly in niches, several meters apart from the sampling boreholes. A plastic tube (inner diameter 4 mm) with a total length up to 100 m connects the borehole with a bypass valve as described in Table 1. This bypass valve is situated close to the instrumented van. It is installed to reduce the natural groundwater flow rate of the borehole (max. flow rate, see Table 1) to the selected flow rate in the LIBD detection cell. Fig. 7 shows the configuration of the bypass valve between a borehole and the LIBD. The length of the PEEK-tubing (inner diameter 2 mm) between bypass valve and LIBD detection cell is 6 - 8 m. A constant flow rate through the detection cell of 4 ml/min is established by volume determination with time. The highest groundwater pressure of 33 bar is detected at the position of the lowest borehole KA3110A. All other max. borehole pressures are summarized in Table 1.

Fig. 7: Bypass valve configuration

Groundwater sampling for chemical analysis

Some days before the in-situ colloid detection campaign all different boreholes have been sampled by SKB. Directly at each borehole valve, a 3 liter glass bottle has been completely filled with the groundwater. Immediately afterwards the bottles have been closed with a screwed-on plastic cap. No preparation of samples is performed. The samples are transported to Karlsruhe after the in-situ campaign for chemical analysis with IC, ICP-AES and DOC detection.

3. Results

LIBD detected colloid size and mass concentration

At the upper boreholes KR0012B, SA1229A, HA1330B, above –200 m depth, respectively, breakdown-probabilities close to 100% are detected with 1.4 mJ constant laser pulse energy for low, as well as for high groundwater flow rate. Therefore, the above described LIBD s-curve interpretation is applied.

This is demonstrated in Fig. 8 for groundwater KR0012B as an example. For a flow rate of 222 ml/min., the threshold energy corresponds to the threshold energy of a ~600 nm reference particle dispersion. From the slope, a colloid mass concentration of ~600 ppb is

derived. The s-curve for a flow rate of 4 ml/min., with a significantly higher threshold energy, characterizes a dispersion with colloids of ~404 nm average diameter and ~300 ppb mass concentration.

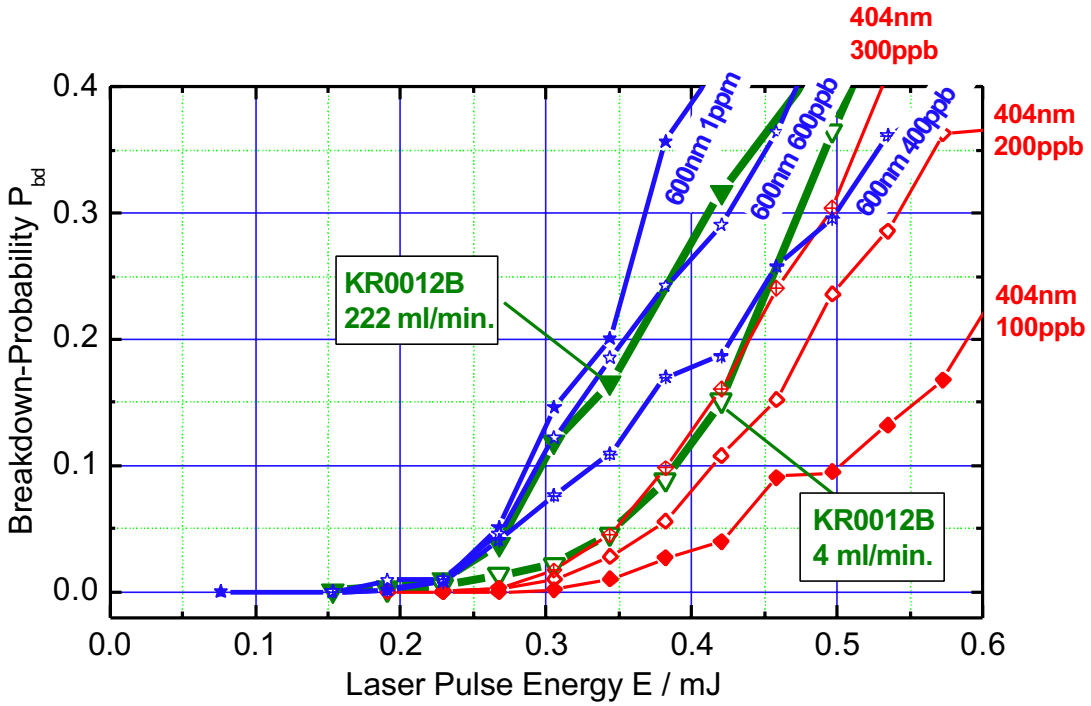

Fig. 8: S-curve interpretation for groundwater KR0012B
(data compared with polystyrene reference particles in ultra pure water)

For breakdown probabilities which are significantly below 100%, average colloid diameter and colloid concentration are generally detected with constant laser pulse energy by applying image processing as described above. The lowest breakdown probability of 0.2% is detected for groundwater KA1755A. For this breakdown probability, which is in the order of the breakdown probability of ultra-pure water an average colloid diameter of 57 nm with a colloid concentration of 14 ppt is evaluated. Additionally, the s-curve interpretation method is applied to verify the data. According to Fig. 9, a colloid diameter of <19 nm and <10 ppt colloid concentration must be derived for this groundwater, which is in the same order of magnitude as the data obtained with constant laser pulse energy.

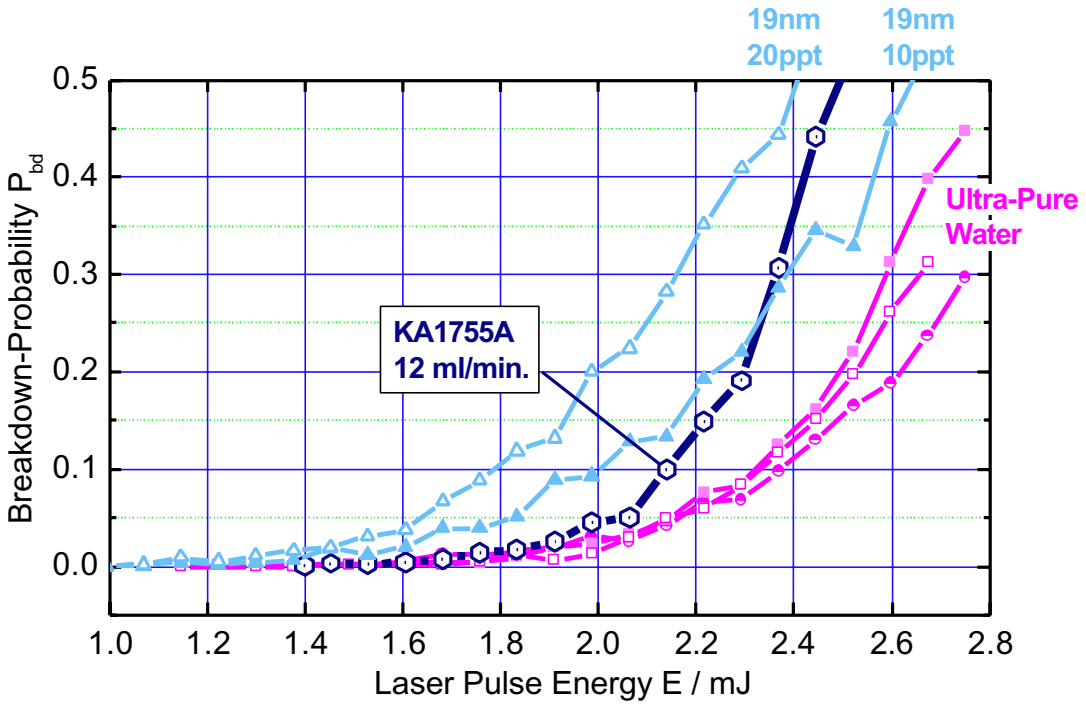

Fig. 9: S-curve interpretation of groundwater KA1755A
(data compared with polystyrene reference particles in ultra pure water and ultra-pure water)

The LIBD data for the different groundwater are summarized in Table 2. At each borehole position the groundwater flow rate adjusted at the bypass valve is varied between 4 ml/min. and the max. flow rate given in Table 1. Groundwater properties arising from visual inspection at site, like "gas generation" (gas bubbles in the dispersion) and "colored dispersion" give some casual information about pressure fluctuations and the amount of colloids. Colloids in KA1755A are detected using 100 m external tubing and no external tubing between bypass valve and borehole in order to investigate the influence of the plastic tubing.

Table 2: Summary of LIBD results

Borehole ID		Elevation m	Tubing Length m	Flow Rate ml/min. (1)	Visual Inspection: Gas-Gen.	Visual Inspection: Colrd. Disp.	LIBD Data Evaluation: Bd. Prob. %	LIBD Data Evaluation: Colloid Diameter nm	LIBD Data Evaluation: Colloid Conc. ppb
1	KR0012B	- 69	0	4	no	yes	100	~404 (2)	~300 (2)
				222			100	~600 (2)	~600 (2)
2	SA1229A	- 168	40	4	no	yes	92	~600 (2)	~190 (2)
				930			100	~300 (2)	~110 (2)
3	HA1330B	- 182	55	4	no	yes	100	~993 (2)	~1 000 (2)
				125			100	~404 (2)	~100 (2)
4	KA1755A	- 235	100	4	yes	no	69.5	631 (3)	630 (3)
				550			3.0	281 (3)	4.1 (3)
			0	12			0.2	<19 (2), 57 (3)	<0.01 (2), 0.014 (3)
				1 400			0.4	129 (3)	0.15 (3)
5	SA2074A	- 282	0	4	no	yes	100	~600 (2)	~600 (2)
				190			38.8	354 (3)	99 (3)
6	SA2273A	- 306	75	4	no	yes	14.5 - 26.0	175 (3)– 263 (3)	9.2 (3)– 35.5 (3)
				900			46.0	218 (3)	53 (3)
7	HA2780A	- 370	70	4	yes	no	2.3 - 18.0	165 (3)– 296 (3)	1.2 (3)– 19 (3)
				11			28.5	456 (3)	102 (3)
				20			63.1	627 (3)	525 (3)
				920			14.5	244 (3)	16.5 (3)
				1 100			17.2	245 (3)	19.6 (3)
8	KA3110A	- 416	0.5	4	no	yes	9.9	365 (3)	22 (3)
				2 400			9.4	333 (3)	18 (3)

(1) Flow rate adjusted at bypass valve
(2) Data s-curve evaluated
(3) Data evaluated with constant laser pulse energy

The different groundwater are sampled and analysed in September 2000 by SKB (Table 3) and one week before the LIBD detection in October 2001 (Table 4) with the analysis at INE. Apart from the total amount of Fe both analysis give comparable results. It is evident, that the lower Fe-content in the October 2001 samples by several orders of magnitude is caused by contact to oxygen. Initially dissolved Fe(II) is oxidized to form FeOOH which is mostly found as precipitated red brown flocs at the bottom of the glass bottles.

Table 3: Groundwater composition
(SKB data, sampling date: Sept. 2000)

Borehole ID	Na	K	Ca	Mg	Cl	SO_4	HCO_3	Br	F	Si	Fe_{tot}	Mn	Li	Sr	DOC	pH
	mg/l	mg/l	mg/l	mg/l	mg/l	mg/l	mg/l	mg/l	mg/l	mg/l	mg/l	mg/l	mg/l	mg/l	mg/l	pHunit
Measurement uncertainty⇒	5%	5%	5%	5%	5%	5%	5%	10%	10%	5%	10%	5%	5%	5%	0.1 mg/l	0.1 unit
1 KR0012B	217	3.7	54	11.6	250	47.0	311	1.5	1.4	6.8	0.253	0.18	0.040	0.89	16.0	7.5
2 SA1229A	1520	25.7	315	131.0	3120	252.0	264	11.9	1.3	6.7	1.833	0.71	0.093	4.87	7.0	7.2
3 HA1330B (1)	1610		648	128.0	3920		252									7.4
4 KA1755A	2960	10.5	4130	35.5	11430	613.0	9	87.5	1.5	4.3	0.190	0.28	2.510	70.00	<1.0	7.8
5 SA2074A	1230	9.3	448	85.1	2770	251.0	169	9.6	1.2	6.1	0.160	0.49	0.150	6.40	5.0	7.7
6 SA2273A	1570	14.3	684	105.0	3770	264.0	159	19.0	1.3	5.7	0.803	0.80	0.317	10.20	5.0	7.4
7 SA2783A (2)	3370	13.5	4980	36.5	13920	655.0	13	109.5	1.7	4.3	0.106	0.30	3.080	84.30	1.0	7.8
8 KA3110A	1470	30.4	372	128.0	3080	277.0	185	11.7	1.6	5.3	1.234	0.76	0.138	5.4	7.0	7.5

(1) Sampling date: Oct. 1992
(2) Similarities with HA2780A

Table 4: Groundwater composition
(INE chemical analysis, sampling by SKB, date: Oct. 2001)

Borehole ID	Na	K	Ca	Mg	Cl	SO_4	NO_3	PO_4	F	Si	Fe_{tot}	Mn	Li	Sr	DOC	
	mg/l	mg/l	mg/l	mg/l	mg/l	mg/l	mg/l	mg/l	mg/l	mg/l	mg/l	mg/l	mg/l	mg/l	mg/l	Pre. (1)
Measurement uncertainty⇒	5%	5%	5%	5%	5%	5%	5%	5%	5%	5%	50%	5%	5%	5%	0.1 mg/l	
1 KR0012B	167	2.1	44	9.4	136	30.7	<0.1	<0.1	0.5	6.75	0.11600	0.141	0.031	0.76	15.7	no
2 SA1229A	1560	32.9	295	128.0	3381	234.2	<0.1	<0.1	5.4	6.15	0.00296	0.714	0.115	4.60	7.0	yes
3 HA1330B	1590	20.8	348	120.0	3496	305.2	<0.1	<0.1	5.7	4.89	0.00283	0.766	0.117	4.86	6.2	yes
4 KA1755A (2)	2940	8.6	3900	32.2	11044	565.7	31.3	28.7	19.3	4.06	0.11300	0.250	2.240	4.06	1.9	no
5 SA2074A	1400	11.2	414	84.6	2913	234.3	<0.1	<0.1	4.7	5.70	0.00249	0.464	0.172	5.80	5.4	no
6 SA2273A	1620	18.6	719	105.0	4234	260.9	<0.1	<0.1	7.1	5.22	0.00344	0.774	0.421	10.60	4.3	yes
7 HA2780A	3400	21.2	4510	48.3	15470	620.4	<0.1	3.7	22.3	4.11	< det.limit	0.250	4.730	66.20	1.5	no
8 KA3110A	1490	45.1	277	133.0	3193	257.9	<0.1	<0.1	4.5	5.09	0.00208	0.737	0.100	3.81	6.3	yes

(1) Precipitation in 3 l sampling bottle (red brown flocs)
(2) Sampling date: Jan. 2002

Interpretation

Colloid concentrations determined by LIBD vary from less than 0.1 ppb to 1000 ppb. They do not only vary in samples taken at different locations, they also depend on flow rates and the lengths of the tubing from the borehole to the LIBD flow through cell at each sampling site. In the case of borehole KA1755A a clear decrease of colloid concentrations appeared

when the tubing length was considerably shortened from 100 m to direct coupling. A decrease of the measured colloid population is also achieved by increasing the flow rate in the long tubing. Both facts indicate colloid generation by to in-diffusion of O_2 through the polyamide tube walls. Dissolved Fe(II) is successively oxidized to form colloidal FeOOH. Both, shortening the tubing length and increasing the sample flow rate diminishes the O_2 input and thus the colloid formation. Increasing the flow rate to very high rates of 1400 ml/min and direct connection of the LIBD to the borehole, entails slighty increased colloid concentration. The reason for this finding is most likely a wash out of colloidal material in the water conducting fractures as a consequence of the shear forces due to the high flow rates (mechanical erosion). As a conclusion it is assumed that the lowest value for the colloid concentration analysed at this sampling location is considered to be as least of all affected by artefacts. Similar relationships regarding the colloid concentration for different water flow rates can also be found in other sampling boreholes. The groundwater sampled at HA2780A contains the lowest Fe concentration of 0.104 mg/l and thus appears to be less sensitive to colloid formation by O_2 contact. As a consequence the lowest colloid concentrations are determined at the lowest flow rates. Higher sample flow rates yield increasing colloid concentrations due to colloid release from the fracture infill. The LIBD signals determined for this water fluctuate significantly with time. They are correlated with pressure changes observed at the borehole outlet. The variation of colloid concentrations therefore can be interpreted as a consequence of colloid release due to pressure changes in the environment of the borehole.

For the following considerations it is assumed that the lowest colloid concentrations measured at each individual borehole are those being "closest to the truth" i.e. artefacts are minimized as much as possible. In general, the amount of colloids being present in a given groundwater are always found to correlate with ionic strength, presence of stabilizing organic matter (fulvic/humic acid) and chemical or mechanical disturbances (see e.g.[20]). In the present study, chemical disturbance due to O_2 access to the sample is minimized by either increasing the water flow rate or by shortening the tubing length. The lacking correlation of measured colloid concentrations with the total Fe concentrations (Fig. 10) indicates the successful suppression of oxidative FeOOH colloid generation. Keeping the original water pressure during analysis by the use of the above described pressure flow through cell avoids release of gases and changes of the chemical milieu due to degassing of e.g. CO_2, H_2S.

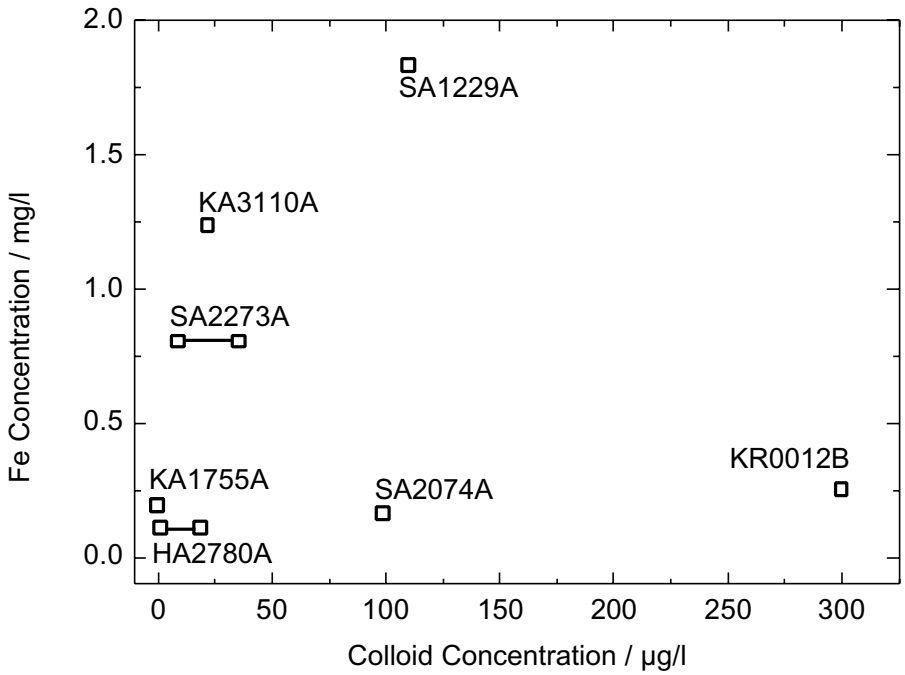

Fig. 10: Groundwater Fe concentration plotted versus colloid concentration in the analysed groundwater samples

The influence of mechanical colloid release has also been attempted to keep at a minimum by variation of the flow rate and collecting samples for a long time period at constant flow rate. Colloid concentrations are determined under steady state conditions and measurement of erroneously high values for colloid populations due to pressure pulses are thus avoided.

If we suppose that chemical and mechanical disturbances are successfully suppressed during the sampling campaign, the variation in colloid concentrations and size has to be explained by the different geochemical groundwater conditions influencing colloid stability.

The dependency of colloid concentration on the groundwater salinity is shown in Fig. 11. A clear decrease of the colloid concentration with increasing salinity (indicated by the respective Cl^--concentration) is stated. This observation is in agreement with findings established in other investigations [21, 22]. The ionic strength dependency of the colloid concentration proves the presence of charge stabilized particles at low ionic strength conditions. At high ionic strength conditions, colloids appear to be destabilized and, therefore, only low concentrations are found. At low ionic strength the stability of even larger particles is increased. This is indicated by the increasing mean colloid diameter with increasing colloid concentrations (Fig. 12).

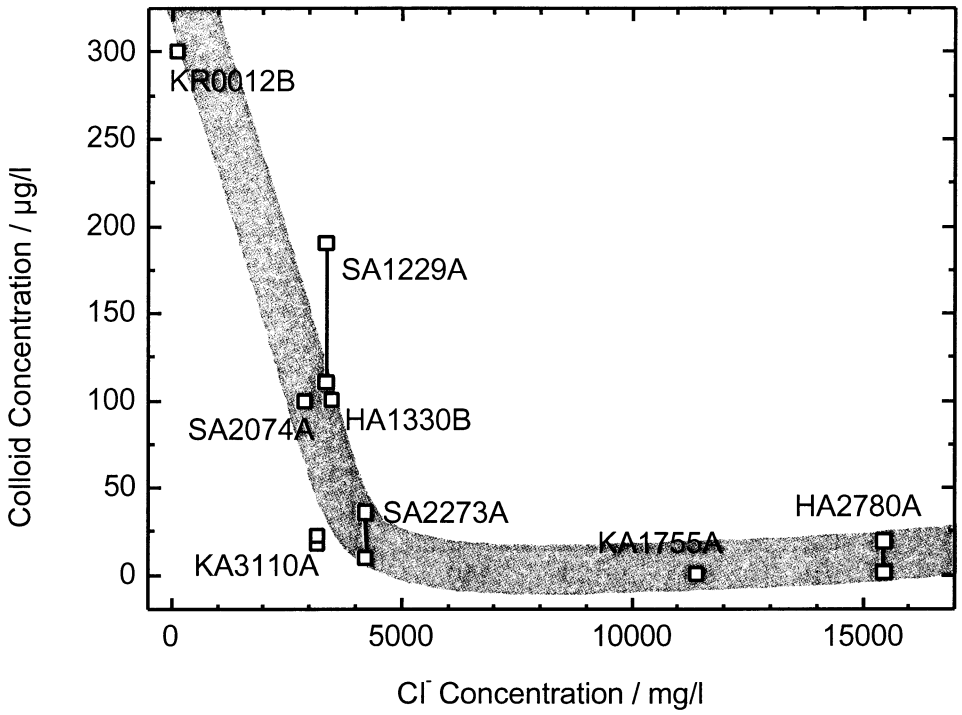

Fig. 11: LIBD analysed colloid concentration as a function of the Cl^- concentration (data from Table 4) as an indicator for salinity (data points connected by bars indicate varying colloid concentrations due to pressure fluctuations)

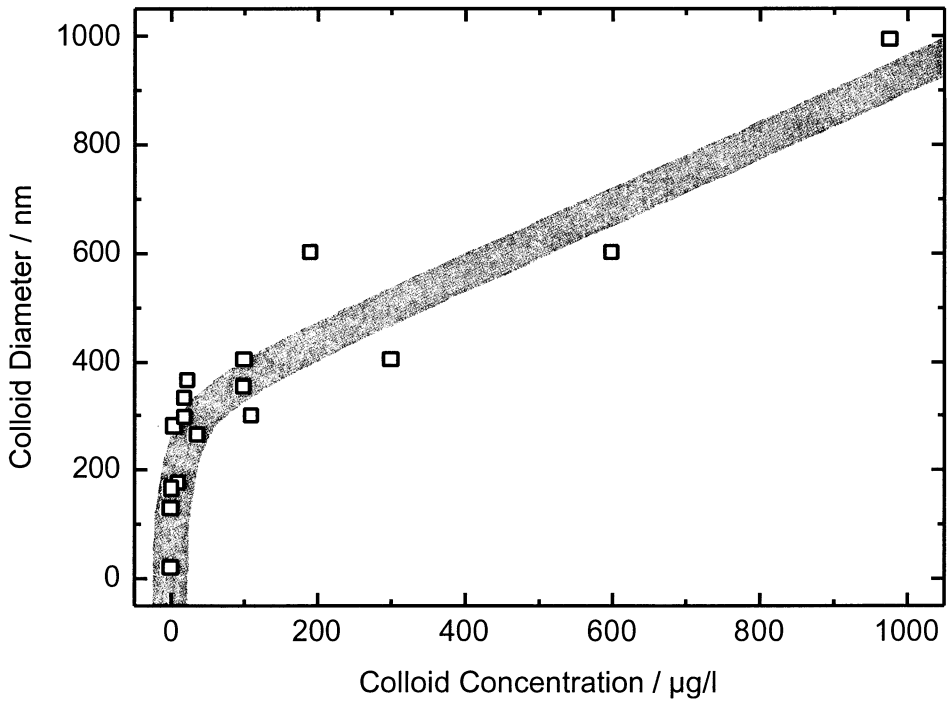

Fig. 12: Correlation of the colloid concentration with the mean colloid diameter determined by LIBD (data from Table 2)

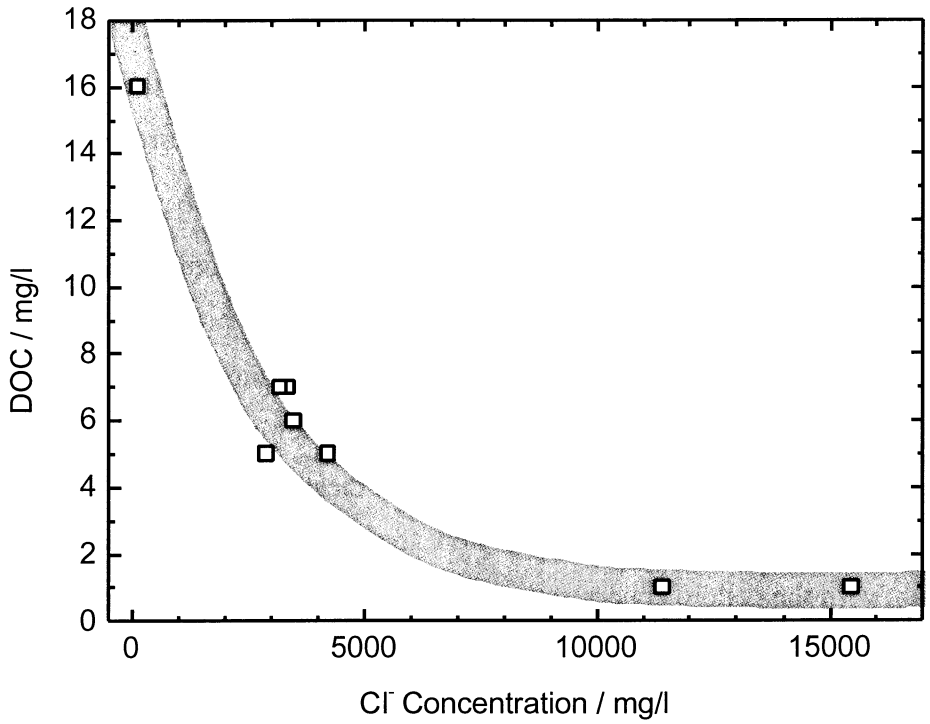

Fig. 13: Dissolved organic carbon DOC versus Cl^- concentration as an indicator for salinity (data from Table 4)

Fig. 13 shows the similar relationship for the dissolved organic carbon (DOC) with salinity as found for the colloids measured by LIBD. One might argue that in view of the strong correlation of colloid concentration and DOC it is primarily fulvic/humic colloids being present in the groundwater. A recent study on humic colloids characterization by LIBD [23] showed that fulvic/humic acid is more or less invisible for LIBD possibly due to their low density. Inorganic or lignite nanoparticles aggregated with fulvic/humic acid, however, can be detected by LIBD. Whether it is purely inorganic colloids or inorganic/organic composites which are determined in the present study cannot be resolved on the basis of the available data. It is however well known that in the presence of organic macromolecules, inorganic colloids are stabilized as organic/inorganic aggregates.

EQ3/6 calculations

Calculations using EQ3/6 [24] are performed in order to identify possible precipitating solids. EQ3/6, release 7.2 together with the database data0.com.R23 has been applied. For speciation and computation of supersaturation of the groundwater, the input for EQ3 is defined using groundwater compositions of Table 3. The Davis activity model is applied. Redox potentials have not measured during the present sampling campaign. Due to the presence of pyrite in the granite, a redox potential of ~ -220mV for the pH given in Table 3 is selected. For calculating

the equilibrium of the groundwater with EQ6, precipitation of pure minerals and solid solutions are taken into account. Precipitation of Si and Fe sulphide bearing phases is computed to less than 1% of the amount of carbonates. Silicate phases are treated hypothetically because Al was not determined in the analyses (Tab. 3).

The concentration of the precipitates calculated from thermodynamic data and the respective solids are given in Tab. 5. It is assumed that the Redox potentials of the groundwater are reducing and, therefore, Fe(III) phases are not supersaturated. Based on the analytical data available for the respective water samples, mainly carbonates appear to be close to saturation or even supersaturated. Even though these scoping calculations can not be interpreted in a straightforward manner, they show some correlation of the degree of supersaturation with the colloid concentration. From the data shown in Tab. 5 and Fig. 14 it might be concluded that colloidal species consist mainly of carbonates. This has to be proved in future studies. The outlying high colloid concentration in the groundwater KR0012B in this correlation (Fig. 14) might be explained by the very low salinity and high DOC in this sample representing very favourable conditions for colloid stabilization.

Table 5: EQ3/6 calculated solid phases

	Borehole ID	Total Precipitate mg/l	Solid Phases
1	KR0012B	29.94	Dolomite, Carbonate-SolidSolution
2	SA1229A	57.27	Dolomite
3	HA1330B	70.65	Dolomite, Fluorite
4	KA1755A	1.80	Carbonate-SolidSolution
5	SA2074A	38.19	Dolomite
6	SA2273A	33.85	Dolomite, Carbonate-SolidSolution
7	SA2783A	2.65	Strontianite
8	KA3110A	0.05	Hematite

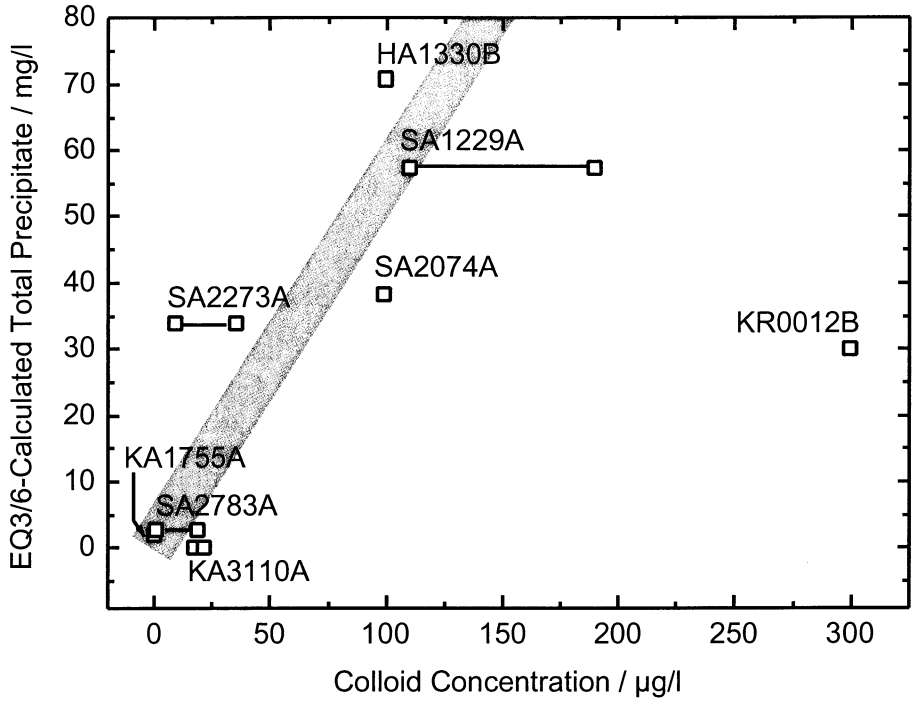

Fig. 14: EQ3/6 calculated total precipitate as a function of the LIBD detected colloid concentration

Conclusions

The present study proves the appropriateness of the mobile LIBD for sensitive in-situ colloid analysis in groundwater. The necessity for an in-situ colloid analysis taking as much as possible care to prevent possible artifacts is also demonstrated. O_2 access to the groundwater and degassing has to be excluded and moderate constant flow rates have to be applied, in order to be sure that only the genuine groundwater colloids are analyzed and possible artifacts are minimized. The data so far show the influence of low salinity and humic like organics on colloid stability in groundwater. Scoping thermodynamic calculations suggest the supersaturation with regard to mainly carbonates as a possible source for colloid formation.

Acknowledgements

The support of the investigations cooperated by SKB and INE/FZK is greatly appreciated. We acknowledge P. Hagman for his technical assistance during the field experiment and C. Mattsén for the groundwater sampling.

References

[1] J. I. Kim, Actinide colloid generation in groundwater, Radiochim. Acta 52/53 (1991) 71.

[2] J. I. Kim, Actinide colloids in natural aquifer systems, MRS Bull. Vol. XIX(12) (1994) 47-53.

[3] J. I. Kim, P. Zeh, B. Delakowitz, Chemical interactions of actinide ions with groundwater colloids in Gorleben aquifer systems, Radiochim. Acta 58/59 (1992) 147-154

[4] R. Artinger, B. Kienzler, W. Schüßler, J.I. Kim, Effects of humic substances on the 241-Am migration in a sandy aquifer: Column experiments with Gorleben groundwater/sediment systems, J.Contam.Hydrol. 35 (1998), 261-275

[5] A.B. Kersting, D.W. Efurd, D.L. Finnegan, D.J. Rokop, D.K. Smith, J.L. Thompson, Migration of plutonium in ground water at the Nevada Test Site, Nature 397 (1999) 56-59.

[6] M. Fillela, J. Zhang, M.E. Newman, J. Buffle, Analytical applications of photon correlation spectroscopy for size distribution measurements of natural colloidal suspensions: capabilities and limitations, Coll.&Surf. *A* 1997, 120, 27-46

[7] C. Degueldre, H. R. Pfeiffer, W. Alexander, B. Werni, R. Bruetsch, Colloid properties in granitic groundwater systems. I: Sampling and charakterisation, Appl. Geochem. 11 (1996).

[8] H. Wimmer, J.I. Kim, Laser-Induzierte optische Spektroskopie zur Speziation von f-Elementen in natürlichen aquatischen Systemen, RCM 00992, Institut für Radiochemie, München (1992)

[9] T. Bundschuh, R. Knopp, J. I. Kim, Laser-induced Breakdown Detection (LIBD) of aquatic colloids with different laser systems, Colloids and Surfaces, Colloids Surf. A, 177 (2001) 47-55.

[10] T. Kitamori, K. Yokose, M. Sakagami, T. Sawada, Detection and counting of ultrafine particles in ultrapure water using laser breakdown acoustic method, Jpn. J. Appl. Phys. 28 (1989) 1195.

[11] F. J. Scherbaum, R. Knopp, J. I. Kim, Counting of particles in aqueous solutions by laser-induced photoacoustic breakdown detection, Appl. Phys. B63 (1996) 299-306.

[12] T. Bundschuh, W. Hauser, J. I. Kim, R. Knopp, F. J. Scherbaum, Determination of colloid size by 2-D optical detection of laser induced plasma, Colloids Surf. A, 180 (2001) 285.

[13] W. Hauser, T. Bundschuh, Verfahren zur Bestimmung der Größe von Partikeln in einer Lösung, Patent: DE 198 33 339 (2000).

[14] W. Hauser, H. Geckeis, J.I. Kim, T. Fierz, A mobile laser-induced breakdown detection system and its application for the in situ-monitoring of colloid migration, Colloids Surf. A, 203 (2002) 37-45.

[15] M. Laaksoharju, Äspö Hard Rock Laboratory, Project description of the Äspö project Colloid with the aim to investigate the stability and mobility of colloids, SKB International Progress Report IPR-01-08 (2001)

[16] L. J. Radziemski, D. A. Cremers, Laser-induced Plasmas and Applications, Marcel Dekker, New York, 1989.

[17] H. Fujimori, T. Matsui, T. Ajiro, K. Yokose, Y. M. Hseuh, S. Izumi, Detection of fine particles in liquids by laser breakdown method, Jpn. J. Appl. Phys. 31 (1992) 1514.

[18] W. Hauser, R. Götz, Druckwellensensor, Patent: DE 196 02 048 (1999).

[19] Evolution of the groundw ater chemistry at the Äspö Hard Rock Laboratory, M. Laaksoharju, B. Wallin (ed.), Proc. of the second Äspö International Geochemistry Workshop, June 6-7, 1995, SKB International Cooperation Report 97-04 (1997).

[20] C. Degueldre, I. Triay, J.I.Kim, P. Vilks, M. Laaksoharju, N. Miekeley, Groundwater colloid properties: a global approach, Appl. Geochem. 15 (2000) 1043-1051.

[21] C. Degueldre, R. Grauer, A. Laube, A. Oess, H. Silby, Colloid properties in granitic systems (II): stability and transport study, Appl. Geochem. 11 (1996), 697-710.

[22] H.Geckeis, B.Grambow, A.Loida, B.Luckscheiter, E.Smailos, J.Quinones, Formation and Stability of colloids under simulated near field conditions, Radiochim. Acta 82 (1998) 123-128

[23] M. Bouby, T. Ngo Manh, H. Geckeis, F. Scherbaum, J. I. Kim, Characterization of aquatic colloids by a combination of LIBD and ICP-MS follo wing the size fractionation, accepted by Radiochim. Acta.

[24] EQ3/6, A Software Package for Geochemical Modeling Version 7.2a, University of California, Lawrence Livermore National Laboratory. Software produced under the Designated Unclassified Subject Area (DUSA) "Yucca" (1990-1993).

Appendix 4

Origin, stability and mobility of humic colloids in Äspö groundwater: Feasibility study

G. Buckau
Institut für Nukleare Entsorgung
Forschungszentrum Karlsruhe GmbH
P.O. Box 3640
76021 Karlsruhe
Germany

M. Wolf
GSF-National Research Center for Environment and Health
Institute of Hydrology
85764 Neuherberg
Germany

Summary

The origin, stability and mobility of colloids in natural aquifer systems surrounding a nuclear waste repository is a key element in developing the basis for long-term safety assessment of nuclear waste disposal. Humic colloids are present in all natural groundwater. They allow analogue studies on humic mobility under natural conditions. In deep granite groundwater, humic colloids are dominated by fulvic acid. Therefore, chemical, spectroscopic and isotopic characterization of fulvic acid from Äspö groundwater has the potential to become a key contribution to evaluation of colloid mobility in granite groundwater. A further potential benefit is the possible contribution to hydrological modeling through quantification and dating of groundwater contributors.

A feasibility study is conducted for the isolation of sufficient amounts of fulvic acid from Äspö groundwaters for this purpose. Eleven groundwaters are investigated for their fulvic acid content. In addition, Baltic water is studied because it is a possible contributor to some of the groundwaters. Dissolved organic carbon (DOC) and UV/Vis spectroscopy of original water samples as well as fulvic acid concentrates is used for quantification of the fulvic acid. The study shows that sufficient fulvic acid is available in all waters. It is also shown that sorption of fulvic acid on precipitates generated during shipping and handling of groundwater samples is not a problem.

The approach for isolation of required amounts of fulvic acid will depend on practical and cost considerations. For chemical, spectroscopic and isotopic (especially ^{14}C) characterization around 200 mg fulvic acid is required (around 100 mg C). In groundwaters where the fulvic acid concentration is around 1 mgC/L or higher, 100 L of groundwater can be sampled and sent to the laboratory for direct treatment. In two of the twelve investigated water samples the fulvic acid concentrations are so low that on-site pre-concentration by reverse osmosis appears to be the method of choice.

1. Objectives

Determine the feasibility for isolation of sufficient amounts of fulvic acid from Äspö groundwaters for chemical, spectroscopic and isotopic characterization.

2. Introduction

Groundwater humic colloids are aquatic humic and fulvic acid in their natural aquatic state, including associated inorganic components. Fulvic acid dominates the organic component of humic colloids in deep granite groundwater. Humic colloids are a fraction of dissolved organic carbon (DOC). This fraction can vary from close to 100 % in groundwaters rich in humic substances, down towards 10 % in groundwaters with very low humic substance concentrations (DOC in the order of 0.1 mgC/L). A previous study on groundwater with

fulvic acid concentrations around 0.02 mgC/L showed that fulvic acid was introduced into the groundwater after the development of a vegetation layer at the end of the last cold maximum of the past ice age. This fulvic acid is still present and shows no significant retardation or decomposition despite the residence time of around 15.000 years [1]. In an aquifer rich in humic substances also no indication of significant decomposition of aquatic humic and fulvic acids was found [2]. This leads into the question to which extent fulvic acid introduced into Äspö groundwater from different sources also shows an ideal tracer behavior. For this purpose, fulvic acid needs to be isolated in sufficient quantities and characterized with respect to chemical composition, spectroscopic properties and isotopic composition. With respect to the latter, especially ^{14}C dating of fulvic acid and comparison with groundwater age from hydrological modeling is important. For this reason the present feasibility study is performed in order to determine if the concentrations of fulvic acid in different Äspö groundwaters are sufficiently high for the required isolation and characterization.

3. Samples

Twelve samples were collected in 2 L glass bottles and shipped to FZK/INE. These are:

SA1327B[1)] (skb: 003465)	SA1229B (skb: 003471)	KAS09
SA2780A[2)] (skb: 003467)	SA2074A (skb: 003468)	Baltic water
KA3110A (skb: 003464)	SA2273A (skb: 003470)	GV1 (011030)
KR0012B (skb: 003466)	KAS03	GV9 (011130)

1): identical with HA 1330B; 2): identical with HA2780A

Origin, physico-chemical properties and chemical composition of the waters are shown in Table 1. Chemical composition determined by INE and SKB on samples of the present sampling campaign show acceptable agreement with each other. One exception is Fe reflecting oxidation of the samples shipped to INE.

4. Quantification of fulvic acid in selected samples

Fulvic acid in natural water is isolated by XAD-8 chromatography (cf. below (4.1)). If the fulvic acid concentration is low, on-site pre-concentration by reverse osmosis is used [3]. For the characterization of fulvic acid about 100 mg carbon is required. Based on the practicability of transporting 100 L water sample to the laboratory for isolation of fulvic acid, on-site pre-concentration is necessary where the fulvic acid concentration is in the order of 1 mgC/L or lower. In order to determine the need for on-site pre-concentration, fulvic acid is quantified in the samples with the two lowest DOC concentrations (SA2780A and KAS 03). For comparison, fulvic acid is also quantified in the groundwater GV9 with a DOC concentration of 18.8 mgC/L. Finally, the sorption of fulvic acid on precipitate generated during shipping and handling is quantified in the groundwater sample SA2273A.

Table 1: Overview of groundwaters with analytical data by SKB and INE. The samples in the present report refer to the lower two parts (SKB and INE October 2001)

Sample	Depth (m)	Seclow/secup (m)	pH	Cond (mS/m)	DOC (mgC/L)	Na	K	Ca	Mg	HCO_3	Cl	SO_4	Br	F (mmol/L)	Si	Fe_{tot}	Mn	Li	Sr	H_2S	NH_4	NO_3	PO_4
SKB: Sept. 2000																							
HA1330B[1)]	182	0/32.5				9	0.09	1.4	0.48	5.10	7.05	0.49	0.02	0.07	0.21	0.005	0.003	0.006	0.01				
HA2783A[2)]	370	0/43.3	7.8		1.0	66	0.66	7.9	5.46	4.33	88.0	2.63	0.15	0.07	0.21	0.033	0.013	0.013	0.06				
KA3110A	416	20.1/26.8	7.5		7.0	129	0.27	103	1.48	0.15	322	6.39	1.09	0.08	0.13	0.003	0.005	0.362	0.80				
KR0012B	69	1.2/10.6	7.5		16.0	53	0.24	11.2	3.55	2.77	78.1	2.61	0.12	0.06	0.19	0.003	0.009	0.022	0.07				
SA1229B	168	6.0/20.5	7.2		7.0	68	0.37	17.1	4.38	2.61	106	2.75	0.24	0.07	0.18	0.014	0.015	0.046	0.12				
SA2074A	282	6.0/38.7	7.7		5.0	147	0.35	124	1.52	0.21	393	6.82	1.37	0.09	0.13	0.002	0.005	0.444	0.96				
SA2273A	306	6.0/20.0	7.4		5.0	64	0.78	9.3	5.33	3.03	86.9	2.89	0.15	0.08	0.17	0.022	0.014	0.020	0.06				
1: Sampling date: Oct. 1992; 2: Similarities with HA2780A																							
SKB: Oct. 2001																							
HA1330B			7.4	970	3.6	68	0.44	8.4	4.92	3.28	83.5	3.25	0.14	0.11	0.18	0.027	0.014	0.014	0.06	0.0003	0.05		
HA2780A			7.6	3250	1.4	144	0.39	111	1.48	0.31	361	6.81	1.26	0.14	0.15	0.002	0.005	0.484	0.86	-	0.01		
KA3110A			7.7	910	5.0	62	0.90	6.4	5.33	3.21	77.0	2.80	0.13	0.05	0.18	0.019	0.013	0.012	0.04	0.0028	0.06		
KR0012B			7.5	116	11.0	7	0.07	1.0	0.33	5.38	4.7	0.39	0.01	0.14	0.24	0.004	0.003	0.005	0.01	0.0013	0.01		
SA1229B			7.3	950	4.8	66	0.67	6.9	5.17	4.33	80.4	2.33	0.15	0.11	0.23	0.033	0.012	0.013	0.05	0.0003	0.11		
SA2074A			7.7	850	4.1	54	0.25	9.9	3.35	2.85	71.1	2.47	0.16	0.14	0.21	0.003	0.009	0.022	0.07	0.0016	0.01		
SA2273A			7.5	1150	3.2	68	0.38	16.9	4.17	2.59	103	2.64	0.20	0.09	0.19	0.014	0.014	0.050	0.12	0.0006	0.03		
INE Oct. 2001																							
SA1327B / HA1330B					6.2	69	0.53	8.7	5.00		98.6	3.18		0.30	0.15	$5x10^{-5}$	0.014	0.017	0.06			<0.002	<0.001
SA2780A / HA2780A					1.5	148	0.54	113	2.01		436	6.46		1.17	0.13	n.d.	0.005	0.682	0.76			<0.002	0.039
KA3110A					6.3	65	1.16	6.9	5.54		90.1	2.69		0.24	0.16	$4x10^{-5}$	0.013	0.014	0.04			<0.002	<0.001
KR0012B					15.7	7	0.05	1.1	0.39		3.8	0.32		0.03	0.21	0.0021	0.003	0.004	0.01			<0.002	<0.001
SA1229B					7.0	68	0.84	7.4	5.33		95.4	2.44		0.28	0.19	$5x10^{-5}$	0.013	0.017	0.05			<0.002	<0.001
SA2074A					5.4	61	0.29	10.4	3.53		82.2	2.44		0.25	0.18	$4x10^{-5}$	0.008	0.025	0.07			<0.002	<0.001
SA2273A					4.3	70	0.48	18.0	4.38		119	2.72		0.38	0.16	$6x10^{-5}$	0.014	0.061	0.12			<0.002	<0.001
KAS03	1003	107/252	7.7	850	1.1	56	0.21	11.4	2.78		94.3	0.21		0.03	0.12	$3x10^{-6}$	0.007	0.051	0.11			<0.002	0.004
KAS09	451	116/150	7.4	870	6.1	69	1.44	4.1	6.33		92.3	3.06		0.24	0.15	$7x10^{-5}$	0.013	0.008	0.03			<0.002	<0.001
Baltic water	(surface)				10.8	54	1.38	1.7	6.21		70.7	2.90		0.13	0.09	0.003	$5x10^{-5}$	0.003	0.01			<0.002	<0.001
GV1	?				56.8	0.019	0.022	0.36	0.22		0.69	0.19		0.01	0.48	0.089	0.003	0.001	$2x10^{-3}$			0.002	<0.001
GV9	?				18.8	0.43	0.042	0.54	0.63		0.37	0.32		0.02	0.28	0.009	0.001	$5x10^{-4}$	$1x10^{-3}$			0.006	<0.001
n.d.: not detected																							

4.1 Experimental

The water samples were filtered with 0.45 micrometer (Roth, Cellulose acetate, E 259.1) syringe-tip filters. UV/Vis spectra were recorded from 200 to 900 nm. Three samples were selected for concentration of fulvic acid by XAD-8 chromatography. Humic and fulvic acid shows strong sorption on XAD-8 resin at low pH. At high pH they desorb. Acidified water (pH 2 through addition of HCl) is pumped through a XAD-8 column (dead volume around 10 mL). Fulvic acid is desorbed with 0.1 M NaOH and collected as a concentrate. Concentrates (concentration factor around ten) are characterized by UV/Vis spectroscopy and measurement of DOC. For the sample SA2780A a sample was also concentrated by a factor of 272. Precipitate in the groundwater SA2273A was collected by a large pipette, acidified, and fulvic acid was isolated by XAD-8 chromatography.

4.2 DOC and UV/Vis spectroscopy of original and acidified water samples

DOC concentrations vary from 1.1 to 56.8 mgC/L (Table 2). In samples with low DOC concentrations, absorption is disturbed by other absorbing components than humic substances (Fig. 1 and Table 2). Estimation of metal ion complexation of fulvic acid shows that considerable part of fulvic acid functional groups are complexed. Furthermore, over-saturated phases may associate with fulvic acid and stabilize in solution. This will have an impact on the UV/Vis spectra. For this reason UV/Vis spectra are recorded on both original and acidified water samples (20μL 10 M HCl to 20 mL water followed by storage for about three weeks). The two samples with the lowest DOC concentrations show considerable deviation from each other with and without acidification, contrary to the other samples where deviation in absorption at 300 nm is around ±10 %. With decreasing DOC concentration (and thus decreasing absorption from humic and fulvic acid) the spectra also of acidified samples become progressively disturbed (Fig. 1 and Table 2). This shows that absorbing groundwater components disturb the spectra in addition to the impact of fulvic acid complexation.

The relationship between absorption at 300 nm (average between original and acidified) and the DOC concentration is:

$$A_{300} = 0.021\ (\pm\ 0.001) \times DOC - 0.037\ (\pm\ 0.013) \qquad (1)$$

The specific absorption of humic acid is considerably higher than for fulvic acid. The sample GV1 contains considerable amounts of humic acid. For this reason this sample has been excluded in calculating the above relationship between absorption and DOC.

Extrapolation to zero absorption at 300 nm results in a DOC value of 1.8 mgC/L. This verifies that DOC consists not only of UV/Vis absorbing humic and fulvic acid but also of non-absorbing organic components. This non-absorbing fraction of DOC is not enriched by XAD-8 chromatography, i.e. does not show hydrophobic character through protonation of functional groups at low pH, and is thus frequently called “hydrophilic organic carbon”.

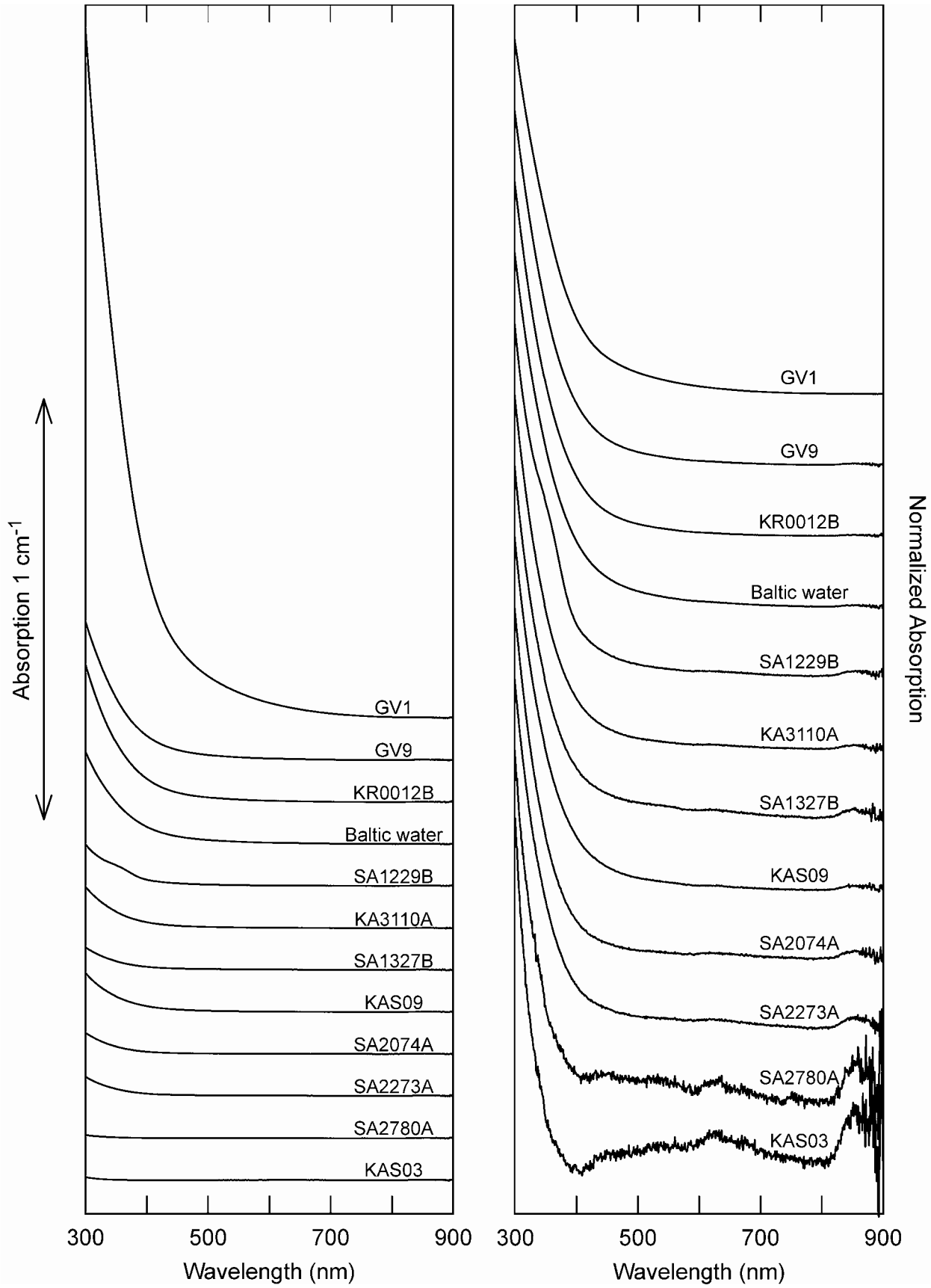

Fig 1: UV/Vis spectra of acidified water samples. Original scale in the left part of the figure, and normalized to the same height (at 300 nm) in the right part.

Table 2: DOC concentration, absorption at 300 nm wavelength of original water and acidified water samples stored for three weeks, and DOC after concentration by different factors by XAD-8 chromatography.

No.	Sample	DOC (mgC/L)	Spectrum[1)]	Abs. 300 nm (original)	Abs. 300 nm (acidified)	DOC (conc.≈x10)[2)]	DOC (conc.x272)
1.	SA1327B	6.2	Background	0.0571	0.0552		
2.	SA2780A	1.5	Disturbed[3)]	0.0102	0.0079	1.1	0.35
3.	KA3110A	6.3		0.101	0.099		
4.	KR0012B	15.7		0.309	0.329		
5.	SA1229 B	7.0	Shoulder	0.103	0.100		
6.	SA2074A	5.4	Background	0.0571	0.0513		
7.	SA2273A	4.3	Background	0.0533	0.0468		
8.	KAS03	1.1	Disturbed[3)]	0.0103	0.0073	1.1	
9.	KAS09	6.1		0.0976	0.0940		
10.	Baltic water	10.8		0.232	0.220		
11.	GV1	56.8		1.751	1.654		
12.	GV9	18.8		0.322	0.331	11.8	

Reproducibility of UV/Vis spectroscopy: Eight measurements of the same sample gave deviations of 0.03 % and 0.04 % for absorption at 300 nm and 400 nm. This should not be confused with correctness.
1: Negative appearance of UV/Vis spectra of acidified samples (cf. Fig. 1).
2: Concentration factors are 7.06, 11.7 and 15.6 for SA2780A, KAS03 and GV9, respectively.
3: Mainly background due to low humic substance concentration

4.3 Determination of fulvic acid in selected waters.

The results of fulvic acid concentration by XAD-8 chromatography are shown in Table 2. At a concentration factor of around 10 (cf. footnote of Table 2 for exact numbers), 63 %, 100 % and 67 % of DOC is evaluated to be fulvic acid for GV9, KAS03 and SA2780A, respectively. These numbers may be elevated through impact of organic contaminants, especially in the two latter samples with low DOC concentrations. By concentration of SA2780A by a factor of 272, 23 % of DOC is recovered as fulvic acid. At this concentration factor and corresponding large volume of water over the small column, losses of fulvic acid are possible. On the other hand, impact of contaminants is negligible. This number therefore, may be considered as a minimum value.

4.4 Fulvic acid in precipitate of SA 2273 A

In this sample, as well as in most of the other groundwaters, the Fe concentration shows drastic decrease in samples after shipping and handling in the laboratory. Precipitate in 2 L of this water was almost quantitatively sampled, acidified (HCl, ≈ pH 2) and left for dissolution of solid phase. The original solid phase was brown. A residual gray solid phase did not dissolve. Residual brown color was left in the column resisting elution with 0.1 M NaOH. This residual color was washed out with 0.1 M HCl. The concentration of fulvic acid, calculated for the total amount of water from which the precipitate originates, is calculated to be 0.25 mgC/L (by application of Eq. (1)). This should be compared with 4.3 mgC/L in the pre-

filtered groundwater sample. The absorption ratio at 300 to 400 nm is found to be 4.05. This is the lowest value found in this study and resembles humic acid rather than fulvic acid. This indicates that a relatively small amount of less hydrophilic humic substance is sorbed/co-precipitated. Humic acid has a higher specific absorption than fulvic acid. Furthermore, applying Eq. 1, all dissolved carbon is set to be fulvic acid. For these reasons the calculation of sorbed humic substance by Eq. (1) results in an over-estimation. Consequently, the amount of sorbed humic substance will be considerable less than the about 6 % calculated from Eq. (1). In summary, sorption of fulvic acid on precipitates from water shipped to the laboratory will not significantly affect isolation of fulvic acid.

5. Conclusions

Fulvic acid concentrations in all investigated water samples allow isolation of sufficient amounts of fulvic acid for the purpose of chemical, spectroscopic and isotopic characterization. In two of the investigated waters, on-situ pre-concentration by reverse osmosis could be considered. As an alternative 300 L or more could be shipped to the laboratory. Inorganic precipitates generated during shipping and handling under normal laboratory conditions will not sorb fulvic acid in amounts that have a significant negative impact.

Acknowledgements

The technical and administrative support from M. Laaksuharju, Geopoint AB, and water sampling, transport and supply with analytical data from C. Mattsén, SKB, is greatly appreciated. For UV/Vis spectroscopy and concentration of fulvic acids by XAD-8 chromatography we thank G. Teichmann and D. Jurrat.

6. References

[1] Buckau G., Artinger R., Kim J.I., Geyer S., Fritz P., Wolf M., Frenzel B. "Development of Climatic and Vegetation Conditions and the Geochemical and Isotopic Composition in the Franconian Albvorland Aquifer System", *Applied Geochemistry*, **15/8**, 2000, 1191-1201.

[2] Buckau G., Artinger R., Fritz P., Geyer S., Kim J.I., Wolf M. "Origin and Mobility of Humic Colloids in the Gorleben Aquifer System", *Applied Geochemistry*, **15/2**, 2000, 171-179.

[3] Artinger R., Buckau G., Geyer S., Wolf M., Kim J.I., Fritz P. "Characterization of Groundwater Humic Substances: Influence of Sedimentary Organic Carbon", *Applied Geochemistry*, **15/1**, 2000, 97-116.

Appendix 5

Characteristics of natural colloids in two groundwater samples from the Äspö HRL-tunnel

Ulla Vuorinen
VTT Processes

1 Introduction

Colloidal particles are of interest for the safety in final disposal of spent nuclear fuel because of their potential for transporting radionuclides from a faulty fuel canister in the repository to the biosphere. In general colloids are defined as small particles in the size range of 10^{-6} to 10^{-3} mm. However, in this context the size of colloids, which usually is of interest is < 0.45 μm, because only colloids which do not sediment in a very slow groundwater flow are potential carriers.

The natural background colloid concentrations and some of their characteristics from various bore holes along the Äspö HRL-tunnel were studied by several groups. In this study two bore holes **HA2780A** (on the 23.10.2001) and **SA2273A** (on the 24-25.10.2001) were sampled, which are in the following text referred to as **GW I** and **GW II**, correspondingly.

2 Sampling

Groundwater from the two bore holes mainly differed in salinity. The groundwater samples were treated on site in a nitrogen (grade 6.0) flushed movable glove-box at ambient temperature and stored in the glove-box until taken to Finland, where the samples were kept in a refrigerator until analysis. The continuous flushing with nitrogen allowed maintaining a slight over pressure throughout the activity. Oxygen content inside the box was measured (Orbisphere) continuously using a probe for *dissolved oxygen*, which also allowed measurement of the oxygen concentration in GW II sample giving a value of 23 ppb.

Centrifugal ultrafiltration tubes (Gelman) and filter membranes (Nuclepore) were used to treat the groundwater samples. In order to avoid particle contamination from air the filters and centrifugal tubes were assembled under laminar flow. In order to diminish oxygen contamination all equipment, membranes, tubes, sample bottles etc, were taken inside a laboratory glove-box (O_2 < 0.1 ppm) via a vacuum chamber. The assembled filters and ultracentrifugation tubes were closed inside plastic jars and all sample bottles were tightly closed before placing them inside tightly closing steel vessels for transportation. The steel vessels were taken out from the glove box and packed for transportation to Äspö HRL. The movable glove-box was flushed with N_2 already in Finland before transporting it to Äspö HRL where N_2 flushing was continued (O_2 down to 868 ppb) for several hours before taking the closed filter jars etc. from the steel vessels into it. N_2 flushing continued throughout the sampling. The actual sampling procedure was not started until the next day. Unfortunately the oxygen meter stopped working in the evening of the first day (last O_2 = 296 ppb at 20.45 on

the 22.10.2001.) and could not be brought to operation before the evening after completing sampling at GW I sampling point. The registered value when the meter started operating again was 6.46 ppb. While working in the glove-box the O_2 value measured varied between 2.5 ppb and 17.8 ppb depending on the temperature and objects needed to be taken into the glove-box via the flushing chamber.

The usage of the centrifuge inside the box produced extra heat increasing the working temperature from the ambient ≈ 15 °C up to ≈ 19-21 °C, which may have an additional effect on formation of carbonates besides the release of dissolved CO_2. These condition changes especially in respect of calcite behaviour were evaluated by modelling calculations (EQ3/6, DATA0.com) using the analysis results (by Paavo Ristola Oy) of both sampling points. As both total Fe and Fe^{2+} were analysed the pare could be used in computing the corresponding Eh. Some of the modelling results are given in Table 2.1. At 15°C in GW I calcite is only saturated, whereas in GW II it is slightly supersaturated. The increasing of the temperature up to 25 °C has an effect on the saturation of calcite by increasing it and thus calcite also becomes supersaturated in GW I indicating possibility for precipitation. Thus calcite may be present as an artefact in the examined colloid samples. (Several other minerals also showed supersaturation but further modelling and evaluation was out of the scope of this work).

Table 2.1 *Results from EQ3 modelling.*

		SA2273A	**HA2780A**
pH $_{given}$		7.7	7.9
Eh	V	0.062	0.055
Electrical imbalance	% of total charge	-1.5	0.5
$\mathbf{I_{true}}$	M	0.128	0.489
$\mathbf{pCO_2}$		-2.7	-4.1
$\mathbf{pO_2}$		-51.0	-50.7
Calcite at 15°C	SI =>	Supersaturated 0.70	Saturated 0.37
Calcite at 25°C	SI =>	Supersaturated 0.85	Supersaturated 0.51

2.1 Setup and filtration

The cumulative fractionation of groundwater samples was performed inside the glove-box, which was installed in the tunnel near by the two sampling points in question. The tubing from the groundwater sampling point was connected via a quick coupling through the glove-

box wall to enable the collection of groundwater directly inside the anoxic glove-box when needed.

Inside the glove-box a small centrifuge was operated with centrifugal ultrafiltration tubes. Three different cut-off sizes were used, 0.3 μm, 300 kD and 10 kD (6 tubes for each size). Groundwater without prefiltration collected in a plastic bottle inside the glove-box was pipetted (10 mL/tube/centrifugation round) in the six ultrafiltration tubes with the same cut-off size and spun for 10 to 30 min at 6 000 rpm in the six-place centrifuge rotor. This allowed 60 mL of groundwater to be handled per spinning round. The filtrates from the receiver tubes were combined and collected in a plastic bottle and a new 10 mL volume of groundwater/tube was added to the remaining concentrate in the tube and the spinning was repeated. When enough groundwater had been treated thus, the concentrates (about 0.5-1.5 mL/tube) were rinsed with anoxic deionised water (10 mL of H_2O/tube) spinning once more in the centrifuge in order to remove salts. Again the filtrates were combined in one plastic bottle and the remaining concentrates were combined in another plastic bottle. Finally the filter tubes were rinsed with 1% HNO_3 (suprapure, 10 mL/tube) and the rinse solutions combined. A schematic of the procedure is shown in Figure 2.1. Altogether 4 different solution types were obtained for chemical analysis for each cut-off value; the filtrates, the concentrate rinse waters, the rinsed concentrates and acid rinses.

In addition to the solution samples filter membranes with two cut-off values, 0.4 μm and 0.05 μm, were prepared for SEM/EDS analysis.60 mL of groundwater was filtered through the membranes using both sequential filtration and separate filtration without additional prefiltration. The membranes used in separate filtrations were washed with 10 mL of deionised anoxic water in order to remove salts. Thus eight filter membranes were obtained. The SEM micrographs and EDS spectra are presented in appendix 1 and 2.

All samples prepared remained inside the glove-box until brought back to Finland.

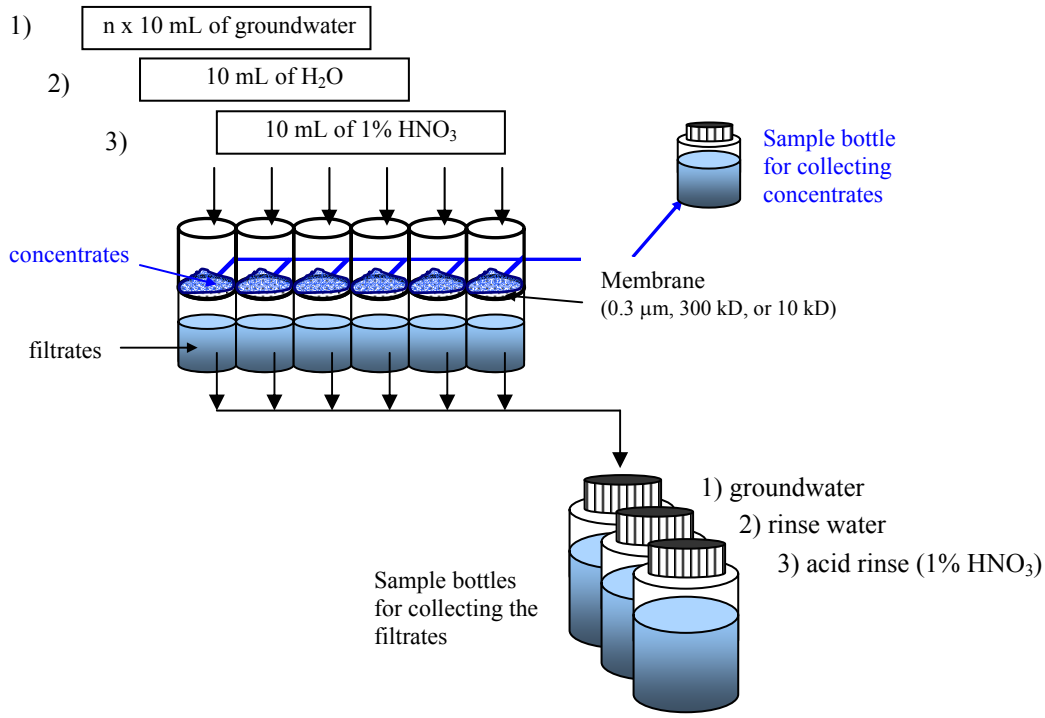

Figure 2.1 *Schematic of the procedure in groundwater sampling.*

3 Analysis results

3.1 Solution analysis

Table 3.1 gives the analysis results for the solution samples collected in the ultrafiltration procedures. Small amounts of collected samples did not allow performance of anion analysis from other fractions than the filtrate, and especially the amount of concentrate was only a few millilitres resulting in rather high detection limits for Al and Si. The few Al results obtained are quite high compared to those obtained in the groundwater analysis (results from Paavo Ristola Oy) giving reason to suspect a possible contamination. The analysis results on filtrate and concentrate washing water clearly show that more salt is retained with the smaller cut-off sizes, more prominently with 10 kD ultrafilters.

Table 3.1 *Analysis results for the various solution samples collected*

		GW I 0.3 µm	GW I 300 kD	GW I 10 kD	GW II 0.3 µm	GW II 300 kD	GW II 10 kD
Concentration factors		*62*	*57*	*18*	*129*	*80*	*46*
Filtrates							
Na	mg/L	**3600**	**3600**	**3600**	**1700**	**1700**	**1700**
K	mg/L	**14**	**14**	**14**	**15**	**14**	**15**
Ca	mg/L	**4800**	**4900**	**4800**	**690**	**700**	**700**
Mg	mg/L	**37**	**37**	**36**	**111**	**112**	**113**
Si	mg/L	**2.4**	**2.4**	**2.4**	**3.3**	**3.3**	**3.3**
Fe_{tot}	mg/L	**0.050**	**0.054**	**0.058**	**0.623**	**0.653**	**0.609**
Al	mg/L	**1.9**	**2.8**	**1.6**	**1.3**	**1.2**	**1.1**
Cl	mg/L	**12000**	**12000**	**12000**	**3600**	**3600**	**3600**
SO_4	mg/L	**650**	**660**	**660**	**310**	**300**	**300**
Br	mg/L	**115**	**118**	**115**	**21**	**21**	**21**
Rinsing water							
Na	mg/L	**160**	**180**	**590**	**80**	**110**	**230**
K	mg/L	**0.67**	**0.75**	**2.26**	**0.79**	**1.02**	**2.02**
Ca	mg/L	**210**	**240**	**770**	**34**	**47**	**95**
Mg	mg/L	**1.6**	**1.8**	**5.8**	**5.6**	**7.1**	**14.3**
Si	mg/L	**0.16**	**0.18**	**0.47**	**0.21**	**0.26**	**0.50**
Fe_{tot}	mg/L	**0.003**	**0.008**	**0.013**	**0.029**	**0.043**	**0.040**
Al	mg/L	*< 0.2*	*< 0.2*	**1.50**	*< 0.2*	*< 0.2*	*< 0.2*
Rinsed concentrate							
Amount of concentrate [mL]		*1.95*	*2.11*	*6.60*	*2.10*	*4.1*	*7.18*
Na	mg/L	**180**	**160**	**480**	**82**	**87**	**160**
K	mg/L	**0.90**	**0.87**	**2.2**	**1.1**	**1.0**	**1.7**
Ca	mg/L	**240**	**220**	**640**	**34**	**36**	**66**
Mg	mg/L	**1.8**	**1.6**	**4.7**	**5.2**	**5.5**	**10.2**
Si	mg/L	*< 0.5*	*< 0.5*	*< 0.5*	*< 0.5*	*< 0.5*	*< 0.5*
Fe_{tot}	mg/L	**0.039**	**0.027**	**0.021**	**0.110**	**0.046**	**0.070**
Al	mg/L	*< 0.6*	*< 0.6*	**2.10**	*< 0.6*	*< 0.6*	*< 0.6*
Acid rinse							
Na	mg/L	**11.4**	**8.3**	**15.2**	**8.6**	**5.0**	**5.4**
K	mg/L	*< 0.2*	*< 0.2*	*< 0.2*	*< 0.2*	*< 0.2*	*< 0.2*
Ca	mg/L	**13.4**	**10.6**	**19.2**	**3.5**	**2.0**	**2.3**
Mg	mg/L	**0.11**	**0.08**	**0.16**	**0.50**	**0.29**	**0.31**
Si	mg/L	*< 0.1*	*< 0.1*	*< 0.1*	*< 0.1*	*< 0.1*	*< 0.1*
Fe_{tot}	mg/L	**0.027**	**0.035**	**0.013**	**0.120**	**0.084**	**0.426**
Al	mg/L	*< 0.2*	*< 0.2*	*< 0.2*	*< 0.2*	*< 0.2*	*< 0.2*

< *denotes below detection limit (given by the value)*

By assuming that Na is in soluble form and represents the behaviour of salt retention then calculating different element concentration ratios and comparing the results between the different solution samples some indications may be seen as the soluble elements should follow the same ratios in the samples;

- The results for Si and Fe in both GW I and GW II samples are indicative of some retention occurring in all three cut-off sizes. Thus there are particles associated with these elements in all three fractions studied; particles > 0.3 μm, size ranges 300 kD – 0.3 μm and 10 kD – 300 kD. However, the highest Fe retention was indicated for the 10 kD cut-off and thus the size range for the majority of Fe associated particles in both groundwater samples is 10 kD – 300 kD. Some Fe may have also become sorbed on the ultrafiltration devices. The majority of Si associated particles in GW I were also retained with the smallest cut-off indicating that the size range is 10 kD – 300 kD. In GW II no clear difference between the size ranges of Si associated particles could be seen.
- The results for acid rinse samples were subtly allusive of Mg retention, indicating Mg association mostly with particles > 0.3 μm for GW I and for GW II the association would involve all three fractions studied.
- Minor retention of Ca was seen in GW II samples in all three size ranges. This can partly be an artefact of calcite precipitation as modelling results indicated.
- Filtrate and washing water results for K indicated slight retention in both GW samples, somewhat more in the two bigger size ranges; > 0.3 μm and 300 kD – 0.3 μm.
- If the suspect values for Al are considered only one (due to results < detection limit) indication of Al retention in GW I was seen for the smallest cut-off size.

3.2 SEM/EDS

The SEM micrographs and the EDS spectra obtained are presented in Appendix 1 and 2 for GW I and GW II groundwater samples correspondingly. In the EDS spectra the peaks of Au come from the gold coating of the specimen, and Cu and Zn peaks from the brassy specimen holder. In addition, Appendix 1 (Figure A9) includes micrographs of blank Nuclepore filters and the corresponding EDS spectrum. It has to be noted that the presented micrographs and the EDS spectra of single particles on a filter membrane specimen do not cover but a small

selection of the specimen area, and thus other kind of particles and elements involved may have remained undetected.

Figures A1-A4 and B1-B4 are of the GW I and GW II samples filtered sequentially and not washed with anoxic water, whereas Figures A5-A8 and B5-B8 are separately filtered GW I and GW II samples without prefiltration and washed with anoxic deionised water.

The high backgrounds in the EDS spectra suggest the presence of lighter elements, e.g., hydrogen, carbon, nitrogen and oxygen, which are not detected by EDS. These elements are major constituents in organic material and thus the high background can be considered as an implication of the presence of organic material, but also e.g. carbonates and hydroxides are possible. There is a distinct difference between the EDS spectra backgrounds of the two groundwater samples, compare e.g., Figs. A1, A3, and A5, with Figs. B1, B3, and B5.

Figure A2 and B2 micrographs of the 0.4 μm membranes show that both groundwater samples contain small particles (much smaller than the cut-off size of 0.4 μm) aggregated quite similarly but the amount is greater on the less saline GW II sample specimen. In addition to the aggregates of small particles also larger particles with different morphology are present. The EDS spectra give the presence of Fe, Ca, Si and Cl, of which Cl is an indication of possible salts remained on the specimen, most probably $CaCl_2$ (Fig. A1) in the case of GW I by the ratio of the Ca and Cl peaks, and in the case of GW II both NaCl and $CaCl_2$ (Fig. B1) may be possible. Fe is associated with the small particle aggregates.

When comparing Figures A4 and B4 of the 0.05 μm membrane specimen of the particle agglomerations the difference in the background level in the EDS spectra is more prominent for GW II again and only small peaks for Ca and Cl are seen. The high background may be due to organic material present. The morphology of the small particle aggregates is very similar to that seen on the 0.4 μm specimen (Fig. B2). EDS spectra of the particle agglomerations show the presence of Fe, Ca, Cl and Si, but for the more saline GW I the peaks of Ca, Cl and Si are much more prominent and also peaks for S and Ti are detected indicating more inorganic nature of the aggregated particles. The ratio of Cl and Ca peaks support the presence of Ca also in other phases than $CaCl_2$.

Further characterisation of the small aggregated particles (e.g., Figs. A2 and B2) is possible by making TEM specimen, however, such study was not included here.

4 Discussion and conclusions

The results from SEM/EDS studies and the indicative results based on ultrafiltration samples are in good agreement of the characteristics of the particle phases present in the two groundwaters. However, the obtained results did not allow calculation of the actual concentration of the element association with the different particle phases.

APPENDIX 1: SEM micrographs and EDS spectra for groundwater sampled at Äspö Hard Rock Tunnel, sampling point **HA2780A = GW I**.

Figures A1-A4 are of GW I sample filtered sequentially through the 0.4 µm and 0.05 µm Nuclepore filters. Figures A5-A8 are of the separately filtered samples using the same pore sizes as in the sequential filtration.

Micrographs were taken of each filter with two different magnifications, 500- and 10 00-fold. For the 500-fold magnification the EDS spectrum is a general one over the filter, whereas in the case of larger magnifications (10 000-fold) the EDS spectra are of particles or an agglomeration, where the target area is about the size of circle with a diameter of 1 µm.

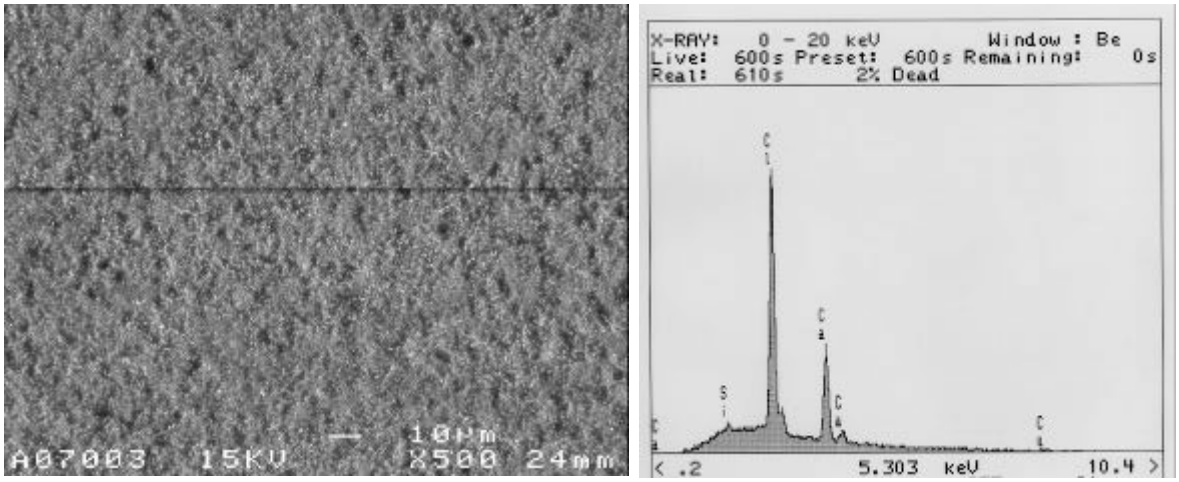

Figure A1. *SEM micrograph of the 0.4 µm filter membrane (magnification= x500) on the left and on the right an EDS spectrum over the filter membrane.*

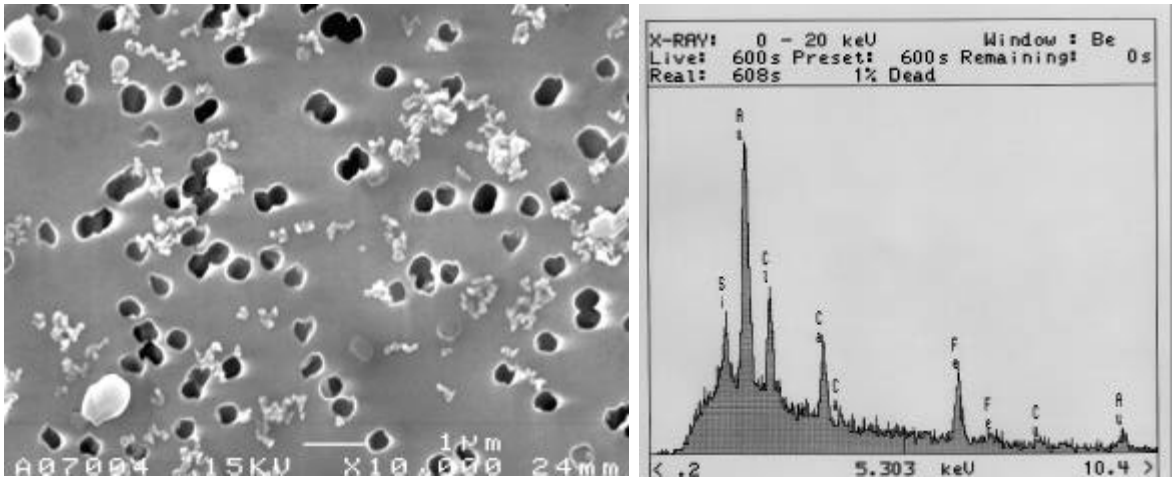

Figure A2. *SEM micrograph of the 0.4 µm filter membrane (magnification= x10 000) on the left and on the right the EDS spectrum of a particle agglomeration.*

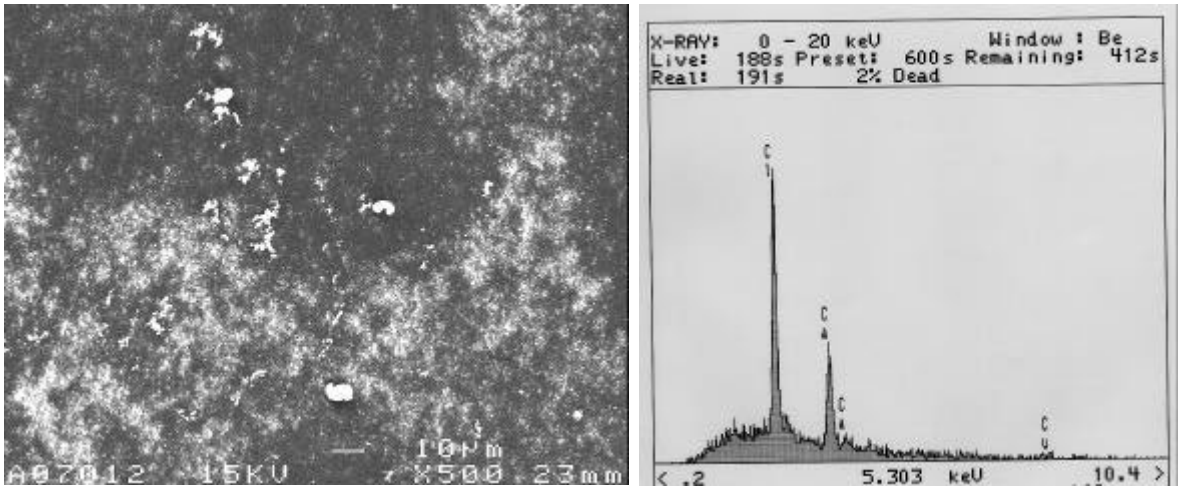

Figure A3. *SEM micrograph of the 0.05 µm filter membrane (magnification= x500) on the left and on the right an EDS spectrum over the filter membrane.*

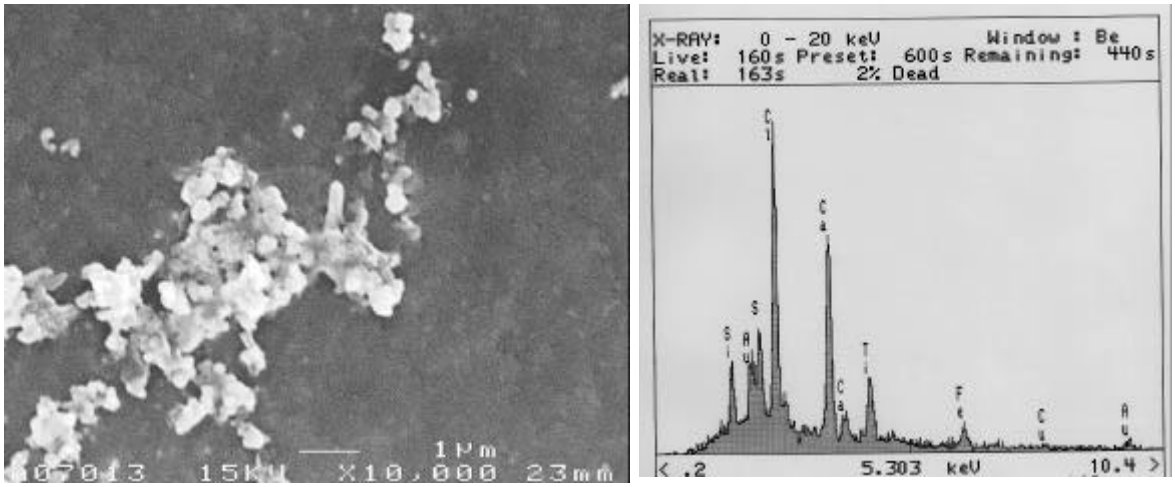

Figure A4. *SEM micrograph of the 0.05 µm filter membrane (magnification= x10 000) on the left and on the right the EDS spectrum of a particle agglomeration.*

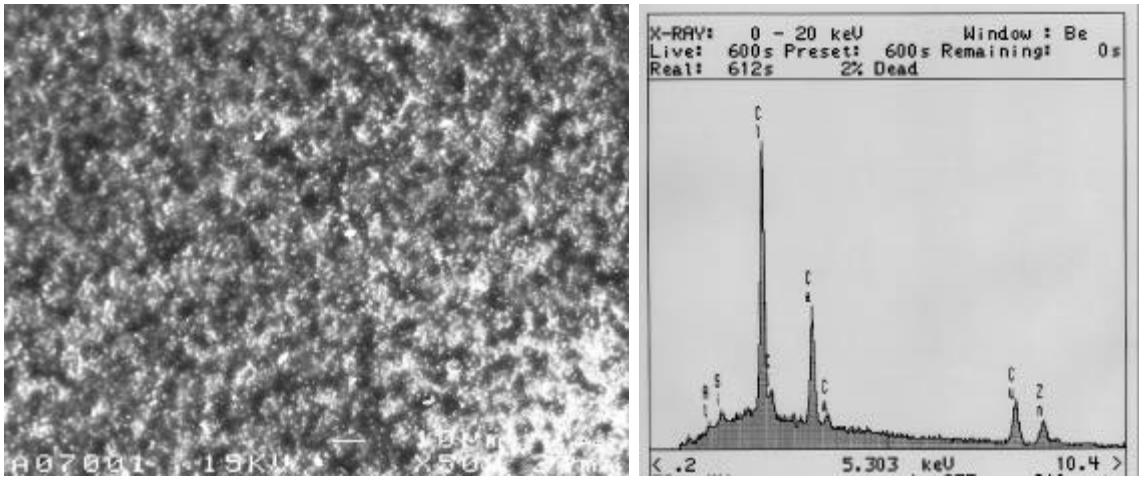

Figure A5. *SEM micrograph of the 0.4 μm filter membrane (magnification= x500) on the left and on the right an EDS spectrum over the filter membrane.*

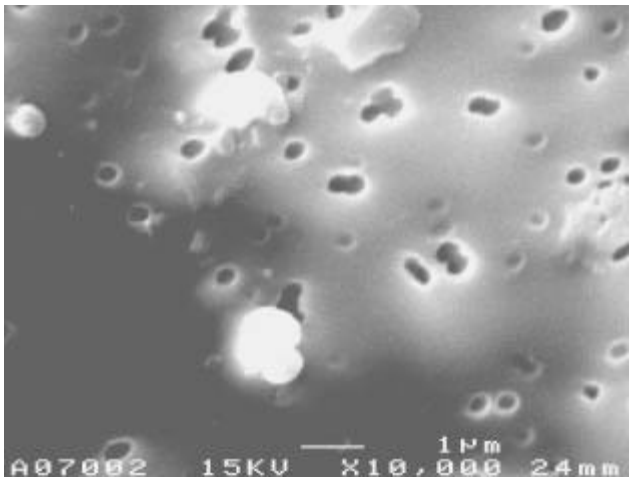

Figure A6. *SEM micrograph of the 0.4 μm filter membrane (magnification= x10 000) on the left. No EDS spectrum was obtained (not enough scattering due to small amount of material on the membrane).*

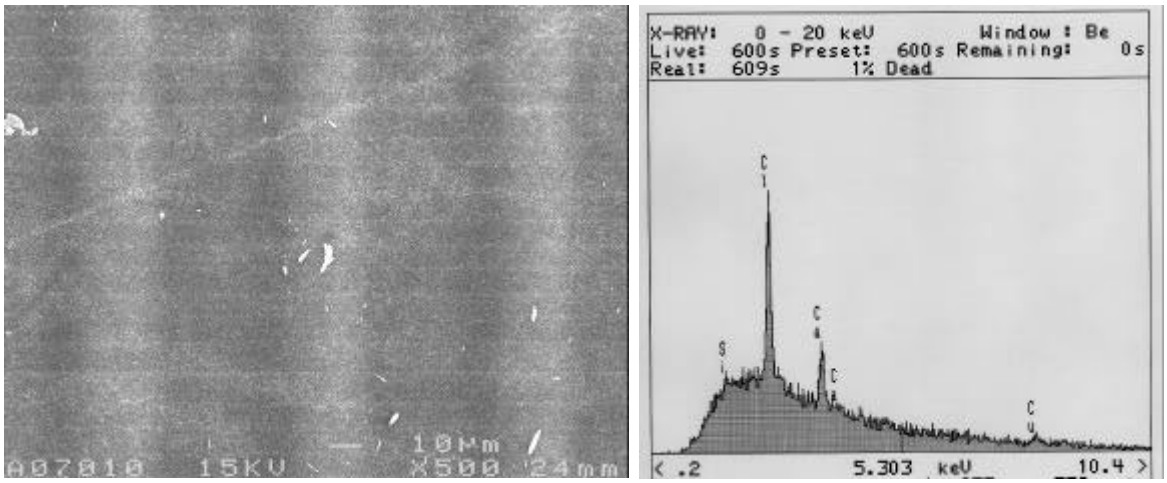

Figure A7*. SEM micrograph of the 0.05 µm filter membrane (magnification= x500) on the left and on the right an EDS spectrum over the filter membrane.*

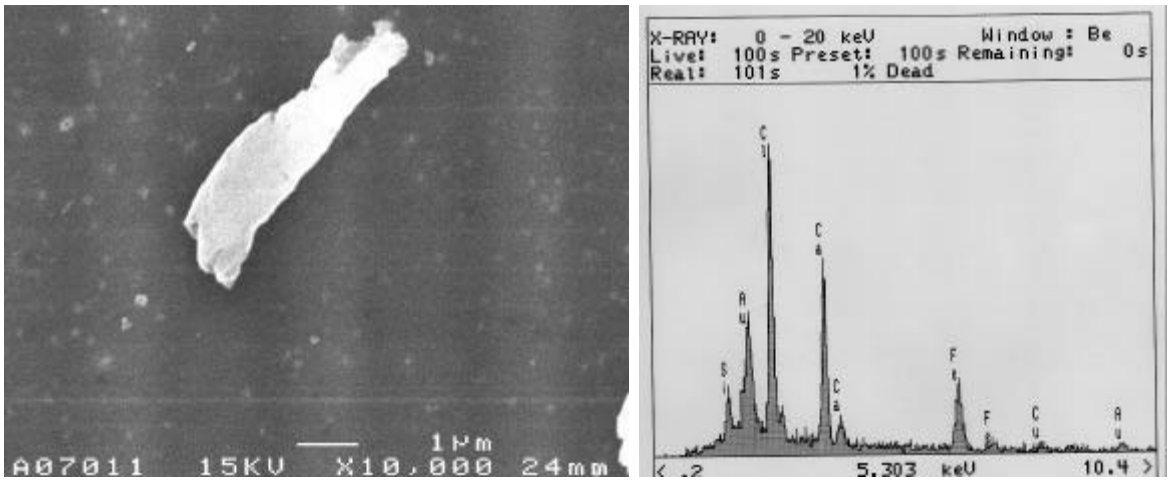

Figure A8. *SEM micrograph of the 0.05 µm filter membrane (magnification= x10 000) on the left and on the right the EDS spectrum of a particles?.*

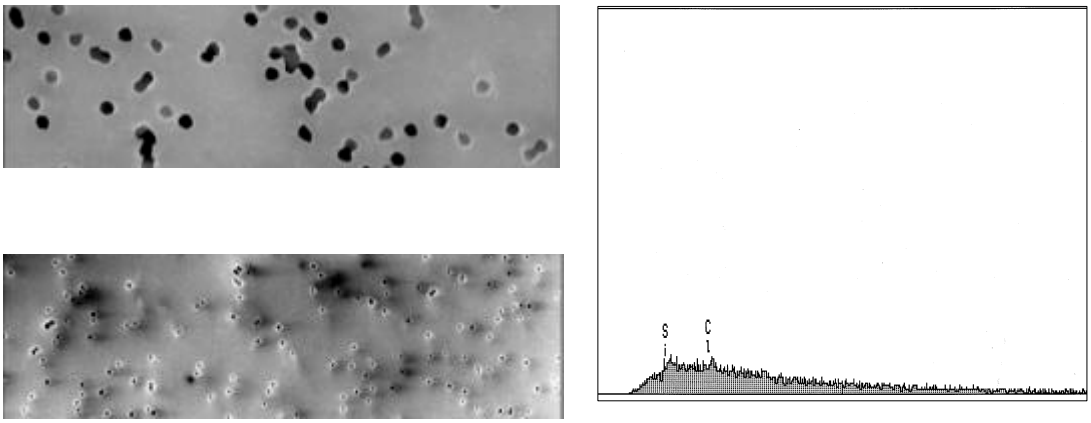

Figure A9. *On the left SEM micrograph of the blank 0.4µm (upper) and 0.1µm (lower) Nuclepore filter membranes (magnification= x10 000) and on the right the EDS spectrum of a blank filter.*

APPENDIX 2: SEM micrographs and EDS spectra for groundwater sampled at Äspö Hard Rock Tunnel, sampling point **SA2273A = GW II**.

Figures B1-B4 are of GW I sample filtered sequentially through the 0.4 µm and 0.05 µm Nuclepore filters. Figures B5-B8 are of the separately filtered samples using the same pore sizes as in the sequential filtration.

Micrographs were taken of each filter with two different magnifications, 500-fold and 10 000- or 5 000-fold. For the 500-fold magnification the EDS spectrum is a general one over the filter, whereas in the case of larger magnifications (5 000- or 10 000-fold) the EDS spectra are of particles or an agglomeration, where the target area is about the size of circle with a diameter of 1 µm.

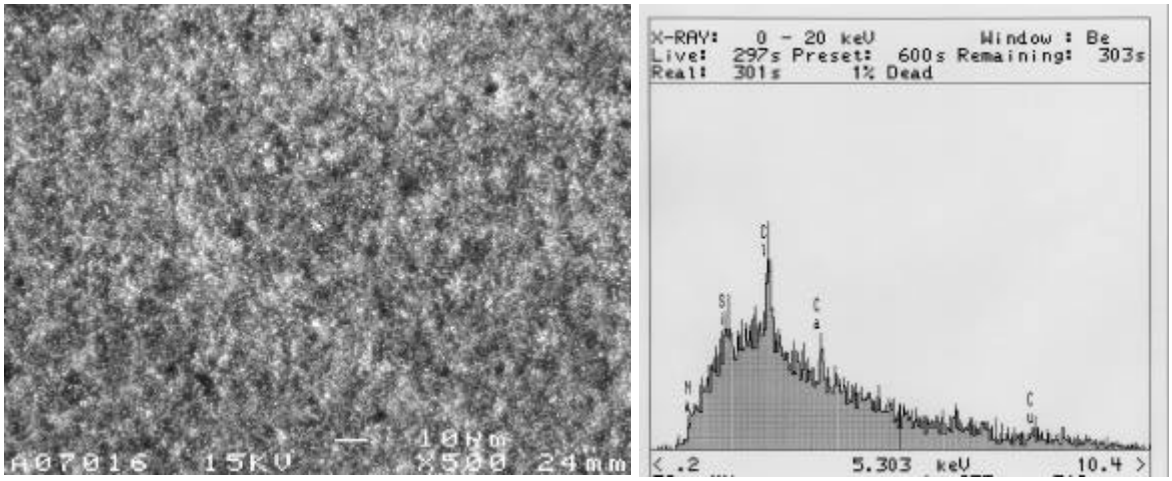

Figure B1. *SEM micrograph of the 0.4 µm filter membrane (magnification= x500) on the left and on the right an EDS spectrum over the filter membrane.*

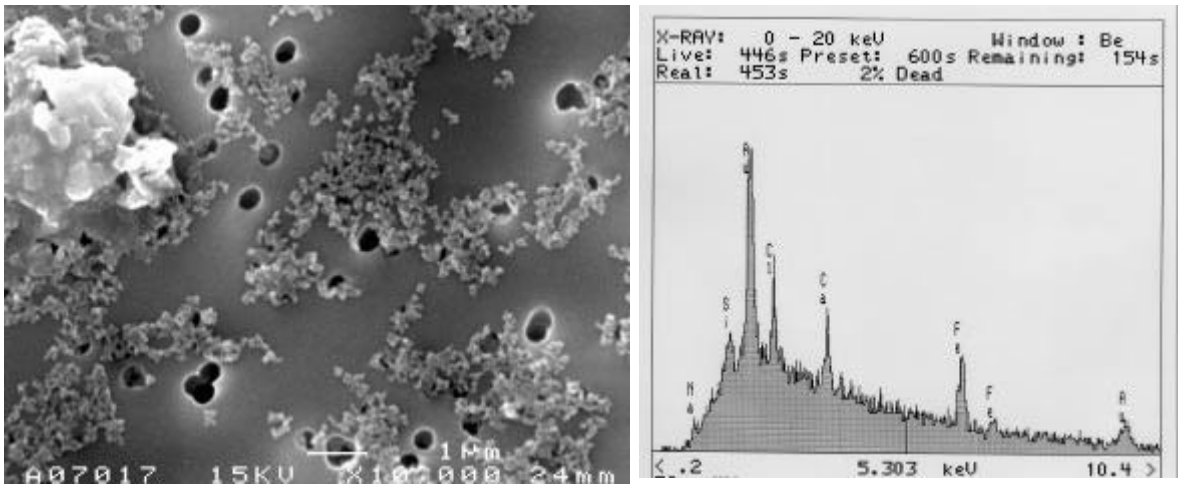

Figure B2. *SEM micrograph of the 0.4 µm filter membrane (magnification= x10 000) on the left and on the right the EDS spectrum of a particle agglomeration.*

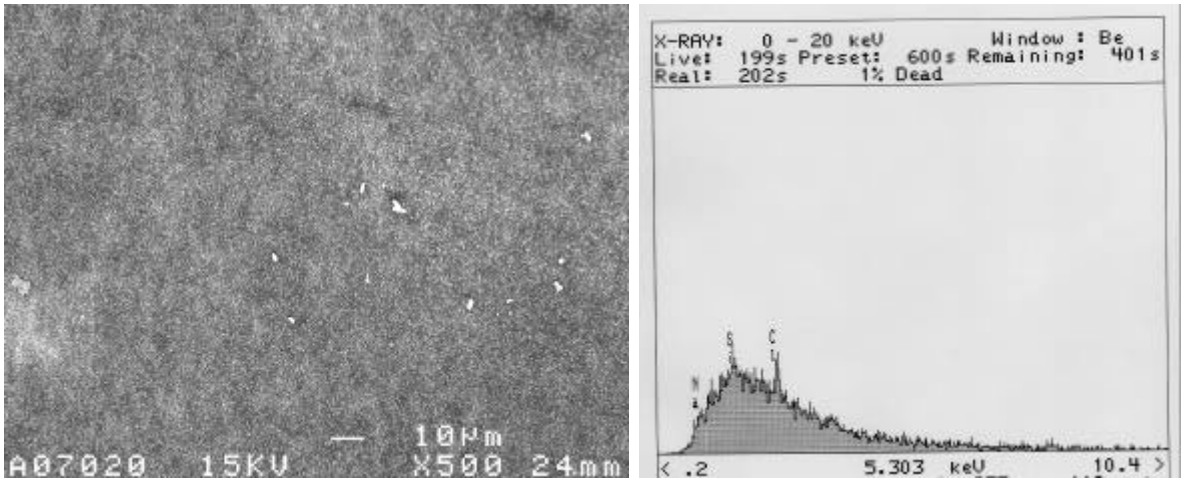

Figure B3. *SEM micrograph of the 0.05 µm filter membrane (magnification= x500) on the left and on the right an EDS spectrum over the filter membrane.*

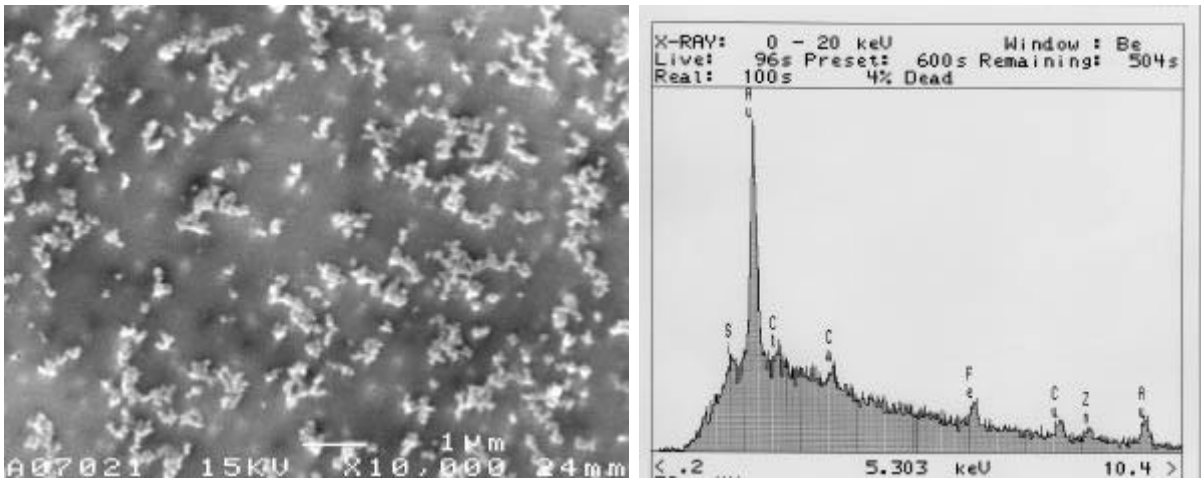

Figure B4. *SEM micrograph of the 0.05 µm filter membrane (magnification= x10 000) on the left and on the right the EDS spectrum of a particle agglomeration.*

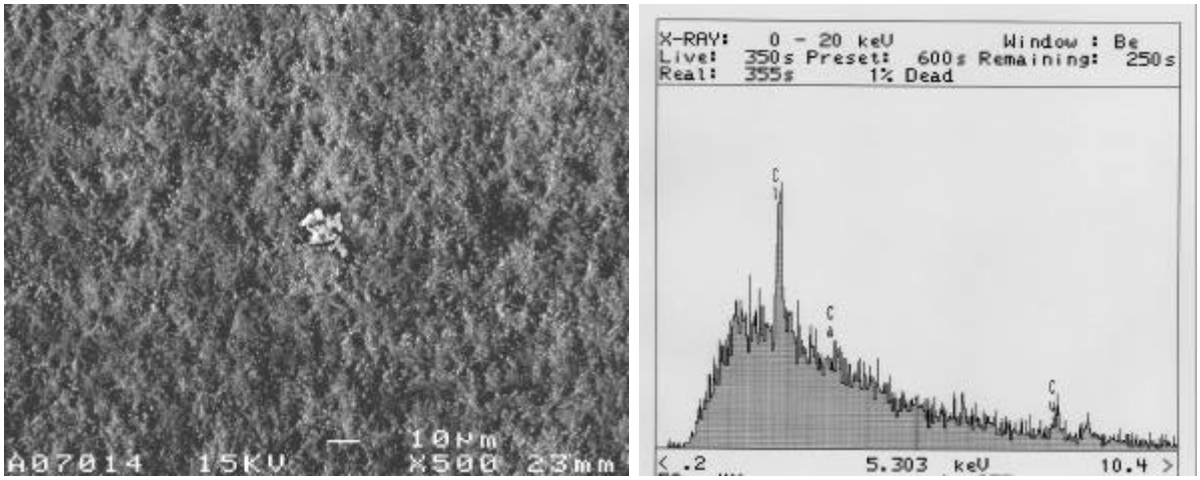

Figure B5. *SEM micrograph of the 0.4 µm filter membrane (magnification= x500) on the left and on the right an EDS spectrum over the filter membrane.*

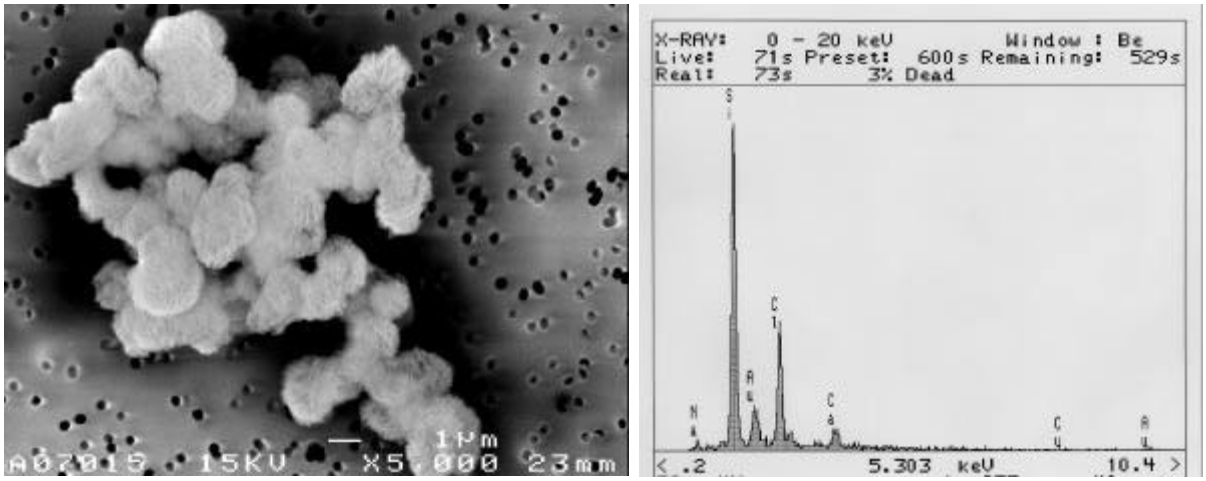

Figure B6. *SEM micrograph of the 0.4 µm filter membrane (magnification= x10 000) on the left and on the right an EDS spectrum of a particle agglomeration.*

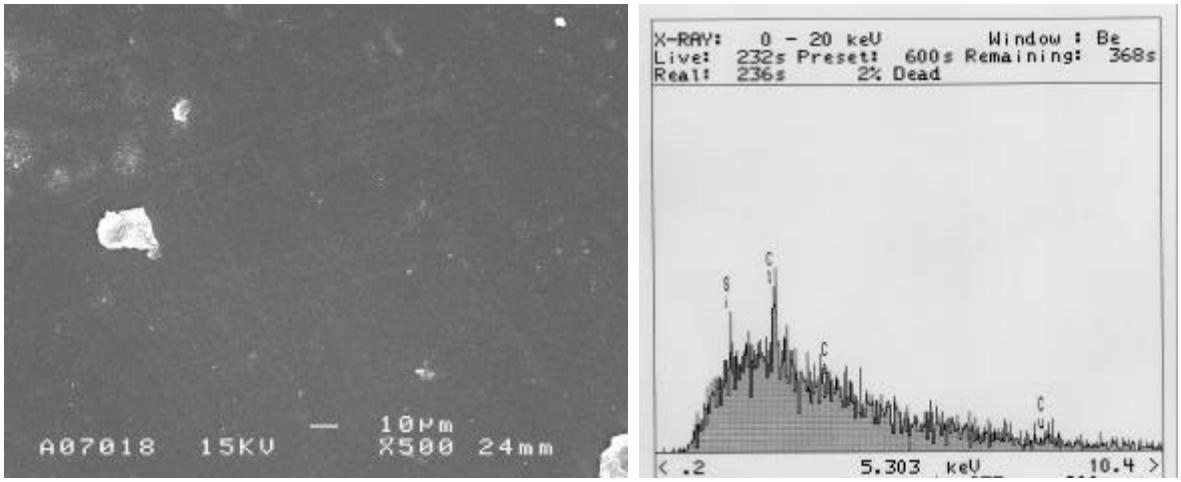

Figure B7*. SEM micrograph of the 0.05 µm filter membrane (magnification= x500) on the left and on the right an EDS spectrum over the filter membrane.*

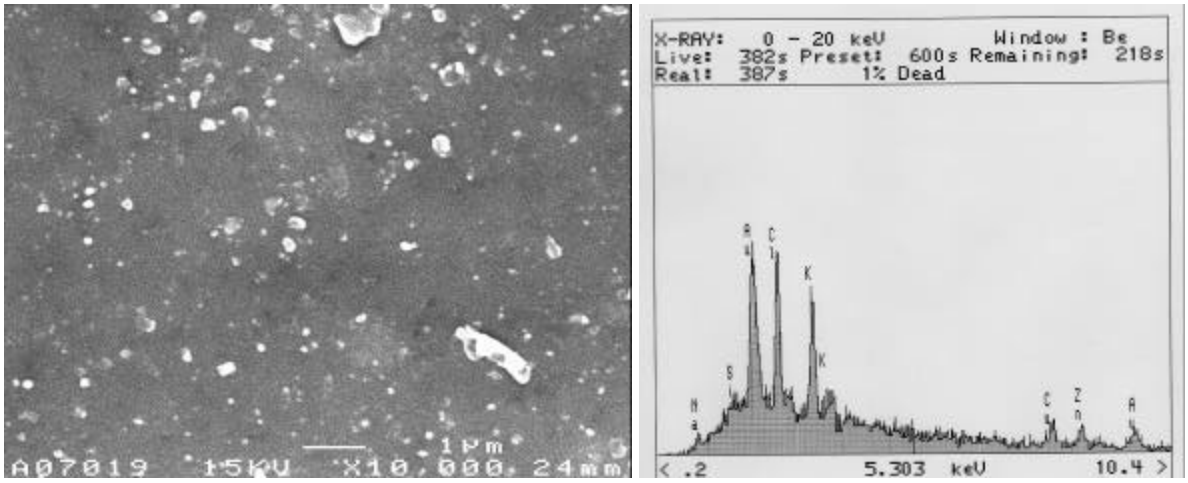

Figure B8. *SEM micrograph of the 0.05 µm filter membrane (magnification= x10 000) on the left and on the right the EDS spectrum of the particles.*

Appendix 6

Groundwater sampling in Äspö tunnel

Minna Rantanen
Consulting Engineers Paavo Ristola, Industry and Power Plant Chemistry

Mia Mäntynen
Posiva Oy

1 Background

The aim of the groundwater sampling for chemical analysis was to compare the sampling techniques and analysis between SKB and POSIVA for QA-purposes and for Posiva to get experience in sampling of groundwater from larger depth from underground facilities for planning of ONKALO phase groundwater sampling.

The boreholes, which were sampled, represented different water types of different salinity range, since it is known that the colloid stability can change with the ion content of the groundwater. The selected boreholes were used to measure the background colloid content, humic substances and microbes. Experimental concepts for the Colloid project were: laboratory experiments, background measurements, borehole specific experiment and possibly fracture specific experiment.

Three groundwater samples were collected by the Posiva team from the following sampling points HA 2780A, SA 2273Aand KA 1755A.

The sampling in Äspö tunnel was carried out 22 – 26 October, 2001.

2 Experimental

The groundwater samples were collected according to Posiva field instructions (Ruotsalainen et. al. 1998). Since 1998 the same system and methods are used in all Posiva's groundwater samplings. The on-line filtering and collecting systems were connected to the sampling line of the borehole. The main part of the samples were filtered through Millipore 0,45 μm filter by an on-line filtering system (e.g. anions, cations, alkalinity, acidity, pH).

Samples for the isotopes (H-3, H-2, O-18,) were taken directly into their own containers. Parameters sensitive to atmospheric contamination or transport delay (e.g. alkalinity, acidity, Fe^{2+}, Fetot, S^{2-}tot, anions, NH_4) were analyzed directly after sampling in the field laboratory at Äspö. The other water samples for parameters to be analyzed in the laboratories in Finland were invariably preserved in accordance with the Posiva field instructions (Ruotsalainen et al. 1998).

2.1 Experimental setup

The on-line collecting systems were set up in the SKB´s field laboratory. Each collecting system

is equipped with a 0,45 µm filter and the system was rinsed and filled with nitrogen gas before taking into operation in the field for groundwater sampling in the Äspö tunnel. The collecting system was connected with a teflon tube and a Swagelock fitting to the borehole. The teflon tube was rinsed with groundwater before the sampling was started.

Each collecting system was filled up with water. Then water sample was bottled in field laboratory by using nitrogen gas to the washed plastic and glass bottles. The samples were handled the way shown in *Table 1*.

Table 1. Methods of sampling, bottling and preservation.

Parameters analysed in the field laboratory	**Sample amount (l) and the type of the container**	**Filtered 0,45 µm**	**Other instructions**
pH, alkalinity and acidity	1 x 0,5 Pyrex-glass bottle	x	titrations carried out in N_2-atmosphere
Conductivity	1 x 0,1 PE	-	
Fe_{tot}, Fe^{2+}	6 x 0,05 acid washed glass volumetric flask	x	4 ml ferrozine buffer solution
Cl	1 x 0,25 PE	x	
NH_4^+	2 x 0,1 PE	-	
S^{2-}	3 x 0,1 Winkler-bottle	Collected under N2-atmosphere, but not filtered	0,5 ml 1 M Zn $(Ac)_2$+ 0,5 ml 1 M NaOH
Parameters Analysed in laboratory	**Sample amount (l) and the type of the container**		
pH, SiO_2	1 x 0,5 PE	x	
Conductivity	2 x 0,5 PE	-	
Anions	1 x 0,2 PE	x	
DIC/DOC	2 x 0,25 l glass bottle with glass stopper	x	
Metals, GFAAS, ICP-MS	1 x 0,2 PE, acid washed bottle	x	1 ml conc. pa^+. HNO_3
PO_4	1 x 0,5 PE	x	5 ml 4 M H_2SO_4
S_{tot}	1 x 0,1 PE	x	
^2H, ^{18}O	2 x 0,01 Venoject tube	-	
^3H	2 x 0, 25 l dark, glass bottle	-	

The samples were kept cold until the delivery to Finland and sending to other laboratories.

2.3 Analysis

Immediately after each sampling, the analyses, which are marked in the *Table 2,* were made in SKB´s field laboratory. The analysis are based on the international standards and methods which are developed further for Posiva´s purposes to analyze groundwater samples of high ionic strength. The recovery tests have been made for ISE, anion and metal analyses. An acceptable

level of the recovery is 80-120%. To check the quality of the results and methods a reference water (OL-SO, Vuorinen et al. 1997) was analyzed both in field and in the laboratories in Finland. The accepted upper and lower limits for OL-SO water have been calculated from the analyze results from several years. The commercial, certified reference waters were used for the metals, DIC and DOC-analyses in Consulting Engineers Paavo Ristola´s Myyrmäki and Hollola laboratories.

3 Results and discussion

The results and analytical methods used are shown in *Table 2.*

Table 2. Results of the water analysis

Analysis	**Unit**	**HA 2780A**	**SA 2273A**	**KA 1755A**	***Standard/Method***
Conductivity 25°C[A]	MS/m	3 480	1 140	3 190	*SFS-EN 27 888, conductivity electrode WTW Tetracon 325*
Conductivity 25°C[B]	MS/m	3 440	1 120	3 220	*SFS-EN 27 888, conductivity electrode Ingold, C 10,3*
pH[A]		7,9	7,7	7,9	*SFS 3021, pH-electrode Orion Ross 82-72BN*
pH[B]		7,6	7,5	7,5	*SFS 3021, pH-electrode Orion Ross 81-72 BN*
Alkalinity, m-value[A]	meq/l	0,24	2,6	0,13	*SFS-EN ISO 9963-1 and Gran-titration by extrapolation, Mettler-Toledo DL-50*
Alkalinity, p-value[A]	meq/l	<0,01	<0,01	<0,01	*SFS-EN ISO 9963-1, Mettler-Toledo DL-50*
Acidity, -p–value[A]	meq/l	0,06	0,24	0,05	*SFS 3005, Mettler-Toledo DL-50*
Bicarbonate, HCO_3[A]	mg/l	15	158	7,9	*SFS 3005, calculated*
Ammonium, NH_4^{+}[A]	mg/l	<0,05	0,89	<0,05	*ASTM 1426, Orion 95-12 ISE*
Sulfide, S^{2-}[A]	mg/l	<0,01	<0,01	<0,01	*SFS 3038, Philips PU 8670 UV-VIS spectrophotometer*
Iron, (tot)[A]	mg/l	0,088	0,78	0,21	*Central Electricity Research Laboratory by ferrozinethio-glycolacidmethod,Philips PU 8670 UV-VIS spectrophotometer*

Analysis	Unit	HA 2780A	SA 2273A	KA 1755A	*Standard/Method*
Iron, Fe^{2+A}	mg/l	0,082	0,76	0,20	*Central Electricity Research Laboratory by ferrozinethioglycolacidmethod, Philips PU 8670 UV-VIS spectrophotometer*
Iron, (tot)[B]	mg/l	0,075	0,79	0,19	*SFS 5074, Perkin-Elmer 4100 ZL HGA*
Chloride, Cl^{B}	mg/l	13 100	3 630	11 800	*SFS 3006, Mettler-Toledo DL-50*
Bromide, Br^{B}	mg/l	97	17	89	*Perkin-Elmer Elan 6000, ICP-MS*
Nitrite, NO_2^{B}	mg/l	<0,05	<0,05	<0,05	*SFS-EN ISO 10304-1, Shimadzu HPLC with UV-detector SPD6-A*
Nitrate, NO_3^{B}	mg/l	< 0,05	<0,05	<0,05	*SFS-EN ISO 10304-1, Shimadzu HPLC with UV-detector SPD6-A*
Phosphate, PO_4^{B}	mg/l	<0,006	<0,006	<0,006	*SFS 3025, Shimadzu UV-VIS 120-02 spectrophotometer*
Sulfate, SO_4^{B}	mg/l	620	270	640	*SFS-EN ISO 10304-1, Dionex DX-100*
Silicate, SiO_2^{B}	mg/l	8,9	12	8,5	*Juoma- ja talousveden tutkimusmenetelmät, Shimadzu UV-VIS 120-02 spectrophotometer*
Dissolved inorganic carbon, DIC[B]	mg C/l	1,7	21	0,8	*ASTM D4839, own developed analyzer with IR-detector*
Dissolved inorganic carbon, DIC[C]	mg C/l	*2,4*	*32,3*	*1,2*	*SFS EN 1484, Shimadzu TOC-5000 analyzer*
Dissolved organic carbon, DOC[B]	mg C/l	0,9	3,6	0,5	*ASTM D4839, own developed analyzer with IR-detector*
Dissolved organic carbon, DOC[C]	mg C/l	*1,0*	*4,8*	*0,7*	*SFS EN 1484, Shimadzu TOC analyzer*
Sulfur, $S_{(tot)}^{B}$	mg/l	*210*	*100*	*210*	*Perkin-Elmer Elan 6000, ICP-MS*
Aluminium, Al^{B}	mg/l	<0,025	0,028	0,007	*Perkin-Elmer Elan 6000, ICP-MS*
Potassium, K^{B}	mg/l	14	15	10	*Perkin-Elmer Elan 6000, ICP-MS*
Calcium, Ca^{B}	mg/l	4 600	670	4 000	*Perkin-Elmer Elan 6000, ICP-MS*
Magnesium, Mg^{B}	mg/l	36	100	37	*Perkin-Elmer Elan 6000, ICP-MS*

Analysis	Unit	HA 2780A	SA 2273A	KA 1755A	*Stamdard/Method*
Sodium, Na^B	mg/l	3 500	1500	3 100	*Perkin-Elmer Elan 6000, ICP-MS*
Manganese, Mn^B	mg/l	0,27	0,85	0,33	*Perkin-Elmer Elan 6000, ICP-MS*
Lithium, Li^B	mg/l	3,8	0,38	3,3	*Perkin-Elmer Elan 6000, ICP-MS*
Strontium, Sr^B	mg/l	80	11	74	*Perkin-Elmer Elan 6000, ICP-MS*
Oxygen 18, $^{18}O^D$	$^o/_{oo}$ SMOW	-12,6	-9,0	-13,4	*Finnigan Mat 251, MS*
Deuterium, $^2H^D$	$^o/_{oo}$ SMOW	*-84,5*	*-65,0*	*-91,7*	*Finnigan Mat 251, MS*
Tritium, $^3H^E$	TU	*1,0*	*8,8*	*0,6*	
TDS	mg/l	*22 100*	*6 400*	*19 800*	*Calculated*

[A] analyzed in Äspö at SKB`s field laboratory

[B] analyzed in Consulting Engineers Paavo Ristola´s laboratory at Myymäki or Hollola

[C] analyzed in Teollisuuden Voima´s Chemistry laboratory at Olkiluoto

[D] analyzed in The Geological Survey of Finland (GTK)

[E] analyzed in The Central Isotope Research Laboratory of the Netherlands (CIO)

The anion-cation ratio was calculated for all samples based on the total amount of anions and cations in meq/l in water samples. The ratio were for the samples HA 2780A 0,992 and SA 2273A 1,029 and KA 1755A 1,023. The ratio should be about one for the accepted results.

The reliability of the analysis can be investigated by calculating ion charge balance of the waters. For water the ion charge balance is neutral. Ion charge balance can be calculated by using equation below, where anions and cations are given in meq/l:

$$E = \frac{Cations - Anions}{Cations + Anions} * 100 \qquad (1)$$

All analyses were acceptable because the ion charge balance for the groundwater sample were between
–1,4 ... 0,4 %. The pH-values were normal for the groundwater samples (pH: 7,5-7,9; F and L). Sulphide was not found from any sample (determination level < 0,01 mg S^{2-}/l). The ratio of Fe^{2+}/Fe_{tot} was calculated for samples on the base of field laboratory analysis (Fe_{tot}: 0,088-0,78 and Fe^{2+}: 0,082-0,76 mg/l; F). The ratio for Fe^{2+}/Fetot varied between 0,932-0,974.

The Gran-titration was carried out for all samples to determined alkalinity values in field laboratory. The contents of bicarbonate (HCO_3, mg/l) were calculated from alkalinities and they were compared with the DIC-analyses made in laboratory. Two different laboratories determined the DIC-content

(Teollisuuden Voima Oy (TVO) and Paavo Ristola, *in Table 2.)* The results were different. The difference varied between 42-53 %. TVO`s DIC-analyses fitted better with the alkalinity results *(Figure 1.)* and they were used.

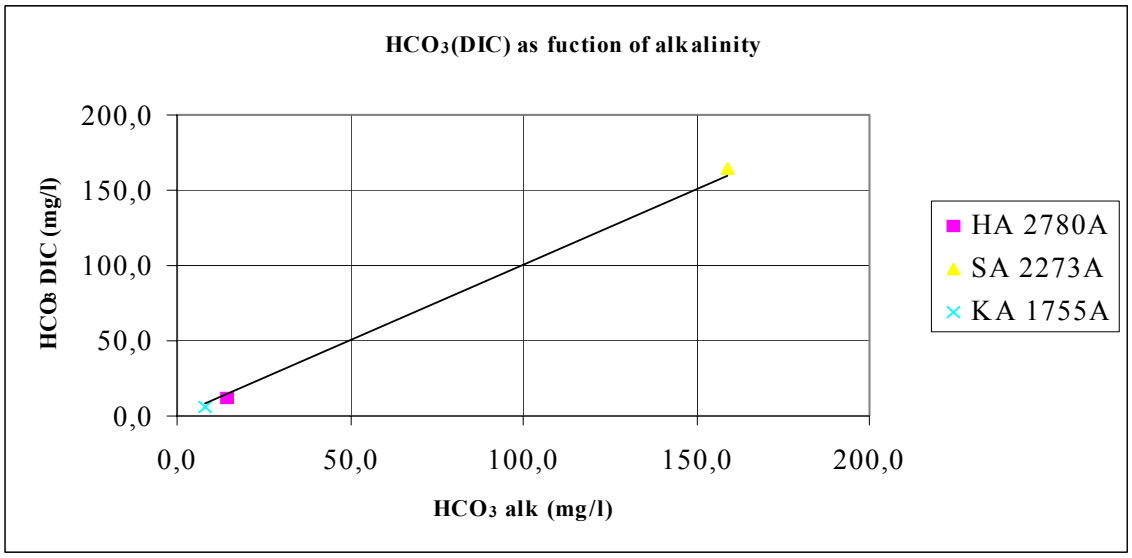

Figure 1. HCO_3 (DIC) results as a function of alkalinity.

According to the classification by Davis & De Wiest (1967) a Ca-Na-Cl water type was found in boreholes HA 2780A and KA 1755A and a Na-Ca-Cl water type in borehole SA 2273A. TDS *(Total Dissolved Solids)* varied between 6 400 ... 22 100 mg/l. Waters can be classified as brackish (1000 <TDS < 10 000 mg/l) and saline (TDS > 10 000 mg/l).

4 Comparing the results of the analysis from SKB and Posiva

Main parameters of the groundwater samples were done both by SKB and Posiva. The groundwater samplings were not done exactly at the same time, but analyses can be considered comparable (*Table 3*).

Table 3. Results of the water analysis both from the SKB and Posiva

Analysis	Unit	HA 2780A		SA 2273A		KA 1755A	
		SKB	Posiva	SKB	Posiva	SKB	Posiva
Conductivity 25°C	mS/m	3250	3 480 [A] 3 440 [B]	1150	1 140 [A] 1 120 [B]	2990	3 190 [A] 3 220 [B]
pH[A]		7,6	7,9 [A] 7,6 [B]	7,5	7,7 [A] 7,5 [B]	7,7	7,9 [A] 7,5 [B]
Bicarbonate, HCO_3[A]	mg/l	19	15	158	158	9,0	7,9
Sulfide, S^{2-}[A]	mg/l	No result	<0,01	0,02	<0,01	No result	<0,01
Iron, (tot)[A]	mg/l	0,09	0,09	0,80	0,78	0,19	0,21
Iron, Fe^{2+}[A]	mg/l	0,10	0,08	0,80	0,76	0,19	0,20
Iron, (tot)[B]	mg/l	0,16	0,08	0,73	0,79	0,19	0,19
Chloride, Cl[B]	mg/l	12 800	13 100	3640	3 630	11 720	11 800
Bromide, Br[B]	mg/l	101,0	97	15,7	17	91,7	89
Sulfate, SO_4[B]	mg/l	650	620	250	270	650	640
Dissolved organic carbon, DOC[B]	mg C/l	1,4	0,9[B] *1,0*[C]	3,2	3,6 [B] *4,8* [C]	1,0	0,5[B] 0,7[C]
Potassium, K[B]	mg/l	15,1	14	14,9	15	11,6	10
Calcium, Ca[B]	mg/l	4450	4 600	675	670	4200	4 000
Magnesium, Mg[B]	mg/l	35,6	36	100	100	36,6	37
Sodium, Na[B]	mg/l	3320	3 500	1570	1500	3050	3 100
Manganese, Mn[B]	mg/l	0,26	0,27	0,78	0,85	0,30	0,33
Lithium, Li[B]	mg/l	3,36	3,8	0,35	0,38	2,92	3,3
Strontium, Sr[B]	mg/l	75,2	80	10,7	11	70,8	74

[A] *analyzed in Äspö at SKB`s field laboratory*

[B] *analyzed in Consulting Engineers Paavo Ristola´s laboratory at Myymäki or Hollola*

[C] *analyzed in Teollisuuden Voima´s Chemistry laboratory at Olkiluoto*

Even though the samples were not taken at the same time almost all results are identical if one considers the uncertainty (± 5 %) in the measurements. Only Li results differs a little bit from each other even after the measuring uncertainty has been taken into account for both measuring results. Li has been analyzed with ICP-MS in Ristola and with ICP-AES in SGAB Analytica. The little differences between the results may be due to the different analytical methods used. According to the observations at Ristola (earlier Fortum) in spring 2001 ICP-AES in not as suitable as ICP-MS for analyzing Li, Cs and Rb concentrations from the saline groundwaters (Rantanen et. al. 2002).

Iron (tot) results done in laboratories for the sample HA2780A differs considerably. Ristola has done iron analysis by GFAAS and SGAB Analytica by ICP. The analysis done in the field with the ferrozine thioglygolacid method gives the same result that the GFAAS method. The difference

between results may be caused by some contamination of the sample. Both methods seems to be suitable for Fe(tot) analysis because they give same results for the other samples.

It seems that Ristola succeeded better in sulfide analysis although all the results are below detection limit. SKB's laboratory had analytical problems with two samples and did not get any results at all from these two samples.

DOC analyses were done in two different laboratories in Finland (Ristola, TVO). Ristola analyzed also the SKB's water samples. The DOC results does not differ much, TVO´s results being slightly higher than Ristola´s but the difference in not significant.

Isotope analyses were done in four different laboratories. Tritium samples were analyzed in the University of Waterloo in Canada (SKB's samples) and in the Central Isotope Research Laboratory of the Netherlands (CIO) (Posivas samples). ^{18}O and Deuterium samples were analyzed in the Institutt Fur Energiteknikk in Norway (IFE) (SKB's samples) and in the Geological Survey of Finland (GTK) (Posivas samples). Results from the isotope analyses are presented in the table 4.

Table 4. Results of the isotope analysis

Analysis	**Unit**	**HA 2780A**		**SA 2273A**		**KA 1755A**	
		SKB	**Posiva**	**SKB**	**Posiva**	**SKB**	**Posiva**
Oxygen 18, ^{18}O	$^{o}/_{oo}$ SMOW	-11,9	-12,6	-8,3	-9,0	-12,8	-13,4
Deuterium, $^{2}H^{D}$	$^{o}/_{oo}$ SMOW	*-85,7*	*-84,5*	*-65,0*	*-65,0*	*-91,9*	*-91,7*
Tritium, ^{3}H	TU	*1,0*	*1,0*	*8,9*	*8,8*	*0,8*	*0,6*

All comparative isotope analysis gives almost the same results. Especially tritium analyses vent very well. The ^{18}O results are generally lower at GSF as compared to results for analyses at IFE. The deuterium results are almost identical, a slightly higher value was reported by GSF for the sample HA2780A. The differences observed in the ^{18}O results calls for additional comparative samplings and parallel analyses.

References:

Davis, S.N. & DeWiest, R.J. 1967. Hydrology, 2. 3., Wiley, New York.
Ruotsalainen et al. 1998. Posivan vesinäytteenoton kenttätyöohje, rev.2, Posiva Työraportti 98-54

Rantanen, M., Paaso, N. & Mäntynen, M. (2002). Pohjavesinäytteiden otto Eurajoen Olkiluodon kairanrei'istä KR9 ja KR11 sekä Korvensuon altaasta vuonna 2001. (is to be published in Finnish)

Vuorinen et al. 1997. Groundwater chemistry of Olkiluoto - Saline and brackish groundwater – recipe for saline reference water, Posiva Working report 97-25.

Appendix 7

Äspö Hard Rock Laboratory

Compilation of groundwater chemistry data
October 2001

Christina Mattsén
Svensk Kärnbränslehantering AB

Contents

List of Tables

List of Appendix

1 Methods and Results

Methods

Water samples, class 4 and 5, have been collected and analysed according to SKB MD 431.011-01. In addition to the ordinary sampling (class 4) we have sampled and analysed carbon isotopes. Table 1 explains the different chemistry classes.

Table 1 *SKB Chemistry Classes*

Class no.	Description	Analyses	Optional
1	Simple sampling, basic control of water type	Electric conductivity pH Uranine*	
2	Simple sampling, control of water type	Electric conductivity pH, Cl, HCO_3 Uranine*	^2H, ^3H, ^{18}O Freeze stored back-up sample
3	Simple sampling, determination of non redox-sensitive major components	Electric conductivity pH, Cl, HCO_3 , SO_4, Br Uranine* Major cations** (except for Fe, Mn), SO_4 as Sulphur on ICP-AES	^2H, ^3H, ^{18}O Freeze stored back-up sample
4	Extensive sampling, complete chemical characterisation	Electric conductivity pH, Cl, HCO_3 , SO_4, Br, Fe (total, ferrous), Uranine*, DOC, major cations** SO_4 as Sulphur on ICP-AES ^2H, ^3H, ^{18}O Freeze stored back-up sample, preserved and non-preserved	HS^- , NH_4
5	Extensive sampling, complete chemical characterisation including special analyses	Electric conductivity pH, Cl, HCO_3 , SO_4, Br, Fe (total, ferrous), Uranine*, DOC, major cations** SO_4 as Sulphur on ICP-AES ^2H, ^3H, ^{18}O Freeze stored back-up sample, preserved and non-preserved	HS^- , NH_4 F, I NO2, NO3, PO4 TOC ^{14}C-age, PMC, $\delta^{13}C$ per mill PDB U, Th (elements and/or isotopes) Other trace elements (INAA and/or ICP-MS) ^{226}Ra, ^{228}Ra, ^{222}Rn Or your decision

* Only measured when uranine was used in the drilling procedure and as long as no extra uranine has been added to the borehole e.g. in tracer tests.
** Major cations are Na, K, Ca, Mg, Si, Fe, Mn, Li, Sr

All sampling sections have been flushed such that five section volumes have been exchanged before sampling.

Water sampled for major components and DOC have been filtered on-line through Colly On-line High Capacity filters (0,45 um). Water for major cations has been filtered on-line through nucleopore filters (0,45um). Unfiltered water were collected for all other isotopes.

Different parameters have been analysed at different laboratories (Table 2).

Table 2*Laboratories used for analyses*

Laboratory	Parameter (method)
Äspö HRL, Sweden	pH, electric conductivity, Cl^-, HCO_3^-, $SO4^{2-}$, Br^-, Fe (total and ferrous), NH_4-N, HS
SGAB Analytica, Sweden	Major cations (ICP-AES)
ALcontrol, Sweden	NH_4-N, NO_2, NO_3, PO_4
Ångströmlaboratoriet, Sweden	Carbon-isotopes
University of Waterloo, Canada	Tritium
Fortum Power and Heat Oy, Finland	DOC
Institutt for Energiteknikk (IFE), Norway	Oxygen-18, Deuterium

Results

Sampled boreholes and sections are listed in Appendix 1 together with Äspö96 coordinates. The water compositions obtained from the analyses are shown in Appendix 2. Environmental isotope analyses are listed in Appendix 3 and Carbon-isotopes in Appendix 4.

The following SICADA queries were applied when extracting data:

gwchemistry/analyses/water/sampling_series, 01-10-15—01-10-16, GWCM

gwchemistry/analyses/water/water_composition, 01-10-15—01-10-16, GWCM

gwchemistry/analyses/water/h_o_isotope, 01-10-15—01-10-16, GWCM

gwchemistry/analyses/water/c_s_isotope, 01-10-15—01-10-16, GWCM

Idcode	Secup* m	Seclow * m	Sample No**	Sampling date	Class No**	Project	Northing Äspö96 (m)	Easting Äspö96 (m)	Elevation Äspö96 (m)
HA1330B	0.0	32.5	3465	2001-10-15	4	GWCM	6975.80	2123.31	-183.13
HA2780A	0.0	43.3	3467	2001-10-16	4	GWCM	7451.30	2159.26	-380.43
KA1755A	88.0	160.0	3469	2001-10-16	4	GWCM	7499.20	2020.44	-279.92
KA3110A	20.1	26.8	3464	2001-10-15	4	GWCM	7299.63	2332.45	-415.94
KR0012B	1.2	10.6	3466	2001-10-15	5	GWCM	6165.91	2167.10	-69.16
SA1229A	6.0	20.5	3471	2001-10-16	4	GWCM	6885.16	2105.46	-171.29
SA2074A	6.0	38.7	3468	2001-10-16	4	GWCM	7290.03	2348.26	-281.68
SA2273A	6.0	20.0	3470	2001-10-16	4	GWCM	7149.70	2221.64	-305.98

* = Secup and Seclow is upper and lower limit of the sampled section
** = Class no shows SKB´s chemistry class

Idcode	Secup m	Seclow m	Sample	Sampling date	Na mg/L	K mg/L	Ca mg/L	Mg mg/L	HCO3 mg/L	Cl mg/L	SO4 mg/L	SO4-S mg/L	Br mg/l	F mg/L	Si mg/L	Fe-ICP mg/L	Fetot mg/L	Fe2+ mg/L
		Measurement uncertainty:			5%	5%	5%	5%	5%	5%	10%	5%	10%	10%	5%	5%	10%	10%
HA1330B	0.0	32.5	3465	2001-10-15	1570	17.1	337	118.0	200	2960	312	121	11.2	2.1	5.8	1.44	1.52	1.54
HA2780A	0.0	43.3	3467	2001-10-16	3320	15.1	4450	35.6	19	12800	654	223	101.0	2.7	4.7	0.156	0.093	0.095
KA1755A	88.0	160.0	3469	2001-10-16	3050	11.6	4200	36.6	9.0	11720	646	225	91.7	2.2	4.5	0.187	0.188	0.190
KA3110A	20.1	26.8	3464	2001-10-15	1430	35.1	257	128.0	196	2730	269	102	10.3	0.9	5.7	0.988	1.040	1.056
KR0012B	1.2	10.6	3466	2001-10-15	172	2.6	40	7.8	328	168	37	14	0.8	2.6	7.6	0.227	0.227	0.226
SA1229A	6.0	20.5	3471	2001-10-16	1520	26.2	277	124.0	264	2850	224	94	12.0	2.0	7.2	1.7	1.84	1.83
SA2074A	6.0	38.7	3468	2001-10-16	1240	9.6	394	80.4	174	2520	237	91	12.8	2.6	6.6	0.163	0.163	0.162
SA2273A	6.0	20.0	3470	2001-10-16	1570	14.9	675	100.0	158	3640	253	102	15.7	1.8	6.2	0.732	0.803	0.799

- = Not analysed
x = No result due to sampling problems
xx = No result due to analytical problems
- "value" = result less than detection limit
SICADA: water_composition, 011015-011016

xxx= only one significant number

Idcode	Secup m	Seclow m	Sample	Mn mg/L	Li mg/L	Sr mg/L	pH pH unit	El, Cond, mS/m	Smpl Flow L/min	Drill water %	DOC mg/L	S2 mg/L	NH4-N mg/L
		Measurement uncertain		5%	5%	5%	0,1 unit	5%			0,1 mg/L	10%	20%
HA1330B	0.0	32.5	3465	0.78	0.10	4.9	7.4	970	0.33	0.04	3.6	0.01	0.67
HA2780A	0.0	43.3	3467	0.26	3.36	75.2	7.6	3250	5	0.03	1.4	xx	0.1
KA1755A	88.0	160.0	3469	0.30	2.92	70.8	7.7	2990	1.1	0.02	1	xx	0.04
KA3110A	20.1	26.8	3464	0.69	0.08	3.7	7.7	910	2	0.05	5	0.09	0.79
KR0012B	1.2	10.6	3466	0.14	0.04	0.8	7.5	116	0.4	0.20	11	0.04	0.09
SA1229A	6.0	20.5	3471	0.66	0.09	4.6	7.3	950	1.5	0.06	4.8	0.01	1.58
SA2074A	6.0	38.7	3468	0.47	0.15	6.0	7.7	850	0.21	0.05	4.1	0.05	0.16
SA2273A	6.0	20.0	3470	0.78	0.35	10.7	7.5	1150	2.4	0.04	3.2	0.02	0.48

- = Not analysed
x = No result due to sampling problems
xx = No result due to analytical problems
- "value" = result less than detection limit
SICADA: water_composition, 011015-011016

xxx= only one significant number

Idcode	Secup m	Seclow m	Sample	Sampling date	D dev SMOW 1 unit	Tr TU 1 unit	O18 dev SMOW 0,2 unit
		Measurement uncertainty:					
HA1330B	0.0	32.5	3465	2001-10-15	-58.5	12.2	-7.2
HA2780A	0.0	43.3	3467	2001-10-16	-85.7	1	-11.9
KA1755A	88.0	160.0	3469	2001-10-16	-91.9	-0.8	-12.8
KA3110A	20.1	26.8	3464	2001-10-15	-58.9	12.2	-7.3
KR0012B	1.2	10.6	3466	2001-10-15	-73.9	13.1	-10.2
SA1229A	6.0	20.5	3471	2001-10-16	-57.3	12	-7.2
SA2074A	6.0	38.7	3468	2001-10-16	-64	10.2	-8.2
SA2273A	6.0	20.0	3470	2001-10-16	-65	8.9	-8.3

- = Not analysed
x = No result due to sampling problems
xx = No result due to analytical problems
SICADA: h_o_isotopes, 011015-011016

Idcode	Secup m	Seclow m	Sample	Sampling date	Percent modern Carbon pmc	C13 dev PDP	Age BP year	Age BP corr year
	Measurement uncertainty:						100 year	
KR0012B	1.2	10.6	3466	2001-10-15	86.9	-14.9	1080	45

- = Not analysed
x = No result due to sampling problems
xx = No result due to analytical problems
SICADA: c_s_isotopes, 011015-011016

Appendix 8

Background inorganic colloid measurements in different Äspö-waters

Susanna Wold and Trygve Eriksen
Royal Institute of Technology
Department of Chemistry / Division of Nuclear Chemistry

1 Background

Complexation of radionuclides by colloids may change the mobility of radionuclides in natural systems. Colloids can serve as a mobile carrier phase for radionuclides. Possible radionuclide carrying colloids in groundwater are clay and humic/fulvic colloids. It is therefore important to study the effect of colloids on radionuclide mobility in bentonite and bedrock barriers of a repository of spent nuclear fuel. In this study the background concentration of inorganic colloid is measured in different types of groundwater, represented by waters from eight bore holes situated at different depth in the bedrock of the Äspö HRL-tunnel. Two different techniques for concentration measurements are compared.

2 Sampling

Eight different bore holes were sampled 23 October. A filter system, with 3000, 450, 220 nm and 220 and 50 nm, were connected in series to the bore hole. The filters were flushed with argon since it is known that colloid formation can be initiated by oxygen exposure. Measured volumes of 50-1000 ml water flowed through the filter system. The low volumes were chosen when filtering through the 220 and 50 nm series to avoid filter clogging. Since the expected colloid concentration is low, large volumes were chosen in the other filter series to allow collection of detectable amounts of colloids. The water flow through the filters was followed throughout the sampling to detect clogging. No clogging was detected. One extra filter for every bore hole was wetted with water and used as blanks. The filters were detached and immediately sealed in plastic cups in an exikator.

Water was collected in pressure vessels of steel. The vessels were flushed with water for about one minute before collecting 500 ml. The pressure vessels and the exikator was transported after sampling to Royal Institute of Technology for analysis.

Experimental

ICP-MS and ICP-AES analysis

The filters were soaked in 0.5 ml 65 % suprapure HNO_3 and 2.5 ml Millipore deionized, triple distilled water in acid washed vessels. After 1.5 h the solutions were diluted to 20 ml with Millipore deionized triple distilled water. After 15 minutes the filters were removed and the diluted solutions were sent to SGAB commercial laboratory for ICP-MS, ICP-AES analysis.

PCS – Dynamic light scattering

The signal in the PCS is roughly proportional to the concentration of colloid particles of different sizes. To enable measurements of particle concentration as well as particle size distributions, the PCS equipment was calibrated with solutions containing latex colloids with defined size distributions.

Water was filtered through 800, 200 and 100 nm syringe filters to plastic cuvettes. The PCS detects gas bubbles as colloids, why it is important to minimise the impact from gas bubbles on the signal. The water was therefore degasing in the cuvettes for a day before analysing with PCS. Degasing the samples is a compromise since oxygen exposure initiates colloid formation.

3 Results

PCS – Dynamic light scattering

All samples contained lower colloid concentrations lower than the PCS detection limit of 0.6 mg/l.

ICP-MS and ICP-AES analysis

The inorganic colloids in Äspö-waters are presumably composed of iron hydroxides, silica and clay mineral. Fe, Si and Al are therefore assumed to represent the inorganic colloids in the analysed Äspö-waters. The colloid content of the different Äspö-waters can be seen in table 1. The concentrations in the solutions sent for analysis were related to the filtered volumes.

Table 1. Colloid content in the Äspö-waters from different bore holes.

		Fe+Si+ Al ppb	Total ppb
KA 3110 A	>50<220 nm	18.4	**21**
	>220<450 nm	1.1	
	>450<3000 nm	1.5	
	>50<3000 nm, total	21.0	
HA 2780 A	>50<220 nm	143.3	**149**
	>220<450 nm	2.8	
	>450<3000 nm	2.8	
	>50<3000 nm, total	148.9	
SA 2273 A	>50<220 nm	0.0	**1**
	>220<450 nm	0.0	
	>450<3000 nm	0.9	
	>50<3000 nm, total	0.9	
SA 2074 A	>50<220 nm	56.9	**87**
	>220<450 nm	11.9	
	>450<3000 nm	18.7	
	>50<3000 nm, total	87.5	
KA 1755 A	>50<220 nm	25.3	**41**
	>220<450 nm	6.4	
	>450<3000 nm	8.8	
	>50<3000 nm, total	40.5	
HA 1330 B	>50<220 nm	3.6	**5**
	>220<450 nm	0.6	
	>450<3000 nm	0.7	
	>50<3000 nm, total	4.9	
SA 1229 A	>50<220 nm	1.8	**3**
	>220<450 nm	1.1	
	>450<3000 nm	0.2	
	>50<3000 nm, total	3.0	
KR 0012 B	>50<220 nm	23.8	**32**
	>220<450 nm	0.6	
	>450<3000 nm	7.4	
	>50<3000 nm, total	31.8	

The colloid concentration in the Äspö-waters is in the range of 1-149 ppb. Colloids in the size range >50<220 nm are dominating in all the Äspö-water samples except for the water sampled in bore hole SA 2273 A. The colloid concentrations are very low and it is therefore questionable to define exact size distributions.

Filtering of water followed by ICP analysis of the leached colloids in solution seems to be a workable method of measuring the colloid content in groundwater with low concentrations of colloids. The PCS technique is not sensitive enough to detect the low concentrations of colloids in this type of groundwater.

Appendix 9

Total number of microorganisms in groundwater sampled during background colloid measurements along the Äspö HRL-tunnel

Karsten Pedersen

1 Background

Colloids are defined as small particles in the size range 10^{-6} to 10^{-3} mm. Colloidal particles are of interest for the safety of spent nuclear fuel because of their potential for transporting radionuclides from a faulty repository canister to the biosphere.

Microorganisms generally range in size between 2 x 10^{-4} to 10^{-2} mm, thereby overlapping colloid particles in size. Their organic character, with many different functional groups directed outwards from the cell surface, e.g. phosphates, amines, hydroxyl- and carboxyl-groups, makes them potent as radionuclide sorbents.

The natural background colloid concentrations from various boreholes along the Äspö HRL-tunnel was studied. The boreholes represented different water types since it is well known that the colloid stability can change with the ion content of the groundwater. This is also true for microorganisms. Additionally, organic content and the chemical composition of the water influence microbe types and numbers. Eight selected boreholes were used to measure the background colloid content, humic substances and microorganisms. The results from microorganism enumerations are presented here.

2 Sampling

Eight different boreholes were sampled 23 October as shown in Table 1. A test rack with 50 ml sterile plastic tubes with screw lids were supplied with 3 ml 30 % formaldehyde. Triplicates of groundwater were collected from each borehole. The sampling was distributed over time, during which other sampling activities also were performed. The samples were cool stored until transport to and analysis in Göteborg.

2.1 Experimental setup and filtration

Selected volumes were filtered on 13 mm diameter, black 0.22 Micron polycarbonate filter (Osmonic Inc.,), using a Millipore stainless steel filtration set-up, equipped with 13 mm funnels. In a first analysis 1 ml was filtered from all samples, using 1/3 atmosphere under-pressure. The counting result guided on the filtered volume in the second analysis. The number of cells counted was aimed to be approximately 500 cells per filter. . The filtration volumes are depicted in Table 1. The filter area was 70 mm^2.

Acridine orange was used for staining the cells. It was blended in a phosphate buffer. The buffer was prepared by dissolving 0.449 g KH_2PO_4 in 500 ml double distilled water, mixed with 0.588 g Na_2HPO_4 in 500 ml double distilled water and adjust pH to 6.7. Phosphate content was 6.6 mM. Ten mg acridine orange was added to 100 ml of buffer. After mixing and filtration through a 0.2 μm filter, sterilization was performed in an autoclave

Table 1. The boreholes were sampled 23 of October at times indicated in the table. The sample volumes filtrated in two repeated analyses are also shown.

Borehole	First analysis time and volume (ml)			Second analysis time and volume (ml)		
	1A	2A	3A	1B	2B	3B
KR0012B	21.32 1	21.50 1	21.53 1	21.32 1	21.50 1	21.53 1
SA1229A	16.32 1	16.38 1	16.47 1	16.32 10	16.38 10	16.47 10
HA1330B	15.35 1	15.45 1	15.55 1	15.35 5	15.45 5	15.55 5
KA1775A*	13.27 3	13.35 3	14.00 3	13.27 10	13.35 10	14.00 10
SA2074A	10.25 1	10.43 1	10.52 1	10.25 10	10.43 10	10.52 10
SA2273A	14.22 1	14.33 1	14.58 1	14.22 10	14.33 10	14.58 10
HA2780A	20.30 1	20.40 1	21.01 1	20.30 10	20.40 10	21.01 10
KA3110A	9.03 1	9.25 1	9.43 1	9.03 1	9.25 1	9.43 1

* KA1775 was filtered three times. The first filtration A, was considered possibly corrupt (contaminated). A third filtration, C was therefore performed.

2.3 Microscopy analysis

Filters were mounted with immersion oil on microscope slides and observed under blue light in an inverted Nikon Diaphot 300 microscope at 1000 times enlargement. A 100 times lens was used. Microbial cells show orange or green fluorescence in this light (See Fig. 2-9). The counted frame size was 100 x 100 um. 15 frames were counted on each filter.

3 Results and discussion

A total of 13158 cells distributed over 24 samples, two (one sample three) repeated filtrations and 375 frames were registered. The results are shown in table 2.

The numbers ranged more than two orders of magnitude, with the highest numbers in the most shallow and the deepest borehole investigated, KR0012B and KA3110A. A comparison of the obtained data with earlier data on total numbers of microorganisms in Fennoscandian Shield groundwater is shown in Fig. 1. The obtained data lies within the range of all available data.

There was an obvious difference in size and appearance between the boreholes, from 0.2 um up to several um. The borehole HA1330B showed the largest cells (Fig. 4), most other

boreholes had small, or very small cells. Se figures 2-9 for details. Thin flaks were observed in KR0012B.

Table 2. Results from two repeated filtrations. See table 1 for sample volumes.

Borehole	First analysis cells ml^{-1} x 10^4			Second analysis cells ml^{-1} x 10^4			Overall mean cells ml^{-1} x 10^4 (S.D.)
	1A	2A	3A	1B	2B	3B	
KR0012B	40	21	27	48	46	22	35 (12)
SA1229A	1.9	2.9	2.1	2.6	2.0	2.0	2.3 (0.4)
HA1330B	(0.13)	(0.14)	(0.14)	1.1	4.2	3.4	2.9 (1.3)
KA1775A	0.67	1.0	2.4	5.3	0.97	1.3	1.9 (1.6)
SA2074A	0.51	0.05	0.7	0.16	0.15	0.15	0.29 (0.2)
SA2273A	0.93	0.79	1.3	3.1	2.2	2.7	1.8 (0.9)
HA2780A	0.37	0.28	0.14	0.52	0.09	0.14	0.26 (15)
KA3110A	26	14	30	27	11	23	22 (7.0)

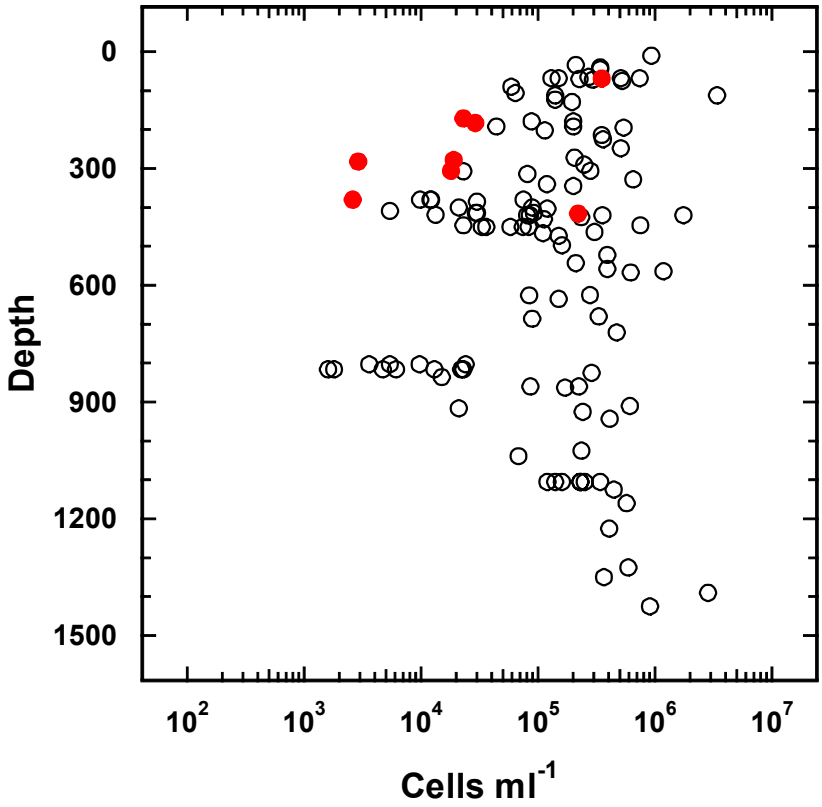

Figure 2. The overall means from Table 2 plotted with the available data base on total numbers of microorganisms fron Stripa research mine, Äspö HRL area, Laxemar boreholes KLX and investigation sites in Finland (Olkiluoto, Hästholmen, Kivetty, Romuvaara) and the natural uranium analogue in Palmottu.

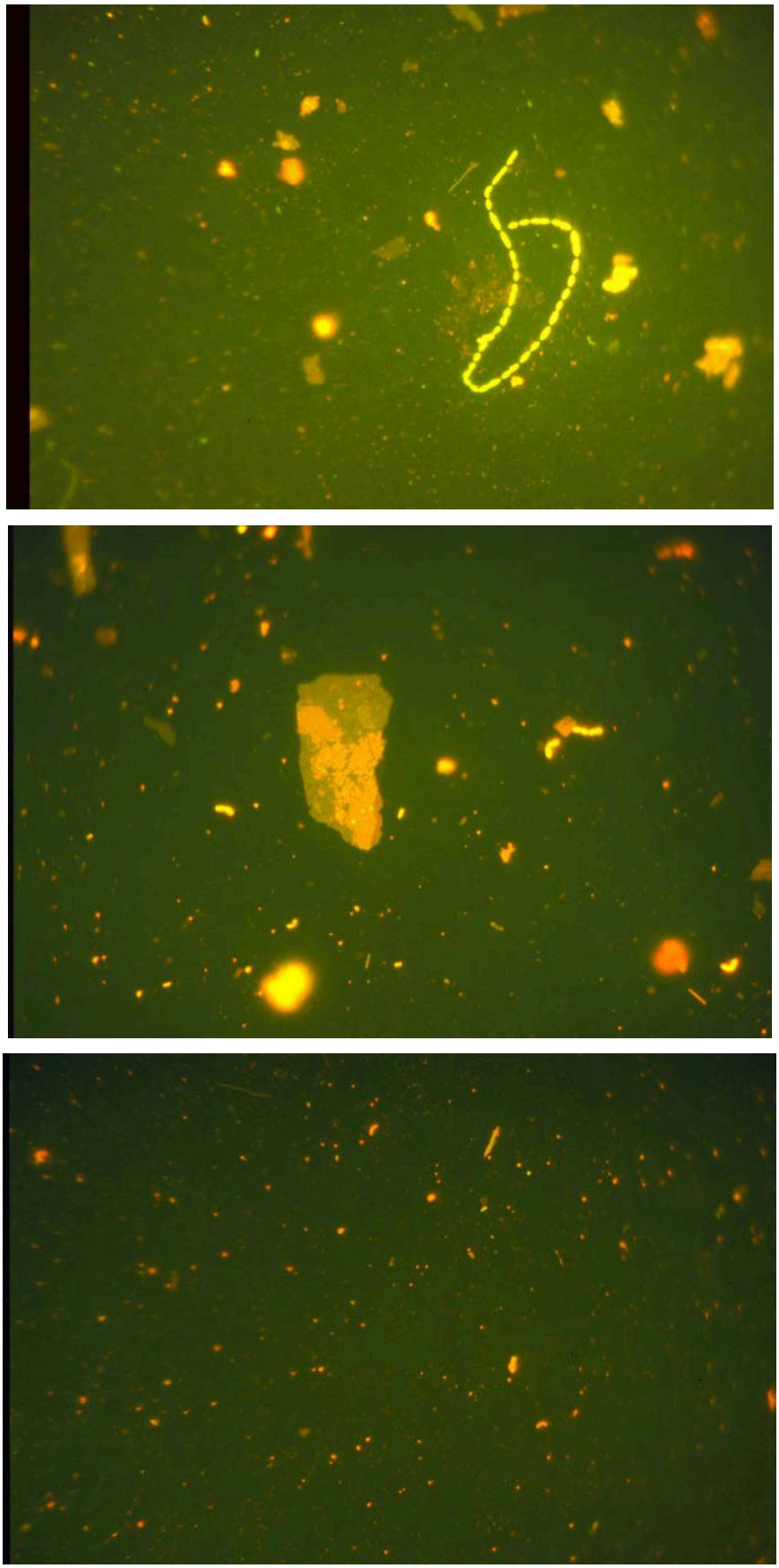

Figure 2. KR0012B, filter 1B, 2B and 3B. Frame size is 130 x 85 μm.

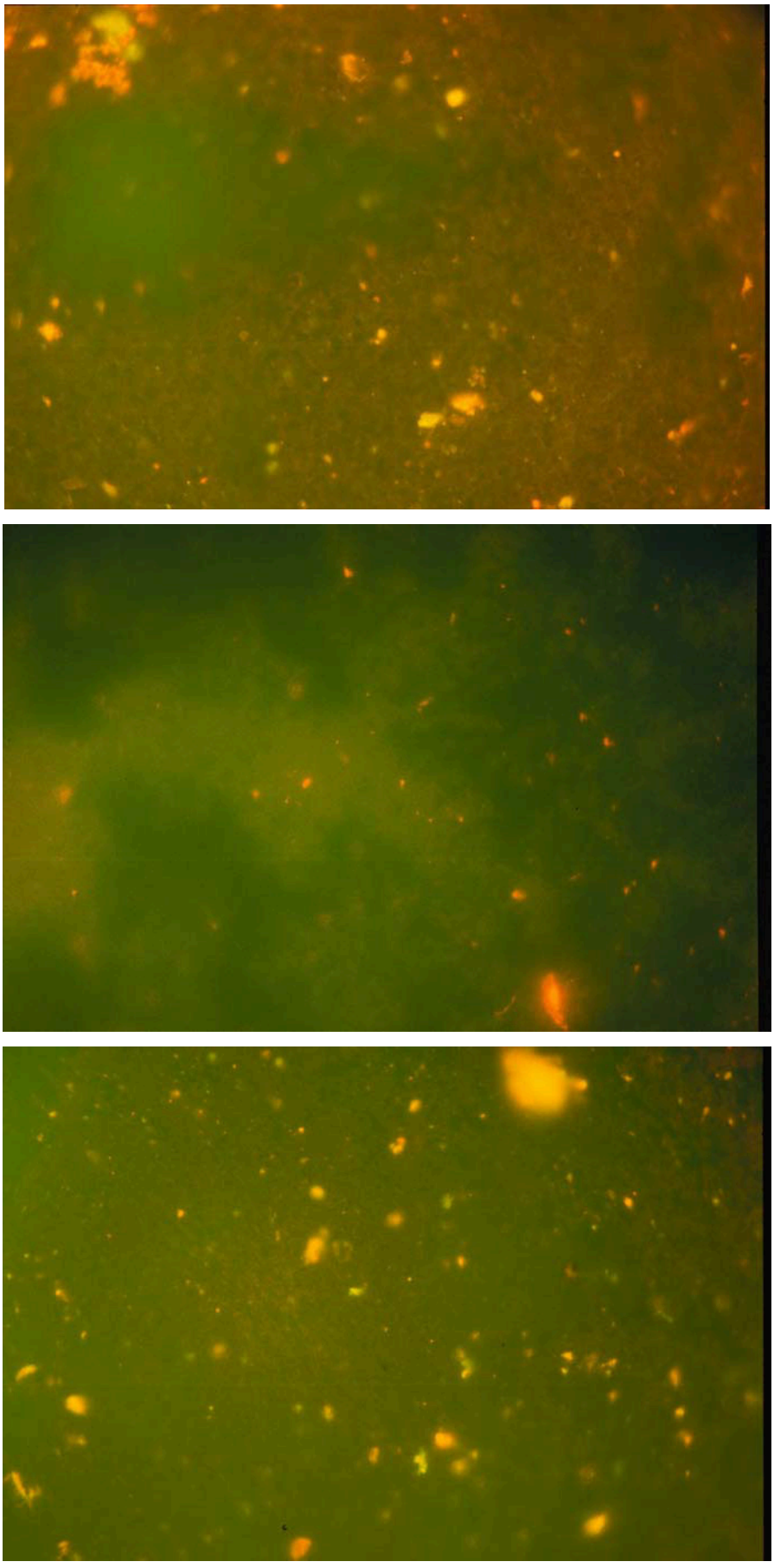

Figure 3. SA1229A filter 1B, 2B and 3B. Frame size is 130 x 85 μm

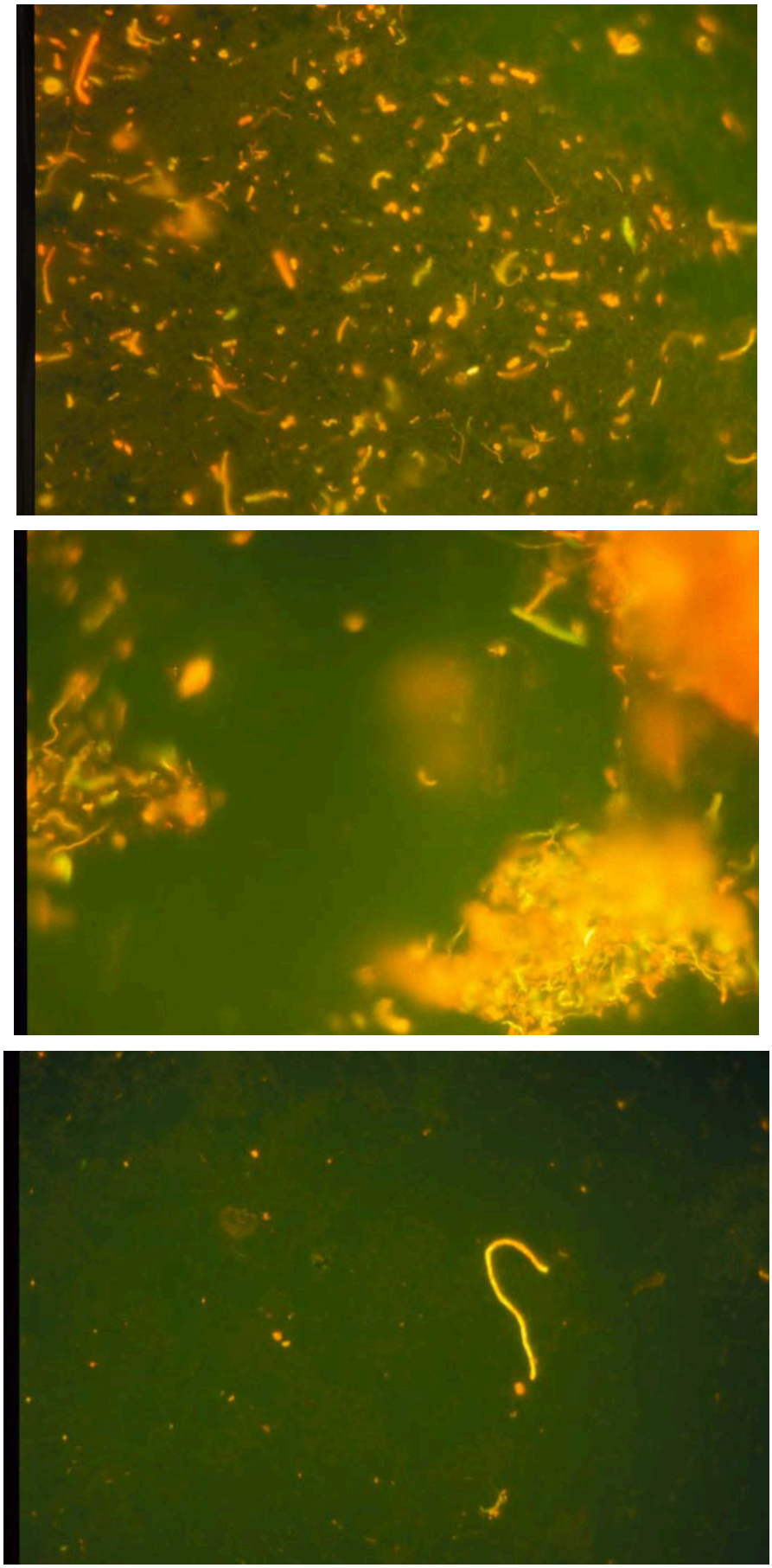

Figure 4. HA1330B, filter 1B, 2B and 3B. Frame size is 130 x 85 µm

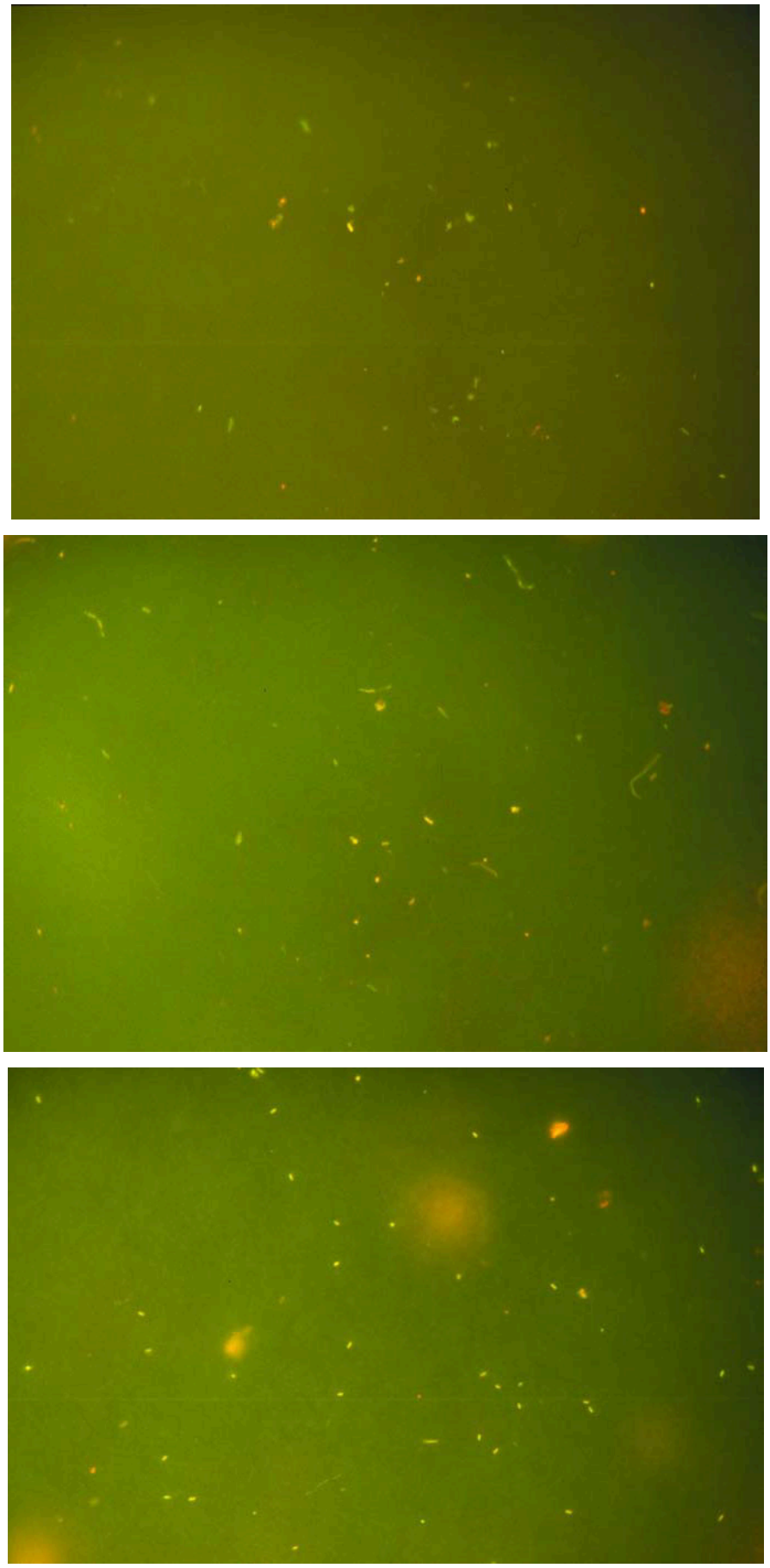

Figure 5. KA1775A, filter 1B, 2B and 3B. Frame size is 130 x 85 µm

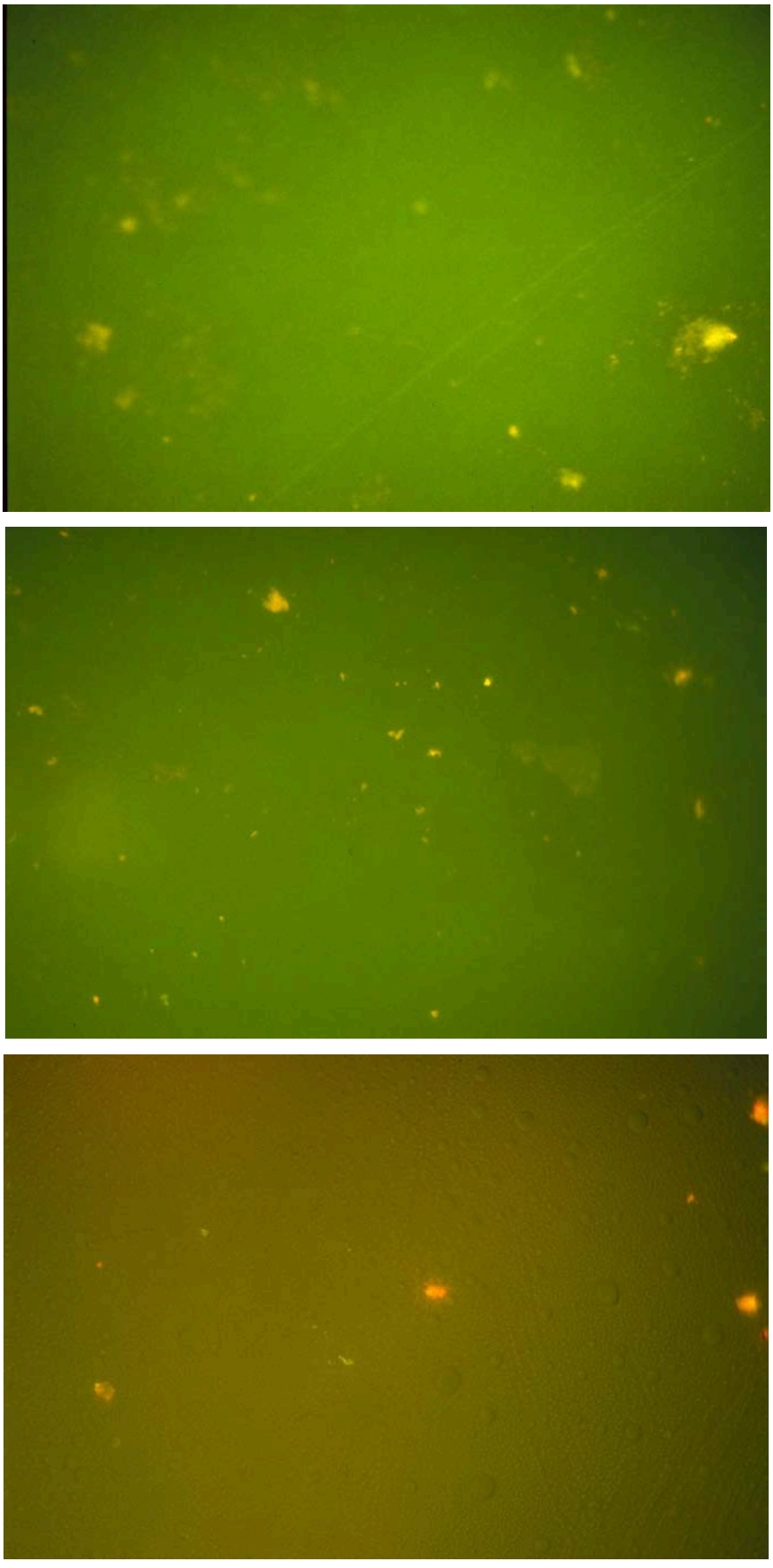

Figure 6. SA2074A, filter 1B, 2B and 3B. Frame size is 130 x 85 µm

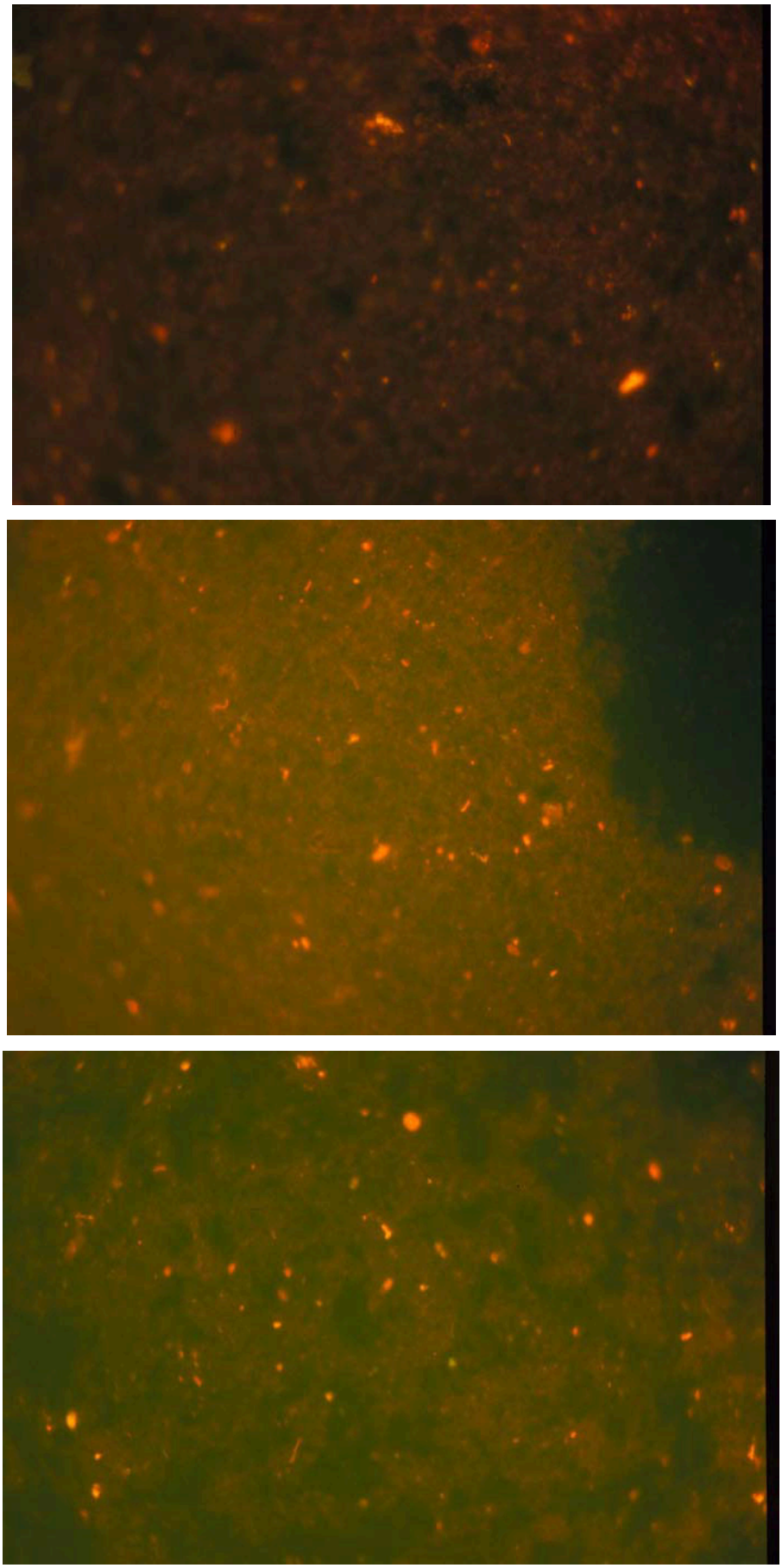

Figure 7. SA2273A, filter 1B, 2B and 3B. Frame size is 130 x 85 μm

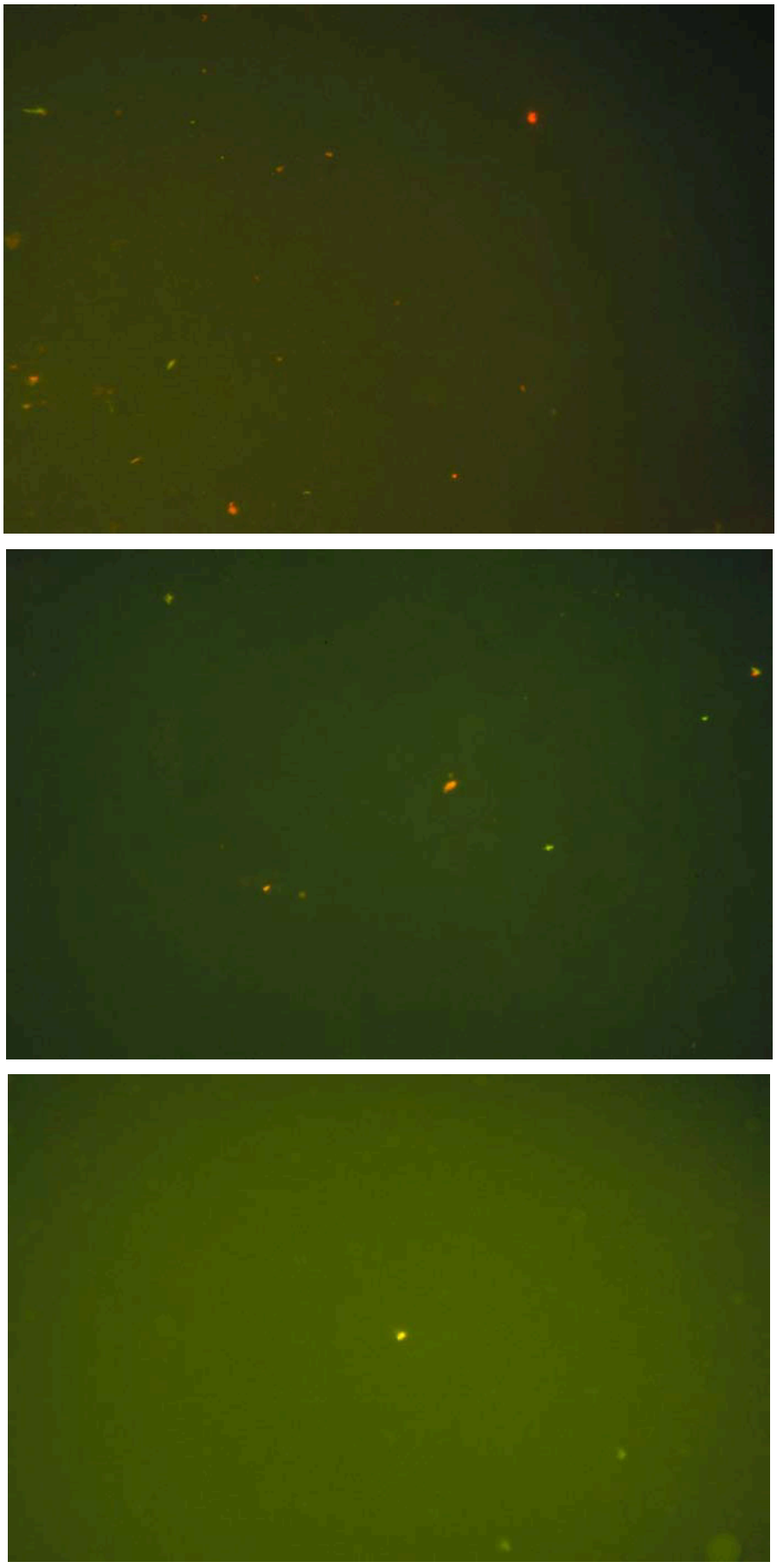

Figure 8. HA2780, filter 1B, 2B and 3B. Frame size is 130 x 85 µm

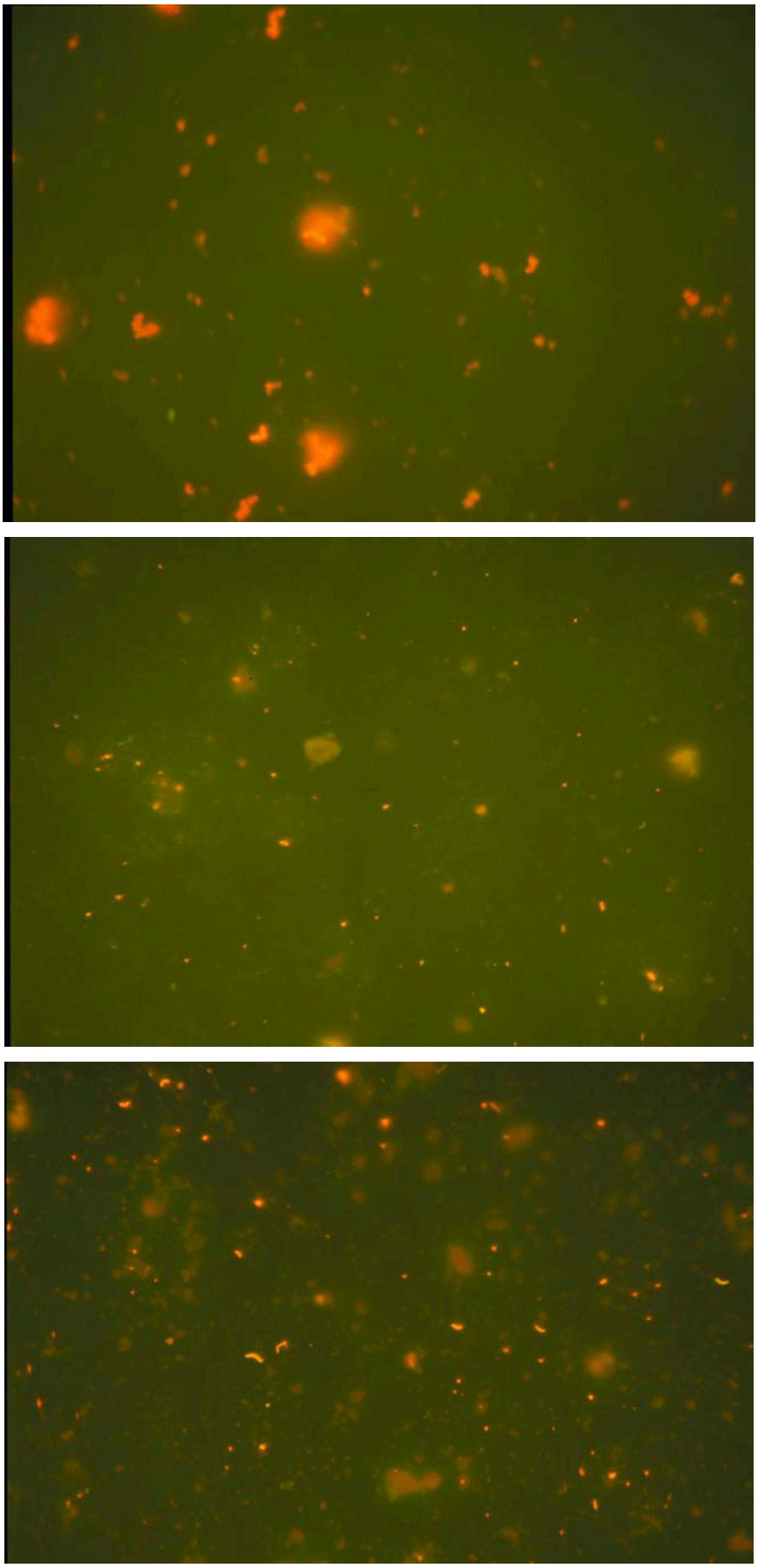

Figure 9 KA3110A, filter 1B, 2B and 3B. Frame size is 130 x 85 µm

Appendix 10

Electric conductivity measurements along the Äspö tunnel

Ioana Gurban
3D Terra
3583 Durocher #1
Montréal, Québec, H2X 2E7 Canada

Background and aim of sampling

The aim of the sampling is to measure the electrical conductivity of all the major water venues at the Äspö tunnel in order to measure the variability of the groundwater chemistry, which may affect the colloid stability. The electrical conductivity data collected along the tunnel is been evaluated and then compared with the borehole data.

The sampling procedure

The water venues along the tunnel were sampled directly in plastic bottles of 100ml capacity. From water venues high up on the tunnel walls or from the tunnel ceiling, the water was sampled by using a funnel adapted to the sampling bottle. The bottles were brought to the Äspö laboratory for analyze, since a mobile electric conductivity-meter was not available.

Number of samples

All the water venues along the tunnel and in the accessible tunnel niches were sampled, by the mean of one water sample for each water venue. For wide water venues representative samples were taken. For example, for a water venue of a width of 10m, a sample was taken in the beginning, one in the middle and the third at the end of the water venue. When possible, water venues were collected from the left side, the right side and the ceiling of the tunnel in order to better capture the variability of the water chemistry. 195 samples were collected along the tunnel in total.

Sampling locations

The sampling locations were all the water venues along the tunnel, identified by A (left side on the tunnel), B (right side on the tunnel) and T (ceiling). The samples were labeled with an ID code according to the SKB procedure.

Results and discussion

A total of 195 samples were taken and analyzed at Äspö laboratory, following the Class1 procedure. The preliminary results for the electrical conductivity are shown in Table 1. The results will be compared with the electrical conductivity measurements from the tunnel boreholes. The modeling and comparison will be realized by using the visualization and interpolation tool Tecplot. Sections along the tunnel will be presented for interpretation and analyze of the variability of the groundwater chemistry along the tunnel.

Table 1: The results of the electrical conductivity measurements along the Äspö tunnel.

Sample nr	Start Date	Idcode	Secup (m)	Seclow (m)	Sample No	Cond (mS/m)	Northing	Easting	Elevation	Coord System
1	10/23/01 3:00	TASA	502	502	3495	120	6366728	1551706	-69.48	RT38-RH00
2	10/23/01 3:00	TASA	170	170	3478	710	6366415	1551815	-23	RT38-RH00
3	10/23/01 3:00	TASA	128	128	3476	410	6366375	1551828	-17.8	RT38-RH00
4	10/23/01 3:00	TASA	282	282	3484	1170	6366520	1551778	-38.68	RT38-RH00
5	10/23/01 3:00	TASA	293	293	3486	1210	6366531	1551774	-40.22	RT38-RH00
6	10/23/01 3:00	TASA	150	150	3475	400	6366396	1551821	-20.2	RT38-RH00
7	10/23/01 3:00	TASA	821	821	3504	940	6367030	1551601	-112.62	RT38-RH00
8	10/23/01 3:00	TASA	293	293	3485	1160	6366531	1551774	-40.22	RT38-RH00
9	10/23/01 3:00	TASA	769	769	3501	740	6366980	1551618	-105.36	RT38-RH00
10	10/23/01 3:00	TASA	220	220	3481	920	6366462	1551798	-30	RT38-RH00
11	10/23/01 3:00	TASA	842	842	3506	980	6367049	1551594	-115.56	RT38-RH00
12	10/23/01 3:00	TASA	267	267	3483	1060	6366506	1551783	-36.58	RT38-RH00
13	10/23/01 3:00	TASA	492	492	3493	310	6366719	1551709	-68.08	RT38-RH00
14	10/23/01 3:00	TASA	320	320	3487	1200	6366556	1551765	-44	RT38-RH00
15	10/23/01 3:00	TASA	949	949	3509	1100	6367152	1551569	-130.54	RT38-RH00
16	10/23/01 3:00	TASA	860	860	3508	960	6367066	1551588	-118.08	RT38-RH00
17	10/23/01 3:00	TASA	839	839	3505	990	6367047	1551595	-115.14	RT38-RH00
18	10/23/01 3:00	TASA	202	202	3479	970	6366445	1551804	-27.48	RT38-RH00
19	10/23/01 3:00	TASA	853	853	3507	970	6367060	1551591	-117.1	RT38-RH00
20	10/23/01 3:00	TASA	687	687	3498	430	6366903	1551645	-95.38	RT38-RH00
21	10/23/01 3:00	TASA	555	555	3497	150	6366778	1551688	-76.9	RT38-RH00
22	10/23/01 3:00	TASA	209	209	3480	1060	6366451	1551802	-28.46	RT38-RH00
23	10/23/01 3:00	TASA	437	437	3490	1000	6366667	1551727	-60.38	RT38-RH00
24	10/23/01 3:00	TASA	83	83	3477	940	6366331	1551835	-13.3	RT38-RH00
25	10/23/01 3:00	TASA	788	788	3503	930	6366998	1551612	-108	RT38-RH00
26	10/23/01 3:00	TASA	470	470	3492	640	6366698	1551716	-65	RT38-RH00
27	10/23/01 3:00	TASA	788	788	3502	710	6366998	1551612	-108	RT38-RH00
28	10/23/01 3:00	TASA	555	555	3496	170	6366778	1551688	-76.9	RT38-RH00
29	10/23/01 3:00	TASA	232	232	3482	1030	6366473	1551794	-31.68	RT38-RH00
30	10/23/01 3:00	TASA	448	448	3491	560	6366677	1551723	-61.92	RT38-RH00
31	10/23/01 3:00	TASA	415	415	3489	660	6366646	1551734	-57.3	RT38-RH00
32	10/23/01 3:00	TASA	410	410	3488	950	6366641	1551736	-56.6	RT38-RH00
33	10/23/01 3:00	TASA	500	500	3494	120	6366726	1551706	-69.2	RT38-RH00
34	10/23/01 3:00	TASA	764	764	3499	860	6366976	1551620	-104.86	RT38-RH00
35	10/23/01 3:00	TASA	765	765	3500	740	6366977	1551620	-104.96	RT38-RH00
36	10/23/01 13:30	NASA1049A	1049	1049	3525	880				
37	10/23/01 13:30	NASA1265A	1265	1265	3545	940				
38	10/23/01 13:30	NASA1272B	1272	1272	3547	935				
39	10/23/01 13:30	NASA2156B	2156	2156	3584	870				
40	10/23/01 13:30	NASA2198A	2198	2198	3587	1160				
41	10/23/01 13:30	NASA2198A	2198	2198	3586	990				
42	10/23/01 13:30	TASA	2542	2542	3598	940	6367761	1551326	-339.01	RT38-RH00
43	10/23/01 13:30	TASA	1070	1070	3529	935	6367268	1551546	-147.48	RT38-RH00
44	10/23/01 13:30	TASA	2340	2340	3594	1110	6367685	1551486	-314.08	RT38-RH00
45	10/23/01 13:30	TASA	2289	2289	3590	1170	6367709	1551531	-306.94	RT38-RH00
46	10/23/01 13:30	TASA	2168	2168	3585	870	6367788	1551607	-291.8	RT38-RH00

47	10/23/01 13:30	TASA	1050	1050	3524	900	6367249	1551552	-144.68	RT38-RH00
48	10/23/01 13:30	TASA	2150	2150	3583	880	6367806	1551607	-289.28	RT38-RH00
49	10/23/01 13:30	TASA	2122	2122	3581	855	6367834	1551608	-285.36	RT38-RH00
50	10/23/01 13:30	TASA	1023	1023	3522	930	6367223	1551561	-140.9	RT38-RH00
51	10/23/01 13:30	TASA	2030	2030	3578	840	6367914	1551586	-274.28	RT38-RH00
52	10/23/01 13:30	TASA	2265	2265	3588	1170	6367721	1551553	-303.58	RT38-RH00
53	10/23/01 13:30	TASA	1065	1065	3527	920	6367263	1551547	-146.78	RT38-RH00
54	10/23/01 13:30	TASA	2310	2310	3592	915	6367699	1551513	-309.88	RT38-RH00
55	10/23/01 13:30	TASA	2348	2348	3595	1280	6367682	1551479	-315.2	RT38-RH00
56	10/23/01 13:30	TASA	2435	2435	3596	1650	6367693	1551402	-325.59	RT38-RH00
57	10/23/01 13:30	TASA	1122	1122	3531	920	6367317	1551528	-154.76	RT38-RH00
58	10/23/01 13:30	TASA	2580	2580	3600	1360	6367799	1551332	-342.8	RT38-RH00
59	10/23/01 13:30	TASA	2020	2020	3577	840	6367919	1551577	-272.88	RT38-RH00
60	10/23/01 13:30	TASA	2015	2015	3576	825	6367922	1551573	-272.18	RT38-RH00
61	10/23/01 13:30	TASA	991	991	3520	950	6367193	1551572	-136.42	RT38-RH00
62	10/23/01 13:30	TASA	2001	2001	3575	825	6367930	1551561	-270.22	RT38-RH00
63	10/23/01 13:30	TASA	2000	2000	3574	830	6367930	1551560	-270.08	RT38-RH00
64	10/23/01 13:30	TASA	978	978	3515	960	6367180	1551573	-134.6	RT38-RH00
65	10/23/01 13:30	TASA	1980	1980	3571	835	6367941	1551543	-267.28	RT38-RH00
66	10/23/01 13:30	TASA	978	978	3518	940	6367180	1551573	-134.6	RT38-RH00
67	10/23/01 13:30	TASA	1870	1870	3569	950	6367958	1551447	-253.68	RT38-RH00
68	10/23/01 13:30	TASA	978	978	3516	980	6367180	1551573	-134.6	RT38-RH00
69	10/23/01 13:30	TASA	1765	1765	3568	3100	6367909	1551354	-239.72	RT38-RH00
70	10/23/01 13:30	TASA	1749	1749	3567	1640	6367894	1551349	-238.12	RT38-RH00
71	10/23/01 13:30	TASA	1735	1735	3565	3110	6367880	1551346	-236.46	RT38-RH00
72	10/23/01 13:30	TASA	969	969	3514	960	6367171	1551572	-133.34	RT38-RH00
73	10/23/01 13:30	TASA	1691	1691	3563	720	6367837	1551338	-230.3	RT38-RH00
74	10/23/01 13:30	TASA	1686	1686	3562	790	6367832	1551338	-229.6	RT38-RH00
75	10/23/01 13:30	TASA	1435	1435	3560	825	6367612	1551424	-198.58	RT38-RH00
76	10/23/01 13:30	TASA	1430	1430	3559	820	6367607	1551426	-197.88	RT38-RH00
77	10/23/01 13:30	TASA	1400	1400	3558	810	6367579	1551436	-193.68	RT38-RH00
78	10/23/01 13:30	TASA	1387	1387	3555	840	6367566	1551440	-191.86	RT38-RH00
79	10/23/01 13:30	TASA	952	952	3510	1190	6367155	1551569	-130.96	RT38-RH00
80	10/23/01 13:30	TASA	1318	1318	3552	940	6367501	1551463	-182.2	RT38-RH00
81	10/23/01 13:30	TASA	1315	1315	3551	940	6367498	1551464	-181.78	RT38-RH00
82	10/23/01 13:30	TASA	952	952	3511	1100	6367155	1551569	-130.96	RT38-RH00
83	10/23/01 13:30	TASA	1306	1306	3550	940	6367490	1551467	-180.52	RT38-RH00
84	10/23/01 13:30	TASA	1305	1305	3549	940	6367489	1551467	-180.38	RT38-RH00
85	10/23/01 13:30	TASA	1272	1272	3548	940	6367458	1551478	-175.76	RT38-RH00
86	10/23/01 13:30	TASA	1340	1340	3554	910	6367522	1551456	-185.28	RT38-RH00
87	10/23/01 13:30	TASA	1265	1265	3544	940	6367451	1551481	-174.78	RT38-RH00
88	10/23/01 13:30	TASA	1728	1728	3564	2950	6367873	1551345	-235.48	RT38-RH00
89	10/23/01 13:30	TASA	978	978	3517	965	6367180	1551573	-134.6	RT38-RH00
90	10/23/01 13:30	TASA	1265	1265	3546	940	6367451	1551481	-174.78	RT38-RH00
91	10/23/01 13:30	TASA	1400	1400	3557	810	6367579	1551436	-193.68	RT38-RH00
92	10/23/01 13:30	TASA	1230	1230	3543	950	6367418	1551492	-169.88	RT38-RH00
93	10/23/01 13:30	TASA	1880	1880	3570	540	6367963	1551456	-255.08	RT38-RH00
94	10/23/01 13:30	TASA	1983	1983	3572	830	6367939	1551546	-267.7	RT38-RH00
95	10/23/01 13:30	TASA	990	990	3519	950	6367192	1551572	-136.28	RT38-RH00

96	10/23/01 13:30	TASA	2000	2000	3573	830	6367930	1551560	-270.08	RT38-RH00
97	10/23/01 13:30	TASA	1205	1205	3542	1020	6367395	1551501	-166.38	RT38-RH00
98	10/23/01 13:30	TASA	1395	1395	3556	820	6367574	1551437	-192.98	RT38-RH00
99	10/23/01 13:30	TASA	955	955	3513	1060	6367157	1551570	-131.38	RT38-RH00
100	10/23/01 13:30	TASA	1200	1200	3539	900	6367390	1551502	-165.68	RT38-RH00
101	10/23/01 13:30	TASA	995	995	3521	930	6367197	1551571	-136.98	RT38-RH00
102	10/23/01 13:30	TASA	2020	2020	3579	840	6367919	1551577	-272.88	RT38-RH00
103	10/23/01 13:30	TASA	2118	2118	3580	835	6367838	1551609	-284.8	RT38-RH00
104	10/23/01 13:30	TASA	1040	1040	3523	940	6367239	1551556	-143.28	RT38-RH00
105	10/23/01 13:30	TASA	2135	2135	3582	870	6367821	1551608	-287.18	RT38-RH00
106	10/23/01 13:30	TASA	1200	1200	3540	900	6367390	1551502	-165.68	RT38-RH00
107	10/23/01 13:30	TASA	1052	1052	3526	900	6367251	1551552	-144.96	RT38-RH00
108	10/23/01 13:30	TASA	2283	2283	3589	1220	6367712	1551537	-306.1	RT38-RH00
109	10/23/01 13:30	TASA	960	960	3512	1100	6367162	1551571	-132.08	RT38-RH00
110	10/23/01 13:30	TASA	1198	1198	3541	900	6367388	1551503	-165.4	RT38-RH00
111	10/23/01 13:30	TASA	2290	2290	3591	1300	6367709	1551530	-307.08	RT38-RH00
112	10/23/01 13:30	TASA	1065	1065	3528	900	6367263	1551547	-146.78	RT38-RH00
113	10/23/01 13:30	TASA	2335	2335	3593	1120	6367688	1551491	-313.38	RT38-RH00
114	10/23/01 13:30	TASA	1197	1197	3538	900	6367387	1551503	-165.26	RT38-RH00
115	10/23/01 13:30	TASA	1121	1121	3530	950	6367316	1551529	-154.62	RT38-RH00
116	10/23/01 13:30	TASA	2478	2478	3597	1060	6367715	1551366	-331.61	RT38-RH00
117	10/23/01 13:30	TASA	1600	1600	3561	835	6367749	1551338	-221.64	RT38-RH00
118	10/23/01 13:30	TASA	1194	1194	3537	910	6367384	1551504	-164.84	RT38-RH00
119	10/23/01 13:30	TASA	2715	2715	3610	2560	6367932	1551355	-359.7	RT38-RH00
120	10/23/01 13:30	TASA	2548	2548	3599	970	6367767	1551326	-339.61	RT38-RH00
121	10/23/01 13:30	TASA	1122	1122	3532	970	6367317	1551528	-154.76	RT38-RH00
122	10/23/01 13:30	TASA	2580	2580	3601	1370	6367799	1551332	-342.8	RT38-RH00
123	10/23/01 13:30	TASA	2671	2671	3608	2040	6367888	1551348	-353.55	RT38-RH00
124	10/23/01 13:30	TASA	1140	1140	3535	1140	6367333	1551522	-157.28	RT38-RH00
125	10/23/01 13:30	TASA	2645	2645	3606	1710	6367863	1551343	-349.91	RT38-RH00
126	10/23/01 13:30	TASA	2650	2650	3607	1640	6367868	1551344	-350.61	RT38-RH00
127	10/23/01 13:30	TASA	1158	1158	3536	910	6367350	1551516	-159.8	RT38-RH00
128	10/23/01 13:30	TASA	2671	2671	3609	1720	6367888	1551348	-353.55	RT38-RH00
129	10/23/01 13:30	TASA	2610	2610	3605	2010	6367828	1551337	-345.02	RT38-RH00
130	10/23/01 13:30	TASA	1135	1135	3534	940	6367329	1551524	-156.58	RT38-RH00
131	10/23/01 13:30	TASA	2605	2605	3603	1810	6367823	1551336	-344.32	RT38-RH00
132	10/23/01 13:30	TASA	1319	1319	3553	940	6367502	1551463	-182.34	RT38-RH00
133	10/23/01 13:30	TASA	1740	1740	3566	3110	6367885	1551347	-237.16	RT38-RH00
134	10/23/01 13:30	TASA	2605	2605	3604	2300	6367823	1551336	-344.32	RT38-RH00
135	10/23/01 13:30	TASA	1124	1124	3533	920	6367318	1551528	-155.04	RT38-RH00
136	10/23/01 13:30	TASA	2587	2587	3602	1410	6367806	1551333	-343.08	RT38-RH00
137	10/24/01 3:00	TASA	3520	3520	3660	975	6367762	1551244	-448.78	RT38-RH00
138	10/24/01 3:00	TASA	3495	3495	3659	980	6367764	1551269	-449.27	RT38-RH00
139	10/24/01 3:00	TASA	3455	3455	3658	1640	6367773	1551308	-449.23	RT38-RH00
140	10/24/01 3:00	TASA	3437	3437	3656	1710	6367779	1551325	-449.81	RT38-RH00
141	10/24/01 3:00	TASA	3437	3437	3657	1600	6367779	1551325	-449.81	RT38-RH00
142	10/24/01 3:00	TASA	3426	3426	3655	1770	6367783	1551335	-449.99	RT38-RH00
143	10/24/01 3:00	TASA	3365	3365	3654	1915	6367806	1551391	-444.78	RT38-RH00
144	10/24/01 3:00	TASA	3314	3314	3653	2180	6367825	1551439	-437.39	RT38-RH00

145	10/24/01 3:00	TASA	3314	3314	3651	2250	6367825	1551439	-437.39	RT38-RH00	
146	10/24/01 3:00	TASA	3312	3312	3650	2320	6367826	1551441	-437.1	RT38-RH00	
147	10/24/01 3:00	TASA	3280	3280	3648	1290	6367838	1551470	-432.46	RT38-RH00	
148	10/24/01 3:00	TASA	3277	3277	3647	1275	6367839	1551473	-432.02	RT38-RH00	
149	10/24/01 3:00	TASA	3275	3275	3646	1255	6367839	1551475	-431.73	RT38-RH00	
150	10/24/01 3:00	TASA	3270	3270	3644	1520	6367841	1551480	-431.01	RT38-RH00	
151	10/24/01 3:00	TASA	3248	3248	3643	1290	6367849	1551500	-427.82	RT38-RH00	
152	10/24/01 3:00	TASA	3248	3248	3642	1320	6367849	1551500	-427.82	RT38-RH00	
153	10/24/01 3:00	TASA	3233	3233	3641	1080	6367855	1551514	-425.64	RT38-RH00	
154	10/24/01 3:00	TASA	3190	3190	3636	825	6367871	1551554	-419.41	RT38-RH00	
155	10/24/01 3:00	TASA	3160	3160	3635	875	6367882	1551582	-418.22	RT38-RH00	
156	10/24/01 3:00	TASA	3135	3135	3634	820	6367892	1551605	-417.69	RT38-RH00	
157	10/24/01 3:00	TASA	3135	3135	3633	830	6367892	1551605	-417.69	RT38-RH00	
158	10/24/01 3:00	TASA	3122	3122	3631	800	6367897	1551617	-416.66	RT38-RH00	
159	10/24/01 3:00	TASA	3122	3122	3632	810	6367897	1551617	-416.66	RT38-RH00	
160	10/24/01 3:00	TASA	3110	3110	3630	750	6367901	1551628	-415	RT38-RH00	
161	10/24/01 3:00	TASA	3275	3275	3645	2110	6367839	1551475	-431.73	RT38-RH00	
162	10/24/01 3:00	TASA	3090	3090	3629	730	6367912	1551644	-412.2	RT38-RH00	
163	10/24/01 3:00	TASA	3090	3090	3627	770	6367912	1551644	-412.2	RT38-RH00	
164	10/24/01 3:00	TASA	3088	3088	3628	740	6367914	1551646	-411.92	RT38-RH00	
165	10/24/01 3:00	TASA	2929	2929	3626	1640	6367994	1551547	-389.66	RT38-RH00	
166	10/24/01 3:00	TASA	3290	3290	3649	2320	6367834	1551461	-433.91	RT38-RH00	
167	10/24/01 3:00	TASA	3314	3314	3652	2100	6367825	1551439	-437.39	RT38-RH00	
168	10/24/01 3:00	TASA	2929	2929	3625	1050	6367994	1551547	-389.66	RT38-RH00	
169	10/24/01 3:00	TASA	2920	2920	3623	790	6367996	1551538	-388.4	RT38-RH00	
170	10/24/01 3:00	TASA	2920	2920	3624	750	6367996	1551538	-388.4	RT38-RH00	
171	10/24/01 3:00	TASA	2917	2917	3621	820	6367997	1551535	-387.98	RT38-RH00	
172	10/24/01 3:00	TASA	2916	2916	3622	980	6367997	1551534	-387.84	RT38-RH00	
173	10/24/01 3:00	TASA	2916	2916	3620	1480	6367997	1551534	-387.84	RT38-RH00	
174	10/24/01 3:00	TASA	2915	2915	3619	1030	6367997	1551533	-387.7	RT38-RH00	
175	10/24/01 3:00	TASA	2900	2900	3618	2495	6368000	1551518	-385.6	RT38-RH00	
176	10/24/01 3:00	TASA	3540	3540	3661	1060	6367761	1551224	-448.34	RT38-RH00	
177	10/24/01 3:00	TASA	2800	2800	3617	2585	6367976	1551426	-371.6	RT38-RH00	
178	10/24/01 3:00	TASA	2770	2770	3616	3280	6367962	1551400	-367.4	RT38-RH00	
179	10/24/01 3:00	TASA	2768	2768	3615	3310	6367961	1551398	-367.12	RT38-RH00	
180	10/24/01 3:00	TASA	2760	2760	3614	3130	6367957	1551391	-366	RT38-RH00	
181	10/24/01 3:00	TASA	2750	2750	3613	3290	6367953	1551382	-364.6	RT38-RH00	
182	10/24/01 3:00	TASA	2740	2740	3612	3245	6367948	1551373	-363.2	RT38-RH00	
183	10/24/01 3:00	TASA	2715	2715	3611	3570	6367932	1551355	-359.7	RT38-RH00	
184	10/24/01 3:00	TASD	72	72	3640	1020	6367812	1551599	-417.22	RT38-RH00	
185	10/24/01 3:00	TASD	60	60	3639	940	6367823	1551594	-417.49	RT38-RH00	
186	10/24/01 3:00	TASD	57	57	3638	1130	6367826	1551593	-417.56	RT38-RH00	
187	10/24/01 3:00	TASD	5	5	3637	1530	6367874	1551574	-418.74	RT38-RH00	
188	10/24/01 3:00	TASF	75	75	3666	2215	6367812	1551327	-456.91	RT38-RH00	
189	10/24/01 3:00	TASF	45	45	3665	1795	6367804	1551298	-453.2	RT38-RH00	
190	10/24/01 3:00	TASF	29	29	3664	1775	6367800	1551283	-451.23	RT38-RH00	
191	10/24/01 3:00	TASH	450	450	3667	1780					
192	10/24/01 3:00	TASH	340	340	3669	1330					
193	10/24/01 3:00	TASH	220	220	3668	1090					

194	10/24/01 3:00	TASI	10	10	3663	960	6367753	1551258	-448.8	RT38-RH00
195	10/24/01 3:00	TASI	1	1	3662	960	6367762	1551257	-449.1	RT38-RH00

Visualization of the sampling points

The geometry of the tunnel volume was modeled with the code TECPLOT. The 195 sampling points were visualized. Figure 1 represents the electrical conductivity value of the sampling points along the tunnel walls. For comparison, the electrical conductivity available from the measurements in the tunnel boreholes during the last 2 years is presented.

a) b)

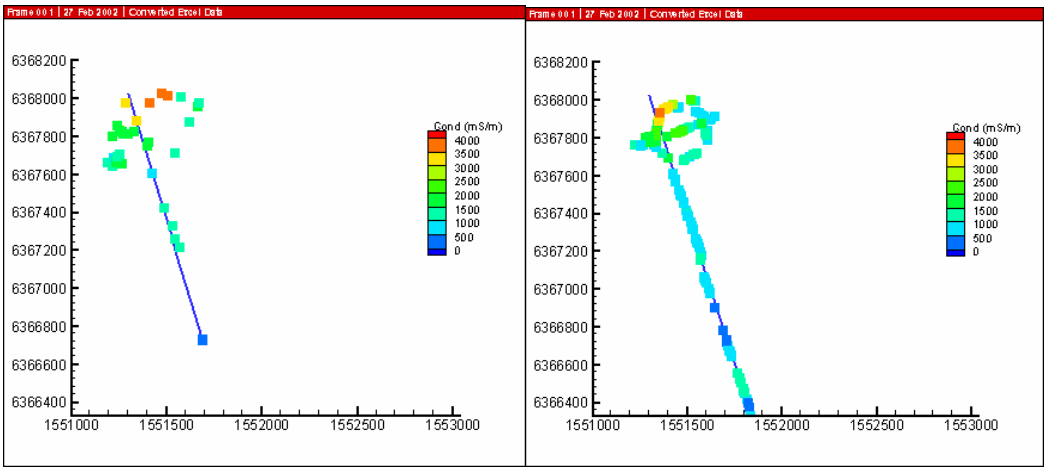

Figure 1: a) Electric conductivity of the groundwater measured in tunnel boreholes; b) Electric conductivity of the groundwater measured along the tunnel wall

The 2 datasets, electrical conductivity measured along the tunnel walls and measured in the tunnel boreholes are compared in Figure 2.

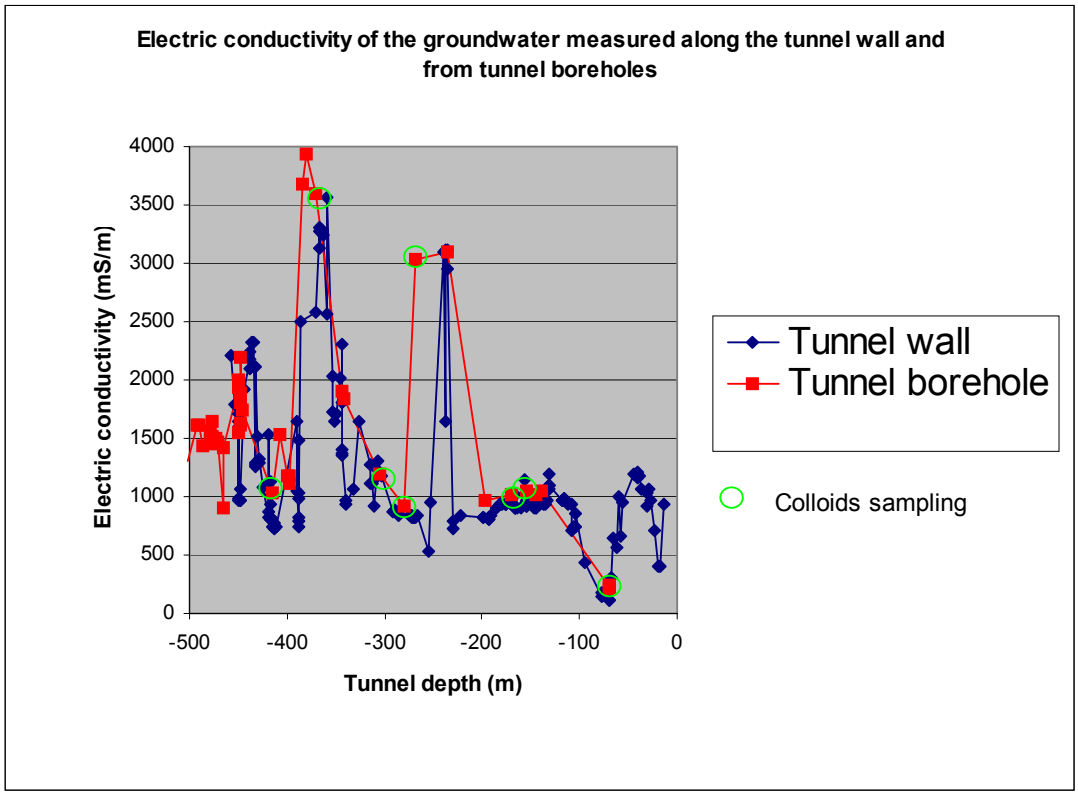

Figure 2: Electrical conductivity data measured along the tunnel walls (blue) and electrical conductivity data measured in the tunnel boreholes (red) versus the tunnel depth. The green circles indicated the 8 boreholes used for colloid sampling.

Conclusions

The aim of the project was to investigate the changes in the groundwater composition along the tunnel wall and to compare the results with the information from the drilled boreholes in the tunnel.

The results indicate that both data sets give the same basic information concerning groundwater composition (salinity) but greater detail variability is seen in the tunnel data. This indicates that tunnel data reflects local variability better than data from boreholes, but when sampling the tunnel wall close to the boreholes the groundwater salinity is the same in the borehole as in the water dripping from the wall.

These results support the colloid project, by showing that the groundwater composition obtained from the boreholes reflect well the major groundwater variability obtained in the whole tunnel.

Appendix 11

Review comments

Claude Degueldre

Äspö Colloid Workshop, Review Note by Claude Degueldre

Review of the presented work

The presentations from the groups were good with detailed tests and experimental results. The results presented concerned mainly groundwater data and data on colloids, bacteria and organics (humic/fulvic). Some specific remarks may be pointed out. A minimum of background on the rock and source terms (various water sources) is required in the general introduction. Some of the data reported during the talks have been given without error bar (standard deviation or estimate) based on precision, without accuracy estimation and without detection limits. In some cases, the data presentation yields confusing figures or unrealistic values such as a negative activity.

-*Tests in the laboratory*

This is a must to understand and identify processes that are not directly observable in situ. Clay Technology AB (O. Karnland) follows systematically the sedimentation of bentonite colloids in batches, contacting bentonite (treated or not) with a range of neutral solutions changing the Na or Ca concentrations. Their pH ranges from 5.9 to 8.5 which is a bit larger that the Äspö groundwater pH (7.1 - 7.8) but which completes the picture. The ICPAES tests of the solution/suspension were carried out systematically without filtration which in some cases yield ambiguous data. The work could be upgraded in these cases by comparing data from the filtered and not filtered phases. In addition, an attachment (sticking) coefficient should be extracted from these data.

The work is completed by PCS analysis (S. Wold). The PCS sensitivity could be somewhat increased selecting more adequate detection angles. Fig. 1- 4 are important. Fig.1-3 should be plotted on a log concentration scale. Connection between O. Karnland and S. Wold reports could be done by deriving attachment (sticking) factor as a function of Na, Ca concentration and pH. The later result can be used by modellers. Data should also be compared from those reported in the literature.

- *Field work*

Results from the German team

The use of LIBD with detection in photospectrometric mode and the development of the high pressure cell to work on line was welcomed (W. Hauser, B. Kienzler). The high pressure cell is an excellent tool for the in situ investigation. The presentation of the report is of high quality. For deriving a concentration the distribution is supposed to be gaussian which is not reflecting the reality, if a correction is possible for continuous distribution, it should be done, otherwise the assumption should be clearly stated. Both Figures 11 & 12 are interesting: they suggest that when the salt concentration decreases the colloid concentration increases and that (Fig. 12) their average diameter increases also. If this is true, this implicates a transport reduction by filtration (size effect) and by sedimentation of the colloid in the low mineralised water (which is the opposite of what is suggested in the literature). However, Table 2 shows data ranging more than in Figure 11 & 12. Fig. 14 is deduced from Table 5: calculated solid phases should not take into account quartz and pyrite, most of the waters are over-saturated with quartz, and in stead of pyrite, troilite should be considered for the iron sulphide colloid phase. For these

calculations presence of organics e.g. fulvic may play an important role. So behind the excellent experimental work, there may be some revisions of the data needed. Finally the very useful LIBD data (artefact-free, from redox Fe(II) oxidation and from calcite precipitation) on the low colloid concentration in the highly saline water confirm what was reported earlier (SKB TR95-24).
The fulvic study makes sense and the work suggested (G. Buckau) on the natural ^{14}C labelled fulvics was supported by the project leader and members. It is difficult to present 12 UV-Vis spectra on the same Figure, also normalised and without scale. What could be done for comparison? Change the order of UV spectra e.g. from DOC poor to DOC rich? It is sometime interesting to present a derivative of the spectra to identify the components. Would it be the case here?
There may be a correlation between DIC and DOC as depicted by the reviewer below (Fig. 1).

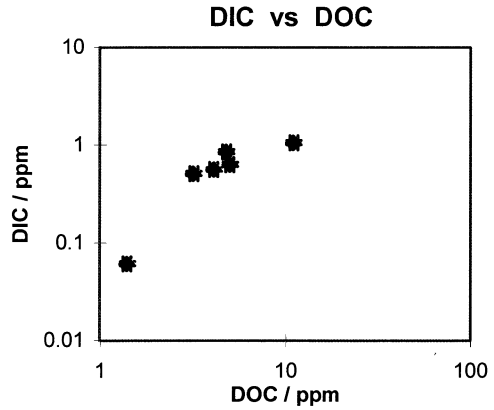

Fig. 1: Correlation between DIC and DOC (derived from SKB data, Tab. 1 in Buckau report)

-Results from the Finnish team
The introduction (M. Snellman) of the Finnish concept was welcomed.
The idea of using centrifugation-filtration is good and the efforts concerning the colloid work are substantial (U. Vuorinen). The work performed by SEM would, however, gain in usefulness if quantification of colloid concentrations was done i.e. provide colloid concentration and size distribution. This quantification performed in term of specific size distributions should be done and compared with the results obtained by LIBD.

-Results from the Swedish groups
The counting of bacteria is always a tremendous work (K. Pedersen). From the microbial entities: bacteria colonies, families, chains, or single entities, what is relevant to be counted for the transport or for the bio-activity? If routine bacteria counting is required the use of a flow cytometer is suggested. The later may be adapted for size distribution, however, the counting at the microscope as realised so far allows morphological discrimination/identification in some cases, which remains essential. May be both manual counting and automatic on line counting could provide useful information for example during systematic studies. The bacteria analysis will also be upgraded with source identification (anthropologic, natural in situ bacteria), but this is in the frame of an

extended study. The correlation bacteria density vs DOC noted by Pedersen (and also by the reviewer) is depicted below (Fig. 2).
If a correlation exists also between DOC and DIC then the correlation bacteria density and DIC would confirm their occurrence by bio-activity (CO_2 source in waters originally depleted in bicarbonate) see Fig. 3.

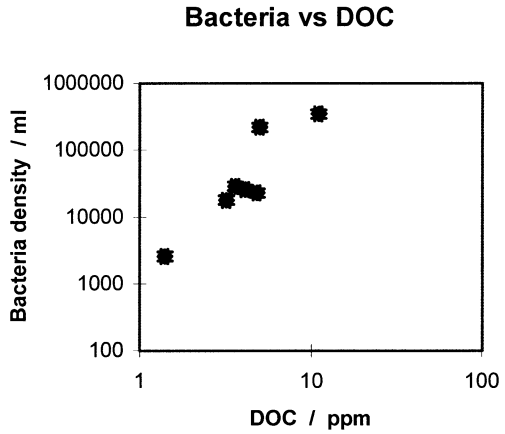

Fig. 2: Correlation between bacteria density and DOC (derived from SKB data, Tab. 1 in Buckau report, and from Tab. 2 in Pedersen in report)

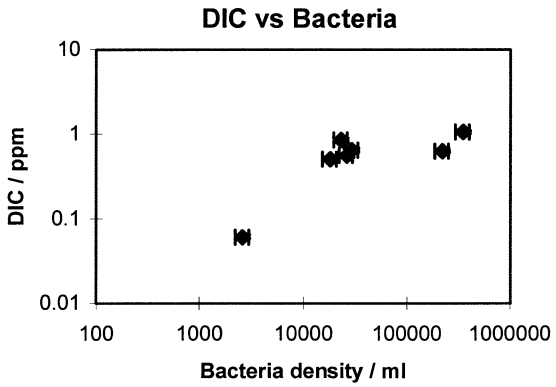

Fig. 3: Correlation between DIC and bacteria density (derived from SKB data, Tab. 1 in Buckau report and from Tab. 2 in Pedersen report)

Review of the concept

To extract useful data from the Äspö Colloid Project and to supply data for a safety related study, it is important to focus on the 3 potential mobile phases:

1. bacteria (natural & anthropogenic e.g. from activities during repository construction)
2. colloids (natural & anthropogenic e.g. from the bentonite buffer)
3. humic/fulvic (natural),

and the interactions between these 3 phases together, as well as with host rock and the nuclides should be studied experimentally. These data should be utilised in models. However, priorities has to be made in the program. The model should take into account the various environments from the site to the biosphere.
In today's program priority concerns the stability of the colloids with emphasis on the natural groundwater colloids and the bentonite colloids. Therefore tests on their coagulation (aggregation) and sedimentation are performed. These tests deliver kinetic information on colloid population stability which is necessary. However, colloid stability studies on geological time scale e.g. considering potential secondary phase formation including groundwater or bentonite colloids should also be suggested. When reviewing the program, one has always to remember the goal: safety of a Scandinavian repository concept over a large distance and a large time scale.

Modelling will be carried out utilising the data from the laboratory and field tests i.e. colloid generation, stability and transport. The first include the tests which were presented and discussed by the program leader (bentonite erosion test), the second the application of the laboratory tests and the use of both approaches (as presented by the reviewer): following the colloid concentration for a given size in the batch as a function of time to calculate the attachment coefficient (e.g. Degueldre et al., 1996), or/and to follow the average size of the colloid population as a function of time during coagulation tests (e.g. Triay et al., 1996). Both approaches are complementary and could be applied using the PCS unit as presented by S. Wold. Colloid transport, was also included in the review talk and concerned colloid partitioning with the host rock. Those concepts and data are important and will support the results obtained so far for the natural entities: bacteria, colloids and organics. Their size distributions summarised in Fig. 4 shows the continuity of the entities size distribution studied in this project.

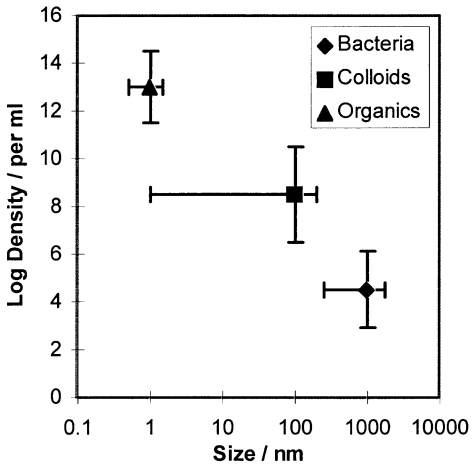

Fig. 4: Size distribution scheme of the studied mobile entities: bacteria, colloids and organics (derived from SKB data, Tab. 1 in Buckau, Tab. 2 in Hauser report and Tab. 2 in Pedersen report)

A conclusion on the effect of colloid in the frame of the migration of safety relevant nuclides will be required. The study will provide important data on the colloid source terms and properties: the generation rate as well as their stability and transport properties for the natural colloids, bacteria and organics, and, for the bentonite colloids: stability and transport potential with emphasis on the colloid facilitated mechanism. The work of the groups must focus on these goals. This is a key issue for the success of the Äspö Colloid Project.

References (both delivered to the Project Leader and S. Wold during the workshop)
Degueldre et al., 1996 Appl. Geochem.
Triay et al., 1996 Los Alamos National Laboratory report.